**AN ABSTRACT OF THE THESIS OF**

Chun-Tien Yeh for the degree of Doctor of Philosophy in Mechanical Engineering presented on April 1, 1992.

Title: Dynamics and Control of a Rigid/Flexible Manipulator.



Abstract approved: _____
Charles E. Smith

Control of high-speed, light-weight robotic manipulators is a challenge because of their special dynamic characteristics. In this work, a two-stage control algorithm for the position control of flexible manipulators is proposed. First, the more complex, flexible robot system is replaced by a simplified hypothetical rigid body system (HRRA) with off-line trajectory planning. This reduces the complexity of the controller design for the flexible robotic arm. A parameter-optimization approach was adopted to minimize the difference between these two models in this stage. Also, a comparison of computational efficiency is made among the methods of calculus-of-variations, dynamic-programming, and the proposed parameter-optimization. At the second stage, simple linear state feedback controllers, based on the simplified hypothetical rigid body model, are proposed to control the actual robotic

system. With the feedback gains selected properly by the pole-placement and linear quadratic methods, the results show satisfactory achievement of the motion objectives.

The algorithm is implemented for a two-link rigid/flexible robotic arm, and the results indicate that the procedure is capable of providing effective control with much simpler computational requirements than those of procedures published previously.

# Dynamics and Control of a Rigid/Flexible Manipulator.

by

Chun-Tien Yeh

A THESIS

submitted to

Oregon State University

in partial fulfillment of

the requirements for the

degree of

Doctor of Philosophy

Completed April 1, 1992

Commencement June 1992

APPROVED:

Redacted for Privacy

Professor of Mechanical Engineering in charge of major

Redacted for Privacy

Head of Department of Mechanical Engineering

Redacted for Privacy

Dean of Graduate School

Date thesis is presented : April 1, 1992

Presented by : Chun-Tien Yeh

ACKNOWLEDGMENTS

It is great pleasure that I acknowledge the inspirational guidance, encouragement and continuing advice of my adviser, Dr. Charles E. Smith, during the completion of this research. Without him this work would not have been possible.

I would also like to express my sincere appreciation to Dr. Timothy C. Kennedy, Dr. Clarence A. Calder and Dr. Andrzej Olas for their advice. Appreciation is also extended to the faculty, staff in the Department of Mechanical Engineering for their advice and help during my years at Oregon State University.

I must also acknowledge my parents for their unending support and my wife Seksiri for her understanding and patience during my studies in Oregon State University.

TABLE OF CONTENTS


CHAPTER 1. INTRODUCTION . . . . . 1
1.1. Background and Motivation . . . . . 1
1.2. Literature Review . . . . . 3
1.3. Study Objectives . . . . . 6

CHAPTER 2. SYSTEM DESCRIPTION . . . . . 9
2.1. Introduction . . . . . 9
2.2. Robotic System . . . . . 10
2.3. Derivation of Equations of Motion of the HRRA System . . . . . 13
2.4. Derivation of Equations of Motion of the RFRA System . . . . . 18
2.5. Linearized Equations of Motion of HRRA . . 26

CHAPTER 3. CONTROL . . . . . 31
3.1. Introduction . . . . . 31
3.2. Conventional Control Strategies . . . . . 31
3.3. Two-Stage Control Method . . . . . 33
3.3.1. Feedforward Control Stage . . . . . 34
3.3.1.1. Off-line motion trajectory planning . . . . . 39
3.3.1.2. Rayleigh-Ritz method . . . . . 42
3.3.1.3. The optimization technique . . 46
3.3.1.4. Trajectory planning design algorithm for RFRA system . . . 51
3.3.2. Feedback Control Stage . . . . . 56
3.3.2.1. Pole-placement method . . . . . 60
3.3.2.2. Linear quadratic method . . . . 62

CHAPTER 4. APPLICATION AND RESULT . . . . . 68
4.1. System Dimensions . . . . . 68
4.2. Open-Loop Trajectory Approximation . . . . 71
4.3. Selection of Performance Index . . . . . 73
4.4. Off-Line Control Simulation Results . . . . 75
4.5. On-Line Control Simulation Results . . . . 120
4.6. Selection of the Weighting Matrices **Q** and **R** . . . . . 129

CHAPTER 5. CONCLUSIONS AND FUTURE WORK . . . . . 131

BIBLIOGRAPHY . . . . . 135

LIST OF FIGURES


| Figure | | Page |
|---|---|---|
| 2.1 | Scheme of the RFRA system. . . . . | 11 |
| 2.2 | Scheme of the HRRA system. . . . . | 12 |
| 3.1 | Conventional FFC (Flexible Feedback Control) method. . . . . | 32 |
| 3.2 | Feedforward control scheme of a RFRA system. . . . . | 35 |
| 3.3 | Off-line trajectory planning for the RFRA System. . . . . | 40 |
| 3.4 | Configurations of a two-link robot in stations A and B. . . . . | 42 |
| 3.5 | Flowchart for determining optimal trajectory. . . . . | 47 |
| 3.6 | Geometric interpretation of Powell's method. . . . . | 50 |
| 3.7a | Computer algoritm using Powell's optimization search method for open-loop trajectory planning. . . . . | 52 |
| 3.7b | Flowchart of Subroutine CPI of computing performance index J for a given set of Ritz constants $C_{ij}$ and $t_f$. . . . . | 53 |
| 3.8 | Scheme of a two-stage control of RFRA System. . . . . | 58 |
| 4.1 | Physical model of RFRA system with cross-section view. . . . . | 69 |
| 4.2 | Motion trajectories of planned paths for case 1 ($m_p$=0 kg): (a) cubic path. (b) cubic poly. + versine path (c) fifth poly. + Fourier type path. . . . . | 79 |
| 4.3 | Motion trajectories of planned paths for case 2 ($m_p$=0.5 kg): (a) cubic path. (b) cubic poly. + versine path. (c) fifth poly. + Fourier type path. . . . . | 80 |

4.4 Motion trajectories of planned path for case 3 (mp = 1 kg): (a) cubic path (b) cubic poly. + versine path. (c) fifth poly. + Fourier type path. . . . . 81

4.5 Actual joint displacements and planned joint displacements using cubic polynomial path for case 1. . . . . 84

4.6 Actual joint displacements and planned joint displacements using cubic polynomial + versine function path for case 1. . . . 85

4.7 Actual joint displacements and planned joint displacements using fifth polynomial + fourier series path for case 1. . . . . 86

4.8 Actual joint velocities and planned joint velocities using cubic ploynomial + versine function path for case 1. . . . . 87

4.9 Actual joint velocities and planned joint velocities using cubic polynomial + versine function path for case 1. . . . . 88

4.10 Actual joint velocities and planned joint velocities using fifth polynomial + Fourier series path for case 1. . . . . 89

4.11 Tracking errors with three types of planned trajectories under no payload condition. . . . . 90

4.12 Tip vibrations with three types of planned trajectories under no payload condition. . 93

4.13 Tip vibrational velocities with three types of planned trajectories under no payload condition. . . . . 94

4.14 Vibrational energy for proposed trajectories with no payload. . . . . 96

4.15 Integrand of control effort ($\tau_1^2+\tau_2^2$) with no payload. . . . . 97

4.16 Actual joint displacements and planned joint displacements using cubic polynomial path for case 2. . . . . 98

4.17 Actual joint displacements and planed joint displacements using cubic polynomial + versine function path for case 2. . . . . 99

4.18 Actual joint displacements and planned joint displacements using fifth polynomial + Fourier series path for case 2. . . . . 100

4.19 Actual joint velocities and planned joint velocities using cubic polynomial for case 2. . . . . 101

4.20 Actual joint velocities and planned joint velocities using cubic polynomial + versine function path for case 2. . . . . 102

4.21 Actual joint velocities and planned joint velocities using fifth polynomial + Fourier series path for case 2. . . . . 103

4.22 Tracking errors for proposed trajectories with payload = 0.5 kg. . . . . 104

4.23 Tip vibrations for proposed trajectories with payload = 0.5 kg. . . . . 105

4.24 Tip vibrational velocities for proposed trajectories with payload = 0.5 kg. . . . 106

4.25 Vibrational energy for proposed trajectories with payload = 0.5 kg. . . . 107

4.26 Integrand of control effort ($\tau_1^2+\tau_2^2$) with payload = 0.5kg. . . . . 108

4.27 Actual joint displacements and planned joint displacements using cubic polynomial path for case 3. . . . . 109

4.28 Actual joint displacements and planned joint velocities using cubic polynomial + versine function path for case 3. . . . . 110

4.29 Actual joint displacements and planned joint displacements using fifth polynomial + Fourier series path for case 3. . . . . 111

4.30 Actual joint velocities and planned joint velocities using cubic polynomial path for case 3. . . . . 112

4.31 Actual joint velocities and planned joint velocities using cubic polynomial + versine function path for case 3. . . . . 113

4.32 Actual joint velocities and planned joint velocities using fifth polynomial + Fourier series path for case 3. . . . . 114

4.33 Tracking errors for proposed trajectories with payload = 1 kg. . . . . 115

4.34 Tip vibration for proposed trajectories with payload = 1 kg. . . . . 116

4.35 Tip vibrational velocities for proposed trajectories with payload = 1 kg. . . . . 117

4.36 Vibrational energy for proposed trajectories with payload = 1 kg. . . . . 118

4.37 Integrand of control effort ($\tau_1^2+\tau_2^2$) with payload = 1 kg. . . . . 119

4.38 Shoulder velocities with proposed controllers ( $m_p$=0kg, $\Delta\tau$=[5,5]N·m, $\zeta=\omega$=[1,1], **Q**=diag[$10^4$,$10^4$,1,1], **R**=diag[$10^{-1}$,$10^{-1}$]) . . . . . 122

4.39 Elbow velocities with proposed controllers ( $m_p$=0kg, $\Delta\tau$=[5,5]N·m, $\zeta=\omega$=[1,1], **Q**=diag[$10^4$,$10^4$,1,1], **R**=diag[$10^{-1}$,$10^{-1}$]). . . 123

4.40 Shoulder velocities with proposed controllers ( $m_p$=0.5 kg, $\Delta\tau$=[5,5] N·m, $\zeta=\omega$=[1,1], **Q**=diag[$10^4$,$10^4$,1,1], R=[$10^{-1}$,$10^{-1}$]). . . . . 124

4.41 Elbow velocities with proposed controller ($m_p$=0.5kg, $\Delta\tau$=[5,5] N·m, $\zeta=\omega$=[1,1], **Q**=[$10^4$,$10^4$,1,1], R=[$10^{-1}$,$10^{-1}$] . . . . . 125

4.42 Shoulder velocities with proposed controllers ($m_p$=1kg, $\Delta\tau$=[5,5]N·m, $\zeta=\omega$=[1,1], **Q**=[$10^4$,$10^4$,1,1], **R**=[$10^{-1}$,$10^{-1}$]). 126

4.43 Elbow velocities with proposed controllers ($m_p$=1kg,$\Delta\tau$=[5,5] N·m, $\zeta=\omega$=[1,1], **Q**=[$10^4$,$10^4$,1,1], **R**=[$10^{-1}$,$10^{-1}$]). . . . . 127

4.44 Joint velocities with LQR controller (**Q**=[$10^6$,$10^6$,1,1] and **R**=[$10^{-1}$,$10^{-1}$], $\Delta\tau$=[5,5]N·m) for $m_p$=0.5kg. . . . . 128

LIST OF TABLES


| Table | | Page |
|---|---|---|
| 1. | System parameters of two-link manipulator . . . . . | 70 |
| 2. | Varying loading conditions for the two-link flexible/rigid manipulator . . . . . | 76 |
| 3. | Determination of optimal trajectories with cubic polynomial plus version function approximation . . . . . | 77 |
| 4. | Determination of optimal trajectories with fifth polynomial plus Fourier-type-based approximation . . . . . | 78 |
| 5. | Summary of open-loop trajectory planning results . . . . . | 91 |

# DYNAMICS AND CONTROL OF A RIGID/FLEXIBLE MANIPULATOR

## CHAPTER 1. INTRODUCTION

### 1.1. Background and Motivation

The kinematics and dynamics of robot manipulators have been studied extensively. Knowing the desired trajectory of the end effector, one can compute an open-loop control strategy to produce that motion. This is known as the direct dynamic problem. In the design of a manipulator, it is generally assumed that the individual links are rigid bodies, an assumption which is warranted in the great majority of current design applications.

In the future, many robots will be used in the areas which require large, light-weight manipulators such as the space shuttle Remote Manipulator System (RMS)(i.e., a remotely controlled anthropomorphic multi-degree of freedom arm used in construction of a space station for periodic repair, clearing and maintenance of satellites on the orbit) or a robot used in forest industry applications where the manipulator must handle very heavy objects compared to the weight of the manipulator. These robots are usually structurally flexible, reflecting the necessity for their light weight based upon minimum energy consumption and cost, as well as handling of heavy payloads.

For those flexible robots which need to handle such tasks, the residual vibration usually delays subsequent operation because longer settling time is required for the next operation. The requirements of precise motion and short settling time call for an effective mean of end-point vibration control for these manipulators.

Traditionally, by increasing the rigidity of the arm, these residual vibrations can be reduced but at higher costs of material and energy consumption required to accelerate the mechanism. This seems to conflict with the demand for increased productivity. Designing lightweight robot manipulators capable of moving larger payloads without increasing the mass of the linkages is of considerable interest.

Control of a flexible robot manipulator is complex. Without proper control, the vibrations caused by the structural elasticity of the links would not only reduce the operation speed but also reduce the accuracy of control, or even cause instability in some cases [Balas,1978]. Therefore, it is necessary to control the structural vibration in the flexible arm for quick, precise tracking of the trajectories and accomplishment of tasks. These requirements make it necessary to take into consideration the dynamic effects of the distributed link flexibility, since high speed operation leads to high inertial forces which in turn cause vibration and diminish

accuracy.

## 1.2. Literature Review

The main consideration in the flexible manipulator motion control is to enable the manipulator end-point to follow the prescribed path with reasonable accuracy and with acceptably small residual vibration amplitudes. This problem can be solved in several ways. Recently, there have been a number of studies reported concerning this subject.

Generally, the researches can be divided into two groups: 1. those using an open-loop approach and 2. those using a closed-loop approach. The open-loop approach is favored by most researchers because it is simple and easy to implement. The main idea of this approach is pre-scheduling the arm trajectories or driving forces to prevent unnecessary excitation of flexible behavior. A performance index in combination with dynamic programming techniques has typically been used to generate this "optimal" trajectory or driving forces in order to suppress vibration. In this category, authors such as Meckle and Seering [1988] suggested using shaped force inputs constructed from a versine series to generate fast motions with minimum residual vibration on a lumped-parameter, two-degree-of-freedom system. Aspinwall [1980] and Singhose [1990] developed the same shaped force

function by the so-called "vector diagram approach" method and by using a shaped profile with a finite Fourier series expansion. Other researchers such as Serna and Bayo [1990] have proposed "parameter-scheduled trajectory planning" using a cubic-rectangular acceleration profile as a generic input to reduce the vibration problem at the trajectory planning level. The study of Biswas and Klafter [1988] also presented an optimal control scheme (open-loop) for a single-axis, flexible manipulator to achieve a desired angular rotation of the link while simultaneously suppressing structural vibrations.

Other open-loop strategies focus on structural design improvements; that is, selecting materials and shapes with higher stiffness-to-weight ratios and higher damping ratios. Thompson [1984] and Liao [1987] suggested fabricating the moving members of manipulators in fiber reinforced composite materials, which can result in high structural stiffness and strength with low mass. Christian and Seering [1989] proposed some general conclusions and guidelines for constructing a flexible robot by considering different types of link geometry and materials. Constrained viscoelastic layer damping treatment has been explored by Book et al. [1985, 1986], Hastings and Book [1986], and Albert et al. [1990] with considerable success in control of flexible arm manipulators.

In contrast to the open-loop strategies, sensor-based, closed-loop vibration control techniques are being developed to control the flexible robot motions. Generally, flexible robots are inherently very complex in structure. They exhibit strong nonlinear and nonstationary behavior. The implementation of conventional control techniques for rigid robots has led to poor performance when robots are operated at high speeds with varying payloads and when structural compliance is present. Therefore, a sophisticated controller design is necessary to insure acceptable robot performance.

Research in the closed-loop control of flexible manipulators can be divided into two categories. The first uses additional sensors with a state estimator to measure the flexible motion (i.e., assumes all state variables to be available). Researchers, such as Book et at. [1975] and Maizza-Neto [1975] analyzed a two-link planar flexible robot arm and proposed three types of linear feedback controller (namely, independent joint control (IJC), general rigid control (GRC), and flexible feedback control (FFC)) with interesting results. Cannon and Schmitz [1984] also reported a successful application of a control scheme for a one-link flexible arm with direct tip position and motor velocity measurements. Various feedback control strategies on similar, very

flexible manipulators have been published Kanoh and Lee [1985], Fukuda [1985], Gebler [1987], Yuan and Book [1988], and Lee [1989].

Instead of controlling the driving torques or forces in order to reduce the vibrations, the second category employs a micromanipulator along with additional sensors to compensate for both static and dynamic structural deflection. A "straightness servo" was used by Zalucky and Hardt [1984] to suppress the bending deflections with satisfactory results.

## 1.3. Study Objectives

Most of the feedback, feed-forward or adaptive control algorithms discussed above (that account for the flexible dynamics) require sophisticated measuring instruments in order to get the information about the deflections (e.g. by strain gauges or by optical sensors). Usually, high speed computations are necessary with these schemes. This disadvantage makes these control strategies unattractive for real time application using current microprocessor technology.

In this study, the focus is on a high-speed, trajectory control such as the one required for the direct-drive, laser cutting robot. To improve speed of response as well as tracking accuracy, the so-called "two-stage control" (i.e., a trajectory planning stage

plus a trajectory tracking stage) is used. This strategy has been extensively used in robot trajectory control by several researchers (Lee and Chung [1984], Singh and Leu [1987]); yet the applications are still limited to rigid link models. In this paper, the two-stage control is used to control flexible manipulator arms so that the dynamic deformations of the arm links can be reduced efficiently and the tracking error can be minimized.

The strategy is to simulate the controllers currently used in industrial robots and to assess the interrelationships between the robot arm flexibility and the controller design. Instead of using constant feedback gains as most of the researchers have, the gains in this work are time varying and are obtained by either a simple pole-placement method [Jamshidi and Malek-Zavarei, 1986] or by an optimal linear quadratic method [Kirt, 1970, Anderson and Moore, 1990] using only the rigid equivalent model. The convenience of this method results from the fact that no additional sensors are used. A conventional linear controller, based on the rigid body model of the robot, is implemented. Simple measurements are sufficient for controlling the actual flexible system.

The particular robot arm considered in this study is a planar two degree-of-freedom manipulator with an elastic forearm. The system is similar to the one used by Schmitz [1989] for space application and is schematically

illustrated in next chapter.

The remaining chapters of this work are arranged as follows: Chapter 2 mainly deals with the derivation of dynamical equations of the example robot arm. The proposed two-stage control strategy is presented in Chapter 3, along with gain selection methods. Chapter 4 presents digital simulation results based on the proposed control strategies and the results are compared with those using conventional control techniques. Discussions and conclusions are presented in the last chapter.

# CHAPTER 2 SYSTEM DESCRIPTION

## 2.1. Introduction

The first step in improving the performance of a robot is to obtain a reasonably accurate dynamic model. In theory, mechanical flexible systems require an infinite number of elastic modes to completely describe their behavior [Book and Majett,1975], However, in practice they are modeled by finite-dimensional systems. The truncated models expressed in modal form can be obtained using several approaches. Intensive studies for deriving the equations of motion of flexible manipulators were done by researchers. The assumed mode method with Lagrange's equations is the most commonly-used procedure, chosen by Book et al. [1975], Maizza-Neto [1975], Cannon and Schmitz [1984], and Benati and Morro [1988]. Huston and Kelly [1982], Schmitz [1989] and Everett [1989] derived the mathematic model by Kane's Method [Kane,1985]. Other Researchers, such as Thompson [1984], Usoro et al. [1986] and Lee et al. [1987] described the elastic deformation of the flexible manipulator arm by using a finite element approximation.

Recently, general-purpose finite element computer programs have become available for generating the mathematical model for the flexible robotic system (e.g., NASTRAN [Sunada and Dubowsky, 1981]). The assumed modes

method is employed in this study.

## 2.2. Robotic System

In this work, the schematic of the general rigid/flexible robotic arm (RFRA) is shown in Figure 2.1. The arm is made of two links; the first link is assumed to be rigid compared with the second link. Both links are uniform in density and cross section, and when undeformed have lengths $L_1$ and $L_2$, respectively, as shown in Figure 2.1. The flexible forearm is connected to the rigid arm by a frictionless pinned joint and the rigid link is connected to a fixed base with a similar joint. The total mass of the elbow joint is described by lumped mass $m_j$ attached at the end of link 1. The payload and the associated gripper at the end of forearm are modeled by a lumped mass, $m_p$, at the end of the second link. The associated torques of the actuators are designated by $\tau_1$ and $\tau_2$. The system is assumed to have planar motion only. Structural damping and gravity were both neglected.

In order to describe the motion of the RFRA system, the over all motion can be understood as a motion of a corresponding hypothetical rigid robotic arm (HRRA) and a flexible motion of the second link with respect to this moving system. Figure 2.2 shows the HRRA system and its associated coordinates. The base is assumed to be fixed in an inertial reference frame, in which the orthonormal

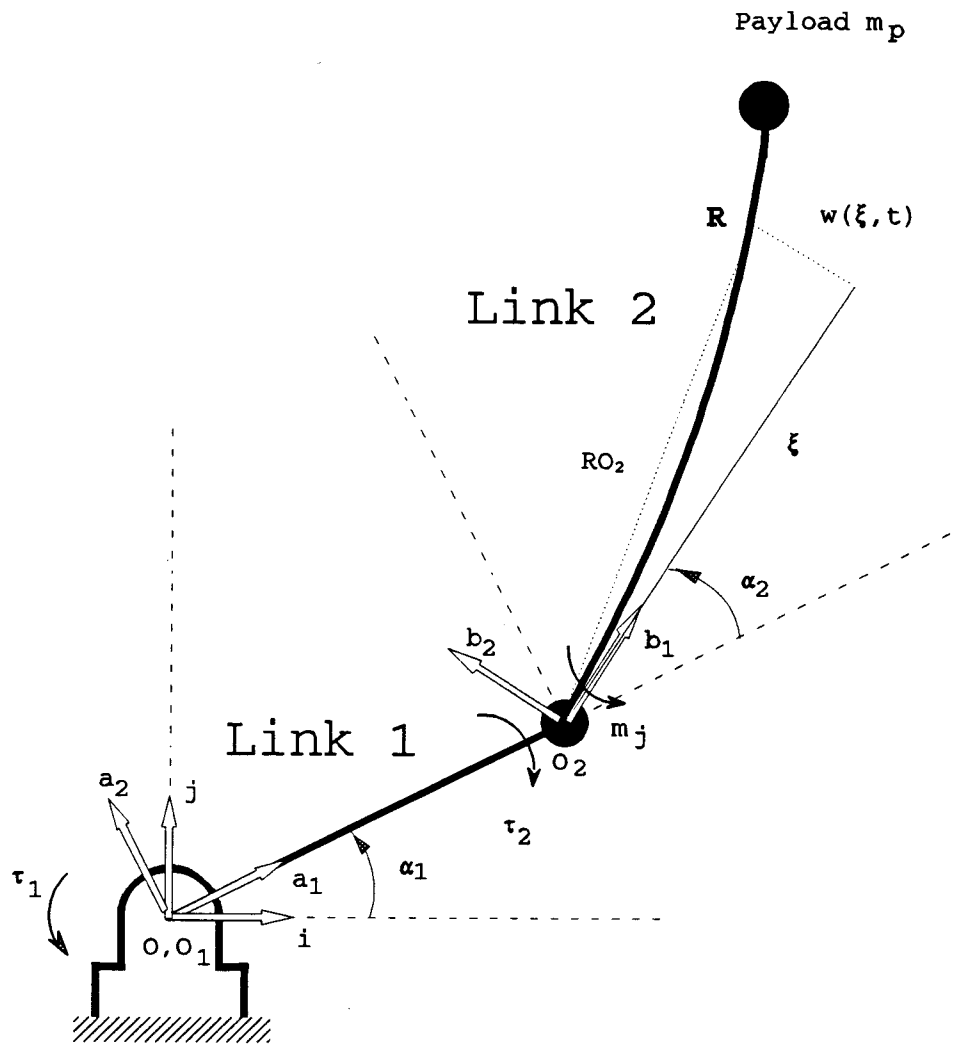


Figure 2.1 Scheme of the RFRA system.

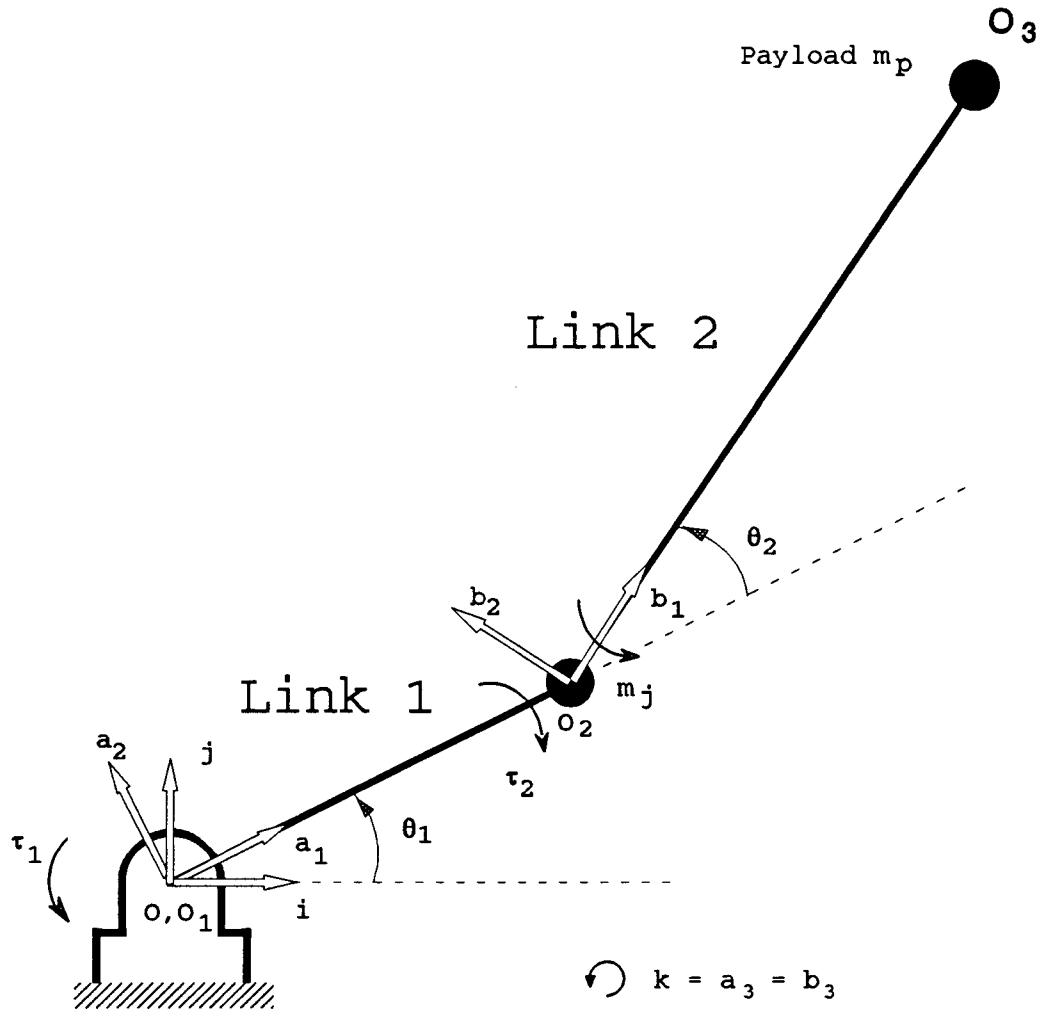


Figure 2.2 Scheme of the HRRA system.

basis $\{\mathbf{i},\mathbf{j},\mathbf{k}\}$ is also fixed. In addition, two orthonormal basis $\{\mathbf{a}_1,\mathbf{a}_2,\mathbf{a}_3\}$ and $\{\mathbf{b}_1,\mathbf{b}_2,\mathbf{b}_3\}$ are fixed to the links 1 and 2, respectively. The first link rotates in the base about $O_1$, and the second link rotates in the first link about point $O_2$. The two joint angles $\theta_1$ and $\theta_2$ are defined by

$$\cos\theta_1 = \mathbf{a}_1 \cdot \mathbf{i}$$

$$\cos\theta_2 = \mathbf{b}_1 \cdot \mathbf{a}_1$$

The configuration of the actual flexible system will be defined to be a variation from that of the HRRA system just described. The variations will consist of joint angles $\alpha_1$ and $\alpha_2$ that may differ from $\theta_1$ and $\theta_2$, together with a bending of the second link. The mathematical models of the HRRA (i.e., Figure 2.2) and the actual RFRA system (i.e., Figure 2.1) will be derived in the following section.

## 2.3. Derivation of Equations of Motion of the HRRA System

The HRRA is an approximate model of the RFRA system by neglecting link bending and represents only rigid body characteristics. Various approaches are available for deriving the equations of motion of a rigid arm manipulator, including Newton-Euler's dynamic formulations [Luh et al., 1980, Craig, 1986], and Lagrange's equations. The equations described by Lagrange are used frequently

because they avoid dealing with constraint forces. However, recent studies have indicated that improvements in computational efficiency can be effected by using Kane's dynamical equation [Kane, 1985] to formulate explicit equation of motion of rigid body robots [Kane,1983].

Because the systems being considered here are not very complex, Lagrange's equations will be used. These equations can be written as

$$\frac{d}{dt}\left(\frac{\partial K}{\partial \dot{\theta}_i}\right) - \frac{\partial K}{\partial \theta_i} + \frac{\partial \Xi}{\partial \theta_i} = \tau_i, \quad i=1,\ldots,n \tag{2.1}$$

where

K = total kinetic energy of the robot arms.

$\Xi$ = total potential energy of the robot arm.

$\theta_i$ = generalized coordinates of the robot arms.

$\dot{\theta}_i$ = first time derivative of the generalized coordinates, $\theta_i$.

$\tau_i$ = generalized forces ( or torques ) applied to the system at joint i to drive link i.

In order to derive the kinetic and potential energy for the HRRA system, the following system parameters have to be defined

$L_1$ = length of link 1.

$L_2$ = length of link 2.

$m_{L1}$ = mass of link 1.

$m_{L2}$ = mass of link 2.

$m_j$ = lumped mass at joint 2.

$m_p$ = mass of the payload.

$\dot{\theta}_1$ = angular velocity in the inertial frame of link 1.

$\dot{\theta}_2$ = angular velocity in link 1 of link 2.

$v_p$ = velocity at the end of link 2.

$v_{ci}$ = velocities of the center of link i. (i=1,2)

$I_{ci}$ = moment inertia of link i r.w.t. its center of mass. (i=1,2)

$J_p$ = moment inertia of payload r.w.t. its center of mass.

The total kinetic energy of the rigid body system can be expressed as

$$K = \frac{1}{2}[m_j L_1^2 + I_{c1} + m_{L1}(\frac{L_1}{2})^2 ]\ \dot{\theta}_1^2 + \frac{1}{2}\ m_p\ V_p^{\ 2} + \frac{1}{2} m_{L2}\ V_{c2}^2 + \frac{1}{2}\ (I_{c2} + J_p)\ (\dot{\theta}_1 + \dot{\theta}_2)^2 \qquad (2.2)$$

Now, with the definitions

$$\omega_1 = \omega_1\ \mathbf{k} = \dot{\theta}_1\ \mathbf{k} \qquad (2.3)$$

$$\omega_2 = \omega_2\ \mathbf{k} = (\dot{\theta}_1+\dot{\theta}_2)\ \mathbf{k} \qquad (2.4)$$

$$s_2 = \sin\theta_2 \qquad (2.5)$$

$$c_2 = \cos\theta_2 \qquad (2.6)$$

the velocities at specific positions can be expressed

$$\boldsymbol{V}_j = L_1 \omega_1 \boldsymbol{a}_2 \tag{2.7}$$

$$\begin{aligned} \boldsymbol{V}_p = \boldsymbol{V}_j + \boldsymbol{\omega}_2 \times L_2 \ (c2\ \boldsymbol{a}_1 + s2\ \boldsymbol{a}_2) \\ - L_2\ \omega_2\ s2\ \boldsymbol{a}_1 + [L_1\ \omega_1 + L_2\ \omega_2\ c2]\ \boldsymbol{b}_2 \end{aligned} \tag{2.8}$$

similarly,

$$\boldsymbol{V}_{c2} = -\frac{1}{2}\ L_2\ \omega_2\ s2\ \boldsymbol{a}_1 + (L_1\ \omega_1 + L_2\ \omega_2\ c2\ )\ \boldsymbol{a}_2 \tag{2.9}$$

Now, with Equations (2.7), (2.8) and (2.9) substituted into Equation (2.2), the expression for kinetic energy K becomes

$$K = N_1\ \dot{\theta}_1^2 + N_2\ (\dot{\theta}_1 + \dot{\theta}_2)^2 + N_3\ \dot{\theta}\ (\dot{\theta}_1 + \dot{\theta}_2\ )\ c2 \tag{2.10}$$

where

$$N_1 = \frac{1}{2}[\,(m_j + m_p + \frac{1}{4}m_{L1} + m_{L2})\ L_1^2 + I_{c1}] \tag{2.11.1}$$

$$N_2 = \frac{1}{2}[\,(m_p + \frac{1}{4}m_{L2})\ L_2^2 + I_{c2} + J_p] \tag{2.11.2}$$

$$N_3 = (m_p + \frac{1}{2}m_{L2})\ L_1\ L_2 \tag{2.11.3}$$

Because the HRRA system is rigid and gravity is neglected,

$$\Xi = 0 \tag{2.12}$$

Substituting the total kinetic energy and potential energy (i.e., Equation (2.10) and (2.12)) into the Lagrange's equations (2.1) leads to the following set of nonlinear, ordinary differential equations

$$\mathbf{u}(t) = \mathbf{M}[\boldsymbol{\theta}(t)]\ddot{\boldsymbol{\theta}}(t) + \mathbf{h}[\boldsymbol{\theta}(t), \dot{\boldsymbol{\theta}}(t)] \tag{2.13}$$

where $\mathbf{M}(\boldsymbol{\theta})$ is a symmetric, 2x2, matrix of inertia coefficients, $\mathbf{h}(\boldsymbol{\theta}, \dot{\boldsymbol{\theta}})$ is a 2x1 matrix of nonlinear components of the coriolis and centrifugal force vector, and $\mathbf{u}(t)$ is an input torque vector.

These matrices are defined as

$$\boldsymbol{M}(\boldsymbol{\theta}) = \begin{bmatrix} M_{11} & M_{12} \\ M_{21} & M_{22} \end{bmatrix} = \begin{bmatrix} 2N_1 + 2N_2 + 2N_3\, c2 & 2N_2 + N_3\, c2 \\ 2N_2 + N_3\, c2 & 2N_2 \end{bmatrix} \tag{2.14.1}$$

$$\boldsymbol{h}(\boldsymbol{\theta}, \dot{\boldsymbol{\theta}}) = \begin{bmatrix} h_1 \\ h_2 \end{bmatrix} = \begin{bmatrix} -N_3\dot{\theta}_2\,(2\dot{\theta}_1 + \dot{\theta}_2)\, s2 \\ N_3\, \dot{\theta}_1^2\, s2 \end{bmatrix} \tag{2.14.2}$$

$$\mathbf{u}(t) = [\tau_1(t), \tau_2(t)]^T \tag{2.14.3}$$

$$\boldsymbol{\theta}(t) = [\theta_1(t), \theta_2(t)]^T \tag{2.14.4}$$

$$\dot{\boldsymbol{\theta}}(t) = [\dot{\theta}_1(t), \dot{\theta}_2(t)]^T \tag{2.14.5}$$

$$\ddot{\boldsymbol{\theta}}(t) = [\ddot{\theta}_1(t), \ddot{\theta}_2(t)]^T \tag{2.14.6}$$

## 2.4. Derivation of Equations of Motion of the RFRA System

Various methods of describing nonrigid, distributed parameter systems have been used by researchers during the past few years. In the section, the derivation follows the method by Neto [1975] and by Book et al. [1975], which is based upon Lagrange's formula and the assumed mode method [Meirovitch,1967].

The following assumptions have been made to simplify the model

(1) The stiffness of the flexible beam in the longitudinal direction is much higher than in the transverse direction, so that only the transverse vibration is considered.
(2) Friction and backlash in the joints are neglected.
(3) Torsional deflection is neglected.
(4) The Euler-Bernoulli model is used for the flexible forearm, for which the rotary inertia and shear deformation effects are neglected.
(5) The resistance of air and internal damping in the beam are negligible.

Based upon the assumed mode method, the deflection $w(\xi,t)$ of the flexible forearm can be written as a linear combination of admissible functions $\phi_i(\xi)$ (i.e., the mode

shapes) multiplied by time-dependent generalized coordinates $z_i(t)$. That is,

$$w(\xi,t) = \sum_{i=1}^{\infty} \phi_i(\xi)\, z_i(t), \quad i=1,\ldots,\infty \tag{2.15}$$

where

$w(\xi,t)$: flexible forearm displacement at $\xi$, $0 \le \xi \le L_2$.

$\phi_i$: admissible functions.

$z_i$: time-dependent modal coordinates.

the admissible functions $\phi_i(\xi)$ will satisfy all the essential boundary conditions.

Assuming that the amplitude of the higher modes of the flexible beam are very small compared to the first ones, the series (i.e., Equation (2.15)) can be truncated after the first two modes (n=2). Then, Equation (2.15) yields

$$w(\xi,t) = \phi_1(\xi) z_1(t) + \phi_2(\xi) z_2(t) \tag{2.16}$$

For numerical analysis of the system, selection of shape functions $\phi_1, \phi_2$ is necessary and may greatly influence the results. The eigenfunctions of a clamp-free beam are the common type of shape functions for discussing the flexible manipulator in many papers [Book et al., 1975, Neto, 1975, Petterson et al, 1990]. The comparison between "clamped-mass" and "pinned-mass" types of

eigenfunctions has been studied by Hastings and Book [1986]. The cubic splines shape function [Smith,1985, Gebler,1985] are proposed in the study, because they yield very good results for many hybrid multi-body system even if only few shape function are used. In addition, they have the advantage of easy differentiation and integration.

The shape functions, in this study, are selected as

$$\phi_1(\xi) = (\frac{\xi}{L_2})^2 \qquad (2.17.1)$$

$$\phi_2(\xi) = (\frac{\xi}{L_2})^3 \qquad (2.17.2)$$

From Figure 2.1, let point **R** be an arbitrary point along the flexible forearm, and $\mathbf{RO}_2$ is the associated position vector from point $\mathbf{O}_2$ to point **R**. Then,

$$RO_2(\xi,t) = [\xi - \frac{1}{2}\int_0^{\xi} (\frac{\partial w}{\partial \xi})^2 d\xi]\, b_1 + w(\xi,t)\, b_2 \qquad (2.18)$$

If the deflection is assumed to be small (i.e., $w(\xi,t) \leq 0.1\ L_2$) and any extension is neglected [Lee and Castelazo, 1987], then Equation (2.18) can be rewritten as

$$\mathbf{RO}_2(\xi,t) = \xi \mathbf{b}_1 + w(\xi,t)\mathbf{b}_2 \qquad (2.19)$$

Now, the respective velocity of the point R is given by

$$V_R = \frac{d\,RO_2}{dt} = -L_1\dot{\alpha}_1 S_1 i + L_1\dot{\alpha}_1 C_1 j - w(\dot{\alpha}_1 + \dot{\alpha}_2)b_1 + [\xi(\dot{\alpha}_1 + \dot{\alpha}_2) + \frac{\partial w}{\partial t}]b_2 \qquad (2.20)$$

where

$$S_1 = \sin \alpha_1 \qquad (2.21.1)$$

$$C_1 = \cos \alpha_2 \qquad (2.21.2)$$

Now, if we defined

$$S_{12} = \sin(\alpha_1+\alpha_2) \qquad (2.22.1)$$

$$C_{12} = \cos(\alpha_1+\alpha_2) \qquad (2.22.2)$$

Then, $\mathbf{b}_1$ and $\mathbf{b}_2$ in equation (2.20) can be further expressed as:

$$\mathbf{b}_1 = C_{12}\mathbf{i} + S_{12}\mathbf{j} \qquad (2.23.1)$$

$$\mathbf{b}_2 = -S_{12}\mathbf{i} + C_{12}\mathbf{j} \qquad (2.23.2)$$

Substituting equations (2.23.1) and (2.23.2) into equation (2.20), the velocity of point R can be expressed as

$$V_R = -[L_1 S_1 \dot{\alpha}_1 + \xi S_{12}(\dot{\alpha}_1+\dot{\alpha}_2) + S_{12} W_t + w C_{12}(\dot{\alpha}_1+\dot{\alpha}_2)]i + [L_1 C_1 \dot{\alpha}_1 + \xi C_{12}(\dot{\alpha}_1+\dot{\alpha}_2) + C_{12} W_t - w S_{12}(\dot{\alpha}_1+\dot{\alpha}_2)]j \qquad (2.24)$$

Neglecting the rotary inertia, the total kinetic energy of the flexible system can be expressed as

$$K = \frac{1}{2}[m_j L_1^2 + I_{cl} + m_{Ll}(\frac{L_1}{2})^2]\dot{\alpha}_1^2 + \frac{1}{2}m_p V_p^2 + \frac{1}{2}\int_0^{L_2} \mu V_R^2 d\xi + \frac{1}{2}J_p(\dot{w}_E')^2 \tag{2.25}$$

where $\mu$ is the lineal mass per unit length of the flexible beam, $V_p$ is the velocity at the end-of-forearm, and $w_E$ is the deflection at the endpoint of second link. Also,

$$\dot{w}=\frac{\partial w}{\partial t} \quad , \quad w'=\frac{\partial w}{\partial \xi} \quad , \quad w''=\frac{\partial^2 w}{\partial \xi^2} \quad , \quad w_E'=\frac{\partial w}{\partial \xi}\Big|_{\xi=L_2}$$

Neglecting shear deformation, the potential energy of the RFRA is

$$\Xi = \frac{1}{2}\int_0^{L_2} EI_z(w'')^2 d\xi \tag{2.26}$$

By substituting the modal expansion (i.e., Equation 2.17) into the potential and kinetic energy equations (i.e., Equation (2.25) and Equation (2.26)) and performing the integrations with the assumption that the links are uniform, the total kinetic energy and the potential energy become

$$K = N_1\dot{\alpha}_1^2 + nw_1\dot{z}_1^2 + nw_2\dot{z}_1\dot{z}_2 + nw_3\dot{z}_2^2 + (nw_4\dot{z}_1 + nw_5\dot{z}_2)(\dot{\alpha}_1+\dot{\alpha}_2)$$

$$+ [N_3C_2 - S_2(nw_6 z_1 + nw_7 z_2)]\dot{\alpha}_1(\dot{\alpha}_1+\dot{\alpha}_2) + (nw_6\dot{z}_1 + nw_7\dot{z}_2)C_2\dot{\alpha}_1$$

$$+ [N_2 + nw_8(z_1+z_2)^2](\dot{\alpha}_1+\dot{\alpha}_2)^2 \qquad (2.27)$$

$$\Xi = nw_9 z_1^2 + nw_{10} z_1 z_2 + nw_{11} z_2^2 \qquad (2.28)$$

where

$$nw_1 = \frac{1}{10}\mu L_2 + \frac{1}{2}m_p + 2\frac{J_p}{L_2^2} \qquad (2.29.1)$$

$$nw_2 = \frac{1}{6}\mu L_2 + m_p + 6\frac{J_p}{L_2^2} \qquad (2.29.2)$$

$$nw_3 = \frac{1}{14}\mu L_2 + \frac{1}{2}m_p + \frac{9}{2}\frac{J_p}{L_2^2} \qquad (2.29.3)$$

$$nw_4 = \frac{1}{4}\mu L_2^2 + m_p L_2 + 2\frac{J_p}{L_2} \qquad (2.29.4)$$

$$nw_5 = \frac{1}{5}\mu L_2^2 + m_p L_2 + 3\frac{J_p}{L_2} \qquad (2.29.5)$$

$$nw_6 = \frac{1}{3}\mu L_1 L_2 + m_p L_1 \qquad (2.29.6)$$

$$nw_7 = \frac{1}{4}\mu L_1 L_2 + m_p L_1 \qquad (2.29.7)$$

$$nw_8 = \frac{1}{2}m_p \qquad (2.29.8)$$

$$nw_9 = 2\frac{EI_Z}{L_2^3} \qquad (2.29.9)$$

$$nw_{10} = 6\frac{EI_z}{L_2^3} \tag{2.29.10}$$

$$nw_{11} = 6\frac{EI_z}{L_2^3} \tag{2.29.11}$$

Again, Lagrange's equations (i.e., Equation (2.1)) yield a set of nonlinear differential equations

$$M_{11}\ddot{\alpha}_1 + M_{12}\ddot{\alpha}_2 + M_{13}\ddot{z}_1 + M_{14}\ddot{z}_2 = -f_1 + \tau_1 \tag{2.30.1}$$

$$M_{21}\ddot{\alpha}_1 + M_{22}\ddot{\alpha}_2 + M_{23}\ddot{z}_1 + M_{24}\ddot{z}_2 = -f_2 + \tau_2 \tag{2.30.2}$$

$$M_{31}\ddot{\alpha}_1 + M_{32}\ddot{\alpha}_2 + M_{33}\ddot{z}_1 + M_{34}\ddot{z}_2 = -f_3 - 2\,nw_9 z_1 - nw_{10} z_2 \tag{2.30.3}$$

$$M_{41}\ddot{\alpha}_1 + M_{42}\ddot{\alpha}_2 + M_{43}\ddot{z}_1 + M_{44}\ddot{z}_2 = -f_4 - nw_{10} z_1 - 2\,nw_{11} z_2 \tag{2.30.4}$$

where the coefficients are given by

$$M_{11} = 2[N_1 + N_2 + N_3 C_2 - S_2(nw_6 z_1 + nw_7 z_2) + nw_8 (z_1+z_2)^2] \tag{2.31.1}$$

$$M_{12} = 2N_2 + N_3 C_2 - S_2(nw_6 z_1 + nw_7 z_2) + 2\,nw_8 (z_1+z_2)^2 \tag{2.31.2}$$

$$M_{13} = nw_4 + C_2\, nw_6 \tag{2.31.3}$$

$$M_{14} = nw_5 + C_2\, nw_7 \tag{2.31.4}$$

$$M_{21} = M_{12} \tag{2.31.5}$$

$$M_{22} = 2N_2 + 2\,nw_8 (z_1+z_2)^2 \tag{2.31.6}$$

$$M_{23} = nw_2 \tag{2.31.7}$$

$$M_{24} = nw_5 \tag{2.31.8}$$

$$M_{31} = M_{13} \tag{2.31.9}$$

$$M_{32} = M_{23} \tag{2.31.10}$$

$$M_{33} = 2\ nw_1 \tag{2.31.11}$$

$$M_{34} = nw_2 \tag{2.31.12}$$

$$M_{41} = M_{14} \tag{2.31.13}$$

$$M_{42} = M_{24} \tag{2.31.14}$$

$$M_{43} = M_{34} \tag{2.31.15}$$

$$M_{44} = 2\ nw_3 \tag{2.31.16}$$

and the nonlinear functions are

$$\begin{aligned} f_1 = {} & -N_3 S_2 \dot{\alpha}_2 (2\dot{\alpha}_1+\dot{\alpha}_2) - S_2 (2\dot{\alpha}_1+\dot{\alpha}_2)(nw_6 \dot{z}_1+nw_7 \dot{z}_2) \\ & -C_2 \dot{\alpha}_2 (2\dot{\alpha}_1+\dot{\alpha}_2)(nw_6 z_1+nw_7 z_2) - S_2 \dot{\alpha}_2 (nw_6 \dot{z}_1+nw_7 \dot{z}_2) \\ & +4\, nw_8 (\dot{\alpha}_1+\dot{\alpha}_2)(z_1+z_2)(\dot{z}_1+\dot{z}_2) \end{aligned} \tag{2.32.1}$$

$$\begin{aligned} f_2 = {} & N_3 S_2 \dot{\alpha}_1^2 + C_2 \dot{\alpha}_1^2 (nw_6 z_1+nw_7 z_2) \\ & +4\, nw_8 (\dot{\alpha}_1+\dot{\alpha}_2)(z_1+z_2)(\dot{z}_1+\dot{z}_2) \end{aligned} \tag{2.32.2}$$

$$f_3 = nw_6 S_2 \dot{\alpha}_1^2 - 2\, nw_8 (\dot{\alpha}_1+\dot{\alpha}_2)^2 (z_1+z_2) \tag{2.32.3}$$

$$f_4 = nw_7 S_2 \dot{\alpha}_1^2 - 2\, nw_8 (\dot{\alpha}_1+\dot{\alpha}_2)^2 (z_1+z_2) \tag{2.32.4}$$

Finally, the resulting dynamic equations of motion for the rigid/flexible manipulator system RFRA can be expressed in the following general matrix form

$$\boldsymbol{A}\,\ddot{\boldsymbol{y}} = \boldsymbol{B}\,\boldsymbol{y} + \boldsymbol{f} + \boldsymbol{C}\,\boldsymbol{u} \tag{2.34}$$

where

$$\boldsymbol{A} = [M_{ij}]\ , \quad i,j = 1,\ldots,4 \tag{2.35.1}$$

$$\boldsymbol{B} = \begin{bmatrix} 0 & 0 & 0 & 0 \\ 0 & 0 & 0 & 0 \\ 0 & 0 & -2\,nw_9 & -nw_{10} \\ 0 & 0 & -nw_{10} & -2\,nw_{11} \end{bmatrix} \tag{2.35.2}$$

$$\boldsymbol{f} = -[f_1\ f_2\ f_3\ f_4]^T \tag{2.35.3}$$

$$\boldsymbol{C} = \begin{bmatrix} 1 & 0 & 0 & 0 \\ 0 & 1 & 0 & 0 \end{bmatrix}^T \tag{2.35.4}$$

$$\boldsymbol{u} = [\tau_1\ \tau_2]^T \tag{2.35.5}$$

$$\boldsymbol{y} = [\alpha_1\ \alpha_2\ z_1\ z_2]^T \tag{2.35.6}$$

## 2.5. Linearized Equations of Motion of HRRA

It can be seen from Equation (2.13), that the equations of motion are highly nonlinear. The design of a feedback controller for this nonlinear system is not easy,

past efforts resulting in very complex designs, as mentioned in the previous chapter. In this work, a motion controller based on a linearized version of the hypothetical rigid body model is proposed to control the flexible manipulator.

The linearized model of Equation (2.13) is derived as follows:

Suppose that the nominal trajectory $\theta^*(t)$ of the nonlinear system is known from the trajectory planning, and the corresponding nominal torques $\mathbf{u}^*(t)$ are also given. Then, both $\theta^*(t)$ and $\mathbf{u}^*(t)$ will satisfy Equation (2.13):

$$\mathbf{u}^*(t) = \mathbf{M}[\theta^*(t)]\ddot{\theta}^*(t) + \mathbf{h}[\theta^*(t), \theta^*(t)] \tag{2.36}$$

Using the Taylor series expansion of Equation (2.13) about the nominal trajectory, and assuming that only the small perturbations are significant (the case most frequently encountered in industrial applications) so that the terms of second and higher power may be neglected. we obtain

$$\begin{aligned} &M(\theta^*)+[\frac{\partial M(\theta)}{\partial \theta}\delta\theta]\ddot{\theta}+M(\theta^*)\delta\ddot{\theta}+h(\theta^*,\dot{\theta}^*)+\frac{\partial h(\theta^*,\dot{\theta}^*)}{\partial \theta}\delta\theta \\ &+\frac{\partial h(\theta^*,\dot{\theta}^*)}{\partial \dot{\theta}}\delta\dot{\theta} = u^*(t)+\Gamma(t) \end{aligned} \tag{2.37}$$

where $\delta\theta(t)=\theta(t)-\theta^*(t)$ is a small deviation of the generalized coordinates from the nominal trajectory, $\Gamma(t)=u(t)-u^*(t)$ is the variation of the vector of driving torques from $u^*(t)$.

Subtracting Equation (2.36) from Equation (2.37) results in a set of linear differential equations with time dependent system parameters.

$$M(\theta^*)\,\delta\ddot{\theta} + P(\theta^*,\dot{\theta}^*)\,\delta\dot{\theta} + Q(\theta^*,\dot{\theta}^*,\ddot{\theta}^*)\,\delta\theta = \Gamma(t) \qquad (2.38)$$

P and Q are matrices of the linearized system given by

$$P(\theta^*,\dot{\theta}^*) = \frac{\partial h(\theta^*,\dot{\theta}^*)}{\partial\dot{\theta}} \qquad (2.39.1)$$

$$Q(\theta^*,\dot{\theta}^*,\ddot{\theta}^*) = \frac{\partial M(\dot{\theta}^*)}{\partial\theta}\ddot{\theta}^* + \frac{\partial h(\theta^*,\dot{\theta}^*)}{\partial\theta} \qquad (2.39.2)$$

where now

$$M_{11} = 2N_1+2N_2+2N_3\,c\theta_2^* \qquad (2.40.1)$$

$$M_{12} = 2N_2 + N_3\,c\theta_2^* \qquad (2.40.2)$$

$$M_{21} = M_{12} \qquad (2.40.3)$$

$$M_{22} = 2N_2 \qquad (2.40.4)$$

$$P_{11} = 0 \qquad (2.40.5)$$

$$P_{12} = -N_3[(2\ddot{\theta}_1^* + \ddot{\theta}_2^*)s\theta_2^* + \dot{\theta}_2^*(2\dot{\theta}_1^* + \dot{\theta}_2^*)c\theta_2^*] \quad (2.40.6)$$

$$P_{21} = 0 \quad (2.40.7)$$

$$P_{22} = -N_3[\ddot{\theta}_2^* - (\dot{\theta}_1^*)^2 c\theta_2^*] \quad (2.40.8)$$

$$Q_{11} = -2N_3\dot{\theta}_2^* s\theta_2^* \quad (2.40.9)$$

$$Q_{12} = -2N_3(\dot{\theta}_1^* + \dot{\theta}_2^*)s\theta_2^* \quad (2.40.10)$$

$$Q_{21} = 2N_3\dot{\theta}_1^* s\theta_2^* \quad (2.40.11)$$

$$Q_{22} = 0 \quad (2.40.12)$$

$$c\theta_2^* = \cos\theta_2^* \quad (2.40.13)$$

$$s\theta_2^* = \sin\theta_2^* \quad (2.40.14)$$

With the state vector $\mathbf{x}$ defined as, $\mathbf{x}=(\delta\theta_1, \delta\theta_2, \delta\dot{\theta}_1, \delta\dot{\theta}_2)^T$, the resulting linearized equation of the hypothetical rigid two-link manipulator can be written as

$$\dot{\boldsymbol{x}}(t) = \boldsymbol{F}(t)\boldsymbol{x}(t) + \boldsymbol{G}(t)\boldsymbol{\Gamma}(t) \ , \ \boldsymbol{x}(0) \ \textit{is given} \quad (2.41)$$

where **F**(t) and **G**(t) denote the 4x4 and 4x2 Jacobian matrices defined, respectively by

$$F(t) = - \begin{bmatrix} 0_{2\times2} & I_{2\times2} \\ M^{-1}P_{2\times2} & -M^{-1}Q_{2\times2} \end{bmatrix}_{4\times4} \tag{2.42.1}$$

$$G = \begin{bmatrix} 0_{2\times2} \\ M^{-1}_{2\times2} \end{bmatrix}_{4\times2} \tag{2.42.2}$$

This system (i.e., Equation (2.41)) represents a set of first-order linear time-varying equations in the perturbations, where the matrices F(t) and G(t) are functions of time. They depend on the instantaneous manipulator position and velocity along the nominal trajectory. Because of the complexity of the manipulator equations of motion, it is convenient to develop a computer-oriented algorithm for constructing the linearized model of the robotic system. Such an approache was given by Vukobratović [1982].

# CHAPTER 3: CONTROL

## 3.1. Introduction

This chapter focuses on the control strategies which were applied to the analysis of controlling flexible manipulators. Several proposed methods will be reviewed in this section. These include the conventional control techniques and the proposed two-stage control in this research. The initial assumptions made in this study for control of the flexible manipulator are that the available actuators are direct-drive motors, with no reducers used between motors and the links. Moreover, all the parameters of the robot, e.g. the payload, can be identified with satisfactory accuracy. Only if this is possible is the use of such a control strategy meaningful.

## 3.2. Conventional Control Strategies

The conventional FFC (Flexible Feedback Control) methods [Book et al, 1975] of controlling a flexible manipulator are as shown in Figure 3.1. In this method, one proceeds exactly in the same way as for the rigid body case, except using a mathematical model which accounts for derivations caused by elastic properties of the arm. Generally, the close-loop feedback control requires additional measurements from the deformation (e.g. by strain gauges or by optical sensors) to improve the

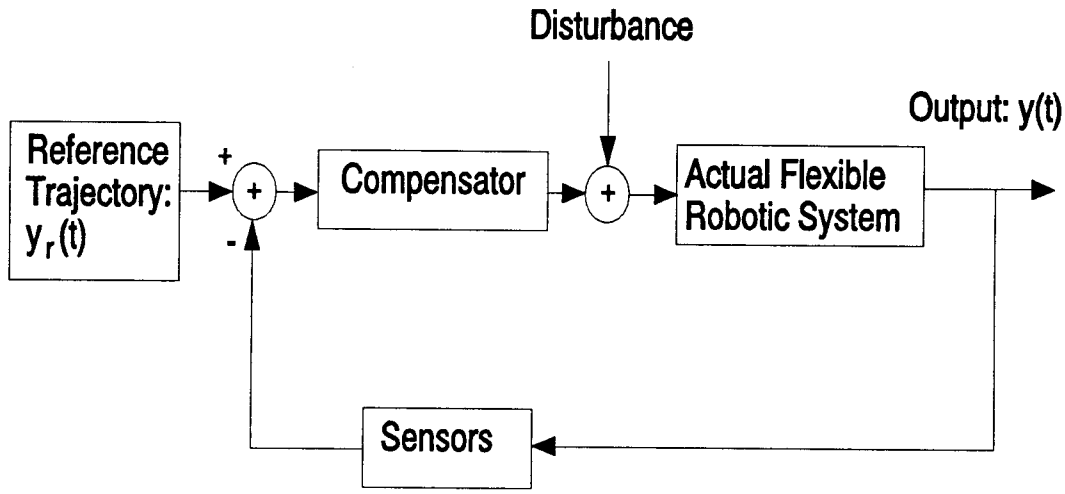


Figure 3.1 Conventional FFC (Flexible Feedback Control) method.

performance of the control and to compensate for the vibrations associated with the flexibilities. This conventional control scheme is costly because it is complicated by the presence of the highly nonlinear terms in Equation (2.34). Even in the case for which the control law can be exactly specified, it would be useful only in very specific cases. This is mainly due to the lack of sensors which are required to measure the entire state with reasonable speed and precision and which are yet robust and cheap enough. Our aim in solving the problem considered above is to avoid the complicated type of design and synthesize as simple a control as possible. In order to reach this goal, a two-stage control method which involves feedforward and feedback control is proposed in this study. This method, in many cases, is quite similar to the control of the rigid body case. This strategy uses only state variables of the hypothetical rigid body for designing feedback controller of the flexible robot. No additional measurements are necessary to control the flexible robot and the control structure can be greatly simplified.

## 3.3. Two-Stage Control Method

The proposed control strategy for the RFRA system can be divided into two stages: 1. Feedforward control with off-line trajectory planning, and 2. Feedback control with

on-line trajectory tracking.

### 3.3.1. Feedforward Control Stage

Figure 3.2 shows the feedforward control scheme of a RFRA system. The intent of the feedforward control is to pre-schedule the nominal control torques $\mathbf{u}^*(t)$ (or forces) to minimize the motion-induced vibrations in the actual RFRA system, while simultaneously achieve a desired tracking accuracy. An optimal control technique with a selected performance index J are typically used to generate this "optimal" input torques u*(t). Generally, the performance index consists of functions of the joint position and joint velocity errors at the final time and the integral of the transverse vibration along the motions.

Mathematically, the problem of feedforward control of a flexible robot can be stated in an optimization fashion as follows:

Finding the optimal control $\mathbf{u}^*(t)$ that causes the flexible robot to follow desired trajectory, $\theta^*(t)$, $\dot{\theta}^*(t)$ and $\ddot{\theta}^*(t)$, such that the performance index,

$$J(u(t)) = \bar{\varphi}[\alpha(t_f), \dot{\alpha}(t_f), z(t_f), \dot{z}(t_f), t_f] + \int_0^{t_f} \bar{L}[\alpha(t), \dot{\alpha}(t), z(t), \dot{z}(t), u(t), t]dt \tag{3.1}$$

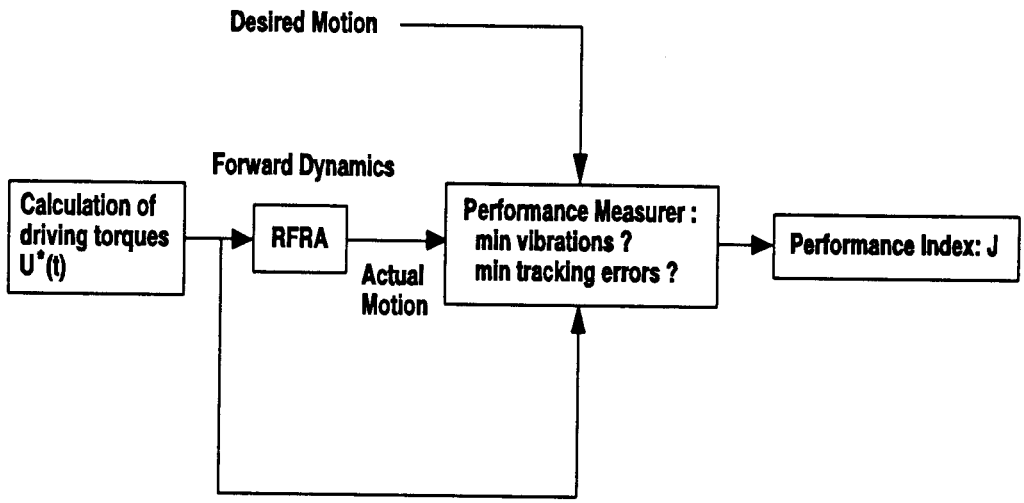


Figure 3.2 Feedforward control scheme of a RFRA system.

is minimized, where $\alpha_1$, $\alpha_2$, $z_1$, $z_2$ are generalized coordinates of the RFRA system, and $\bar{\varphi}$ and $\bar{L}$ are selected functions of these arguments. When faced with such an optimal control problem, it is typical to apply a variational method to solve the problem [Kirt, 1970]. The method can be simply described as follows: with the state variables $\mathbf{q}$ defined as

$$\boldsymbol{q} = \begin{bmatrix} q_1 \\ q_2 \\ q_3 \\ q_4 \\ q_5 \\ q_6 \\ q_7 \\ q_8 \end{bmatrix} = \begin{bmatrix} \alpha_1 \\ \alpha_2 \\ z_1 \\ z_2 \\ \dot{\alpha}_1 \\ \dot{\alpha}_2 \\ \dot{z}_1 \\ \dot{z}_2 \end{bmatrix} \tag{3.2}$$

the nonlinear dynamic equation of the RFRA system (Equation (2.34)) becomes

$$\dot{\boldsymbol{q}}(t) = \boldsymbol{a}\,[\boldsymbol{q}(t), \boldsymbol{u}(t), t] \tag{3.3}$$

By substituting Equation (3.3) into Equation (3.1), the associated performance index in Equation (3.1) can be rewritten as

$$J(u) = \bar{\varphi}[q(t_f), t_f] + \int_0^{t_f} \bar{L}[q(t), u(t), t]\, dt \qquad (3.4)$$

By introducing the Lagrange multiplier $\lambda(t)$ and adjoining Equation (3.3) to Equation (3.4), we obtain

$$J(u) = \bar{\varphi}[q(t_f), t_f] + \int_0^{t_f} \{\bar{L}[q(t), u(t), t] + \lambda^T(t)\{a[q(t), u(t), t] - \dot{q}(t)\}\}dt \qquad (3.5)$$

For convenience, a scalar function H, called the Hamiltonian, is defined as follows:

$$H[q(t), u(t), \lambda(t), t] = \bar{L}[q(t), u(t), t] + \lambda^T(t)\, a[q(t), u(t), t] \qquad (3.6)$$

The variational method leads to the necessary conditions for minimizing the performance index J subjected to the motion constraint given by Equation (3.3).

This can be written as follows [Kirt,1964, Bryson and Ho, 1981]:

$$\dot{q}(t) = \frac{\partial H}{\partial \lambda}[q(t), u(t), \lambda(t), t] \tag{3.7}$$

$$\dot{\lambda}(t) = -\frac{\partial H}{\partial q}[q(t), u(t), \lambda(t), t] \tag{3.8}$$

$$0 = \frac{\partial H}{\partial u}[q(t), u(t), \lambda(t), t] \tag{3.9}$$

with boundary conditions (assuming that the final time and final states are not fixed)

$$q(t_0) = q_0 \tag{3.10}$$

$$\frac{\partial \bar{\varphi}}{\partial q}[q(t_f), t_f] - \lambda(t_f) = o \tag{3.11}$$

$$H[q(t_f), u(t_f), \lambda(t_f), t_f] + \frac{\partial \bar{\varphi}}{\partial t}[q(t_f), t_f] = 0 \tag{3.12}$$

Analytic solution for the optimal control torques is difficult because of the highly non-linear, time-varying differential equations (3.7)-(3.12). Generally, numerical integration can be applied to solve this problem [Kirt, 1970]. Unfortunately, there is another factor that prevents us from simply solving the nonlinear different equation by numerical integration - <u>the boundary conditions for Equation (3.10), (3.11) and (3.12) are split;</u> i.e., some are given for $t=t_0$, and others are given for $t=t_f$. Such problems are called two-point boundary-value problems (TPBVP). The problem is rather difficult to solve because of the combination of split boundary values and the nonlinearity of the differential equation. Numerical procedures for solving TPBVP's exist but are still difficult even with a high-speed computer.

In order to solve the previous optimal control problem without solving the complicate TPBVP problem, the trajectory planning approach [Nagurka and Yen, 1987, and Yen and Nagurka, 1988] is proposed:

By substituting the equation of motion for the HRRA

$$\mathbf{u}(t) = \mathbf{M}[\boldsymbol{\theta}(t)]\ddot{\boldsymbol{\theta}}(t) + \mathbf{h}[\boldsymbol{\theta}(t), \dot{\boldsymbol{\theta}}(t)] \tag{2.13}$$

into Equation (3.1), the performance index J becomes

$$\begin{aligned} & J[\boldsymbol{\theta}(t), \dot{\boldsymbol{\theta}}(t), \ddot{\boldsymbol{\theta}}(t)] \\ & = \varphi[\boldsymbol{\theta}(t_f), \dot{\boldsymbol{\theta}}(t_f), \ddot{\boldsymbol{\theta}}(t_f), \boldsymbol{\alpha}(t_f), \dot{\boldsymbol{\alpha}}(t_f), \ddot{\boldsymbol{\alpha}}(t_f), \boldsymbol{z}(t_f), \dot{\boldsymbol{z}}(t_f), \ddot{\boldsymbol{z}}(t_f), t_f] \\ & + \int_0^{t_f} L[\boldsymbol{\theta}(t), \dot{\boldsymbol{\theta}}(t), \ddot{\boldsymbol{\theta}}(t), \boldsymbol{\alpha}(t), \dot{\boldsymbol{\alpha}}(t), \ddot{\boldsymbol{\alpha}}(t), \boldsymbol{z}(t), \dot{\boldsymbol{z}}(t), \ddot{\boldsymbol{z}}(t), t] dt \end{aligned} \tag{3.13}$$

Now, the open-loop optimal control problem of choosing an optimal control input $\mathbf{u}^*(t)$ to minimize the performance index J (Equation (3.1)) is converted to a trajectory planning problem of choosing the optimal joint displacement $\boldsymbol{\theta}^*(t)$ from the simplified HRRA model. The off-line trajectory planning procedure is outlined in Figure 3.3.

3.3.1.1. Off-line motion trajectory planning

Trajectory planning has been used in controlling manipulators for purposes of minimum traveling time [Luh and Lin, 1981, Bobrow et al., 1985, Shin and Mckay, 1985a, 1985b, 1986, Geering et al., 1986], minimum energy cost

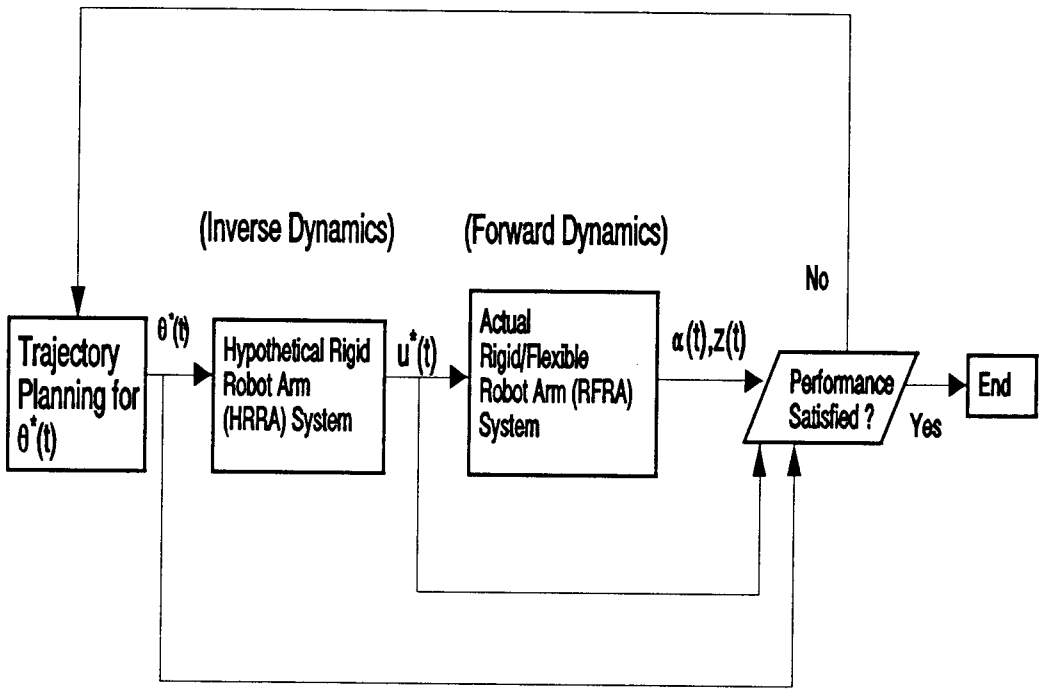


Figure 3.3 Off-line trajectory planning for the RFRA System.

[Schmitt et al., 1985] or some other criterion [Pfeiffer and Johanni, 1986] depending on the form of performance index used. Based on the reports made by Vukobratović [1982], Nagurka and Yen [1987], and Yen and Nagurka [1988], it can also be used to simplify the controller design for rigid manipulators. This study extends the concept to the control of flexible manipulators. The basic concept is a pre-selected "optimal" nominal trajectory based on the simplified HRRA system and minimization of criterion J (Eq.(3.1)). The corresponding nominal control of the "optimal" nominal trajectory are then fed to drive the actual RFRA system. By such an approach, the behaviour of the simplified HRRA is expected to be very "close" to the behaviour of the real RFRA system around the "optimal" nominal trajectory. Thus, at the second stage, a simpler feedback controller based on the simplified HRRA system is more adequate when applied to the actual RFRA system. The performance index J in this stage is selected to control and position the actual flexible manipulator quickly and precisely without large beam vibration during and after moving a robotic arm from one given station to another station (Figure 3.4).

The general Raleigh-Ritz approximation method [Reddy,1985] is then incorporated with a parameter-optimization method in this research because it is very efficient and easy to program.

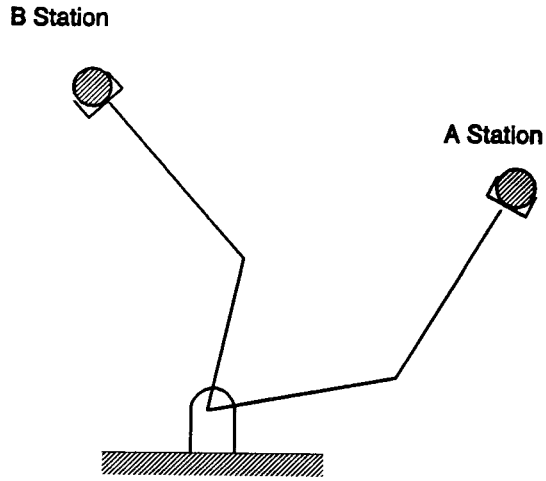


Figure 3.4 Configurations of a two-link robot in stations A and B.

3.3.1.2. Rayleigh-Ritz method

The essential basis of this method is the substitution of an approximation in place of the true optimal trajectory, and can be described as follows:

Let the set of functions $\{\eta_1, \eta_2, \ldots\}$ be continuous and differentiable in the region of $[t_0, t_f]$, and assume that the joint function $\theta_i(t)$ can be expressed as a linear combination of the $\eta_i$'s, valid in the region $[t_0, t_f]$; that is,

$$\theta_i(t) = \sum_{j=1}^{\infty} C_{ij}\, \eta_j(t) \quad ,i=1,..,n, \quad t_0 \le t \le t_f \tag{3.14}$$

where the $C_{ij}$ are constants call Ritz coefficients.

If the expansion expressed by Equation (3.14) is

possible for joint functions $\eta_i(t)$, then the $\eta$'s are termed a complete set in the region $[t_0, t_f]$. Suppose $\theta_i(t)$ is approximated by a subset of the complete set (i.e., Equation (3.14) is truncated to include only a finite number of terms). Then the approximate solution of the joint displacement can be expressed as

$$\theta_i(t) \approx \sum_{j=1}^{k} C_{ij}\, \eta_j(t) \quad ,i=1,..,n, \quad t_0 \le t \le t_f \tag{3.15}$$

this approximate solution (3.15) is expected to converge to the actual solution as $k \to \infty$.

Because of the nonhomogeneous boundary conditions in most of the robotic applications, the Ritz approximation in Equation (3.15) can be modified in the alternative form

$$\theta_i(t) \approx \sum_{j=1}^{k} C_{ij}\, \eta_j(t) + \kappa_{i0}(t) \qquad i=1,\ldots,n, \quad t_0 \le t \le t_f \tag{3.16}$$

where $\kappa_{i0}$ are the functions which satisfy the joint initial and final conditions. i.e.,

$$\begin{aligned} \kappa_{i0}(t_0) &= \theta_i(t_0) \ , \ \kappa_{i0}(t_f) = \theta_i(t_f) \\ \dot{\kappa}_{i0}(t_0) &= \dot{\theta}_i(t_0) \ , \ \dot{\kappa}_{i0}(t_f) = \dot{\theta}_i(t_f) \\ \ddot{\kappa}_{i0}(t_0) &= \ddot{\theta}_i(t_0) \ , \ \ddot{\kappa}_{i0}(t_f) = \ddot{\theta}_i(t_f) \end{aligned} \tag{3.17}$$

Thus, in order for $\theta_i(t)$ to satisfy the boundary conditions, $\eta_j(t)$ and their first two derivatives must be zero at t=0 and $t=t_f$:

$$\eta_j(t_0)=\eta_j(t_f)=0,\ \dot{\eta}_j(t_0)=\dot{\eta}_j(t_f)=0,\ \ddot{\eta}_j(t_0)=\ddot{\eta}_j(t_f)=0 \qquad (3.18)$$

There are several classes of functions that meet this requirement, including power series, Bessel series, Legendre polynomials, and trigonometric functions with increasing harmonic terms [Reddy, 1986]. Although the choice of $\eta_i$ and $\kappa_{i0}$ are arbitrary, one choice of functions might give better accuracy over others, or be computationally more efficient than others. Two approximations proposed by Schmitt et al. [1986] and Nagurka and Yen [1987] will be used for comparison in controlling structural vibration in the flexible link, and the result is discussed in detail in chapter 4.

Once the complete set $\{\eta_j\}$ and $\kappa_{i0}$ are chosen, the trajectory planning is greatly simplified by use of Raleigh-Ritz approximation.

Now,

$$\begin{aligned}\tau_1 &= \tau_1(\theta_1,\ldots,\theta_n,\dot{\theta}_1,\ldots,\dot{\theta}_n,\ddot{\theta}_1,\ldots,\ddot{\theta}_n)\\ &\vdots\\ \tau_n &= \tau_n(\theta_1,\ldots,\theta_n,\dot{\theta}_1,\ldots,\dot{\theta}_n,\ddot{\theta}_1,\ldots,\ddot{\theta}_n)\end{aligned} \qquad (3.19)$$

and

$$\begin{aligned}\theta_1 &= \theta_1(t, C_{11}, C_{12}, \ldots, C_{1j}) \\ &\vdots \\ \theta_n &= \theta_n(t, C_{n1}, C_{n2}, \ldots, C_{nj})\end{aligned} \tag{3.20}$$

Substituting Equation (3.19) and (3.20) into Equation (3.13) yields

$$J(C_{ij}, t_f) = \varphi(C_{ij}, t_f) + \int_0^{t_f} L(C_{ij}, t)\,dt \tag{3.21}$$

After carrying out the integration over the time domain, the performance index J becomes an ordinary function of parameters $C_{ij}$ and $t_f$. Therefore, for minimizing J, the operating time $t_f$ and the time-invariant constant $C_{ij}$s are the ones that need to be determined, not the time dependent $\theta_i(t)$.

To minimize the performance index J, the constants $C_{ij}$ and $t_f$ are choosen such that

$$\frac{\partial J(C_{ij}, t_f)}{\partial C_{ij}} = \frac{\partial \varphi(C_{ij}, t_f)}{\partial C_{ij}} + \int_0^{t_f} \frac{\partial L(C_{ij}, t)}{\partial C_{ij}}\,dt = 0 \tag{3.22.1}$$

$$\frac{\partial J(C_{ij}, t_f)}{\partial t_f} = \frac{\partial \varphi(C_{ij}, t_f)}{\partial t_f} + \frac{\partial}{\partial t_f}\int_0^{t_f} L(C_{ij}, t)\,dt = 0 \tag{3.22.2}$$

These are the necessary conditions for minimizing J, which result in a set of nonlinear algebraic Equations which can be solved either analytically or numerically. Symbol and algebraic manipulation language such as MACSYMA

[1983] can be used to solve nonlinear algebraic Equation analytically for $C_{ij}$ anf $t_f$. Again, if the order is high and the choosen performance index is complicated, the analytic solutions are almost impossible to get.

In this study a special algorithm similar to which Nagurka and Yen [1987] used for trajectory planning of rigid body manipulators is proposed to treat this problem. Figure 3.5 shows the flowchart for determining the optimal trajectory.

The $C_{ij}$ and/or $t_f$ can be evaluated by many well-developed numerical optimization techniques [Beveridge and Schechter,1970, Nelder and Mead,1965] and by commercially available Optimization algorithms such as SUMT (Sequential Unconstrained Minimization Techniques) [Fiacco and McCormick,1969]. Because of a lack of gradient information of the performance index J, the zero-order Powell's method [Powell,1964] has been adopted to solve the foregoing nonlinear programming problem.

3.3.1.3. The optimization technique

Powell's method, together with modification subsequent to its original development, is one of the most efficient and reliable and certainly the most popular of the zero-order optimization methods when first derivatives of the function are not available. Detailed discussion of its mathematical ramifications not covered here may be found

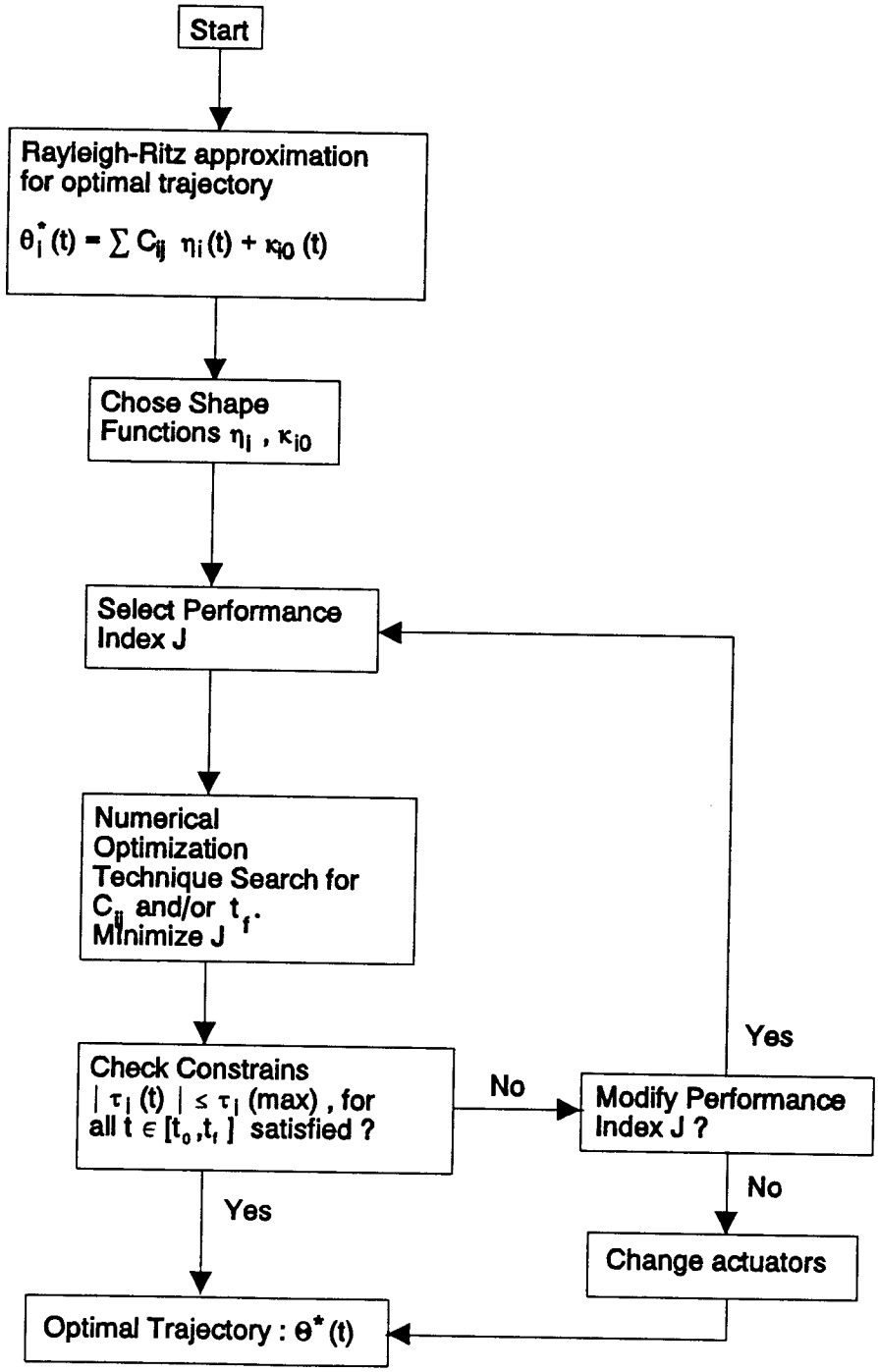


Figure 3.5 Flowchart for determining optimal trajectory.

in the original reference by Powell.

The method is based on the concept of conjugate directions which can be stated as follows:

$\mathbf{s}^i$ and $\mathbf{s}^j$ are conjugate if:

$(\mathbf{s}^i)^T \mathcal{H} \mathbf{s}^j = 0$. for all $i \neq j$, $i,j=1,\ldots,m$

where $\mathcal{H}$ is the Hessian matrix defined by

$$\mathcal{H} = \begin{bmatrix} \frac{\partial^2 J(X)}{\partial X_1^2} & \frac{\partial^2 J(X)}{\partial X_1 \partial X_2} & \cdots & \frac{\partial^2 J(X)}{\partial X_1 \partial X_m} \\ \frac{\partial^2 J(X)}{\partial X_2 \partial X_1} & \frac{\partial^2 J(X)}{\partial X_2^2} & \cdots & \frac{\partial^2 J(X)}{\partial X_2 \partial X_m} \\ \vdots & \vdots & \vdots & \vdots \\ \frac{\partial^2 J(X)}{\partial X_m \partial X_1} & \frac{\partial^2 J(X)}{\partial X_m \partial X_2} & \cdots & \frac{\partial^2 J(X)}{\partial X_m^2} \end{bmatrix} \tag{3.23}$$

here $\mathbf{X}$ is the m-dimension vector of design variables, and J is the function to be optimized.

It is important to understand that the concept of conjugacy forms the basis of most of the more powerful search algorithm. The principal significance is that, if we are given a function J which is quadratic. i.e., of the form

$$J(X) = \sum_{i=1}^{m} \sum_{j=1}^{m} a_{ij} X_i X_j + \sum_{k=1}^{m} b_k X_k + c \tag{3.24}$$

or, in matrix notation,

$$J(X) = X^T A X + X^T B + c \tag{3.25}$$

this quadratic function will be minimized in m or fewer conjugate search directions. Note that although most engineering problems are not quadratic, they can still be approximated well by a second-order Taylor series expansion (quadratic approximation) near the optimum. Indeed, Powell has shown that even when the given function J is not of quadratic type, this method is still better than other zero-order methods.

The basic concept of Powell's method can be shown geometrically in Figure 3.6 for a two-variable case, and is understood intuitively as follows:

First, search in m coordinate directions, $\mathbf{S}^m$ (m=1,2), where each search consists of updating the **X** vector according to

$$X^m = X^{m-1} + \alpha_m^* S^m \tag{3.26}$$

wherein the scalar quantity $\alpha_m^*$ defines the distance that we wish to move in direction $\mathbf{S}^m$.

Note that the coordinate directions are not usually conjugate but provide a starting point from which conjugate directions are built.

Having completed the m unidirectional searches, a conjugate direction $\mathbf{S}^3$ is created by connecting the initial design variables $\mathbf{X}^0$ with the current design $\mathbf{X}^2$. An

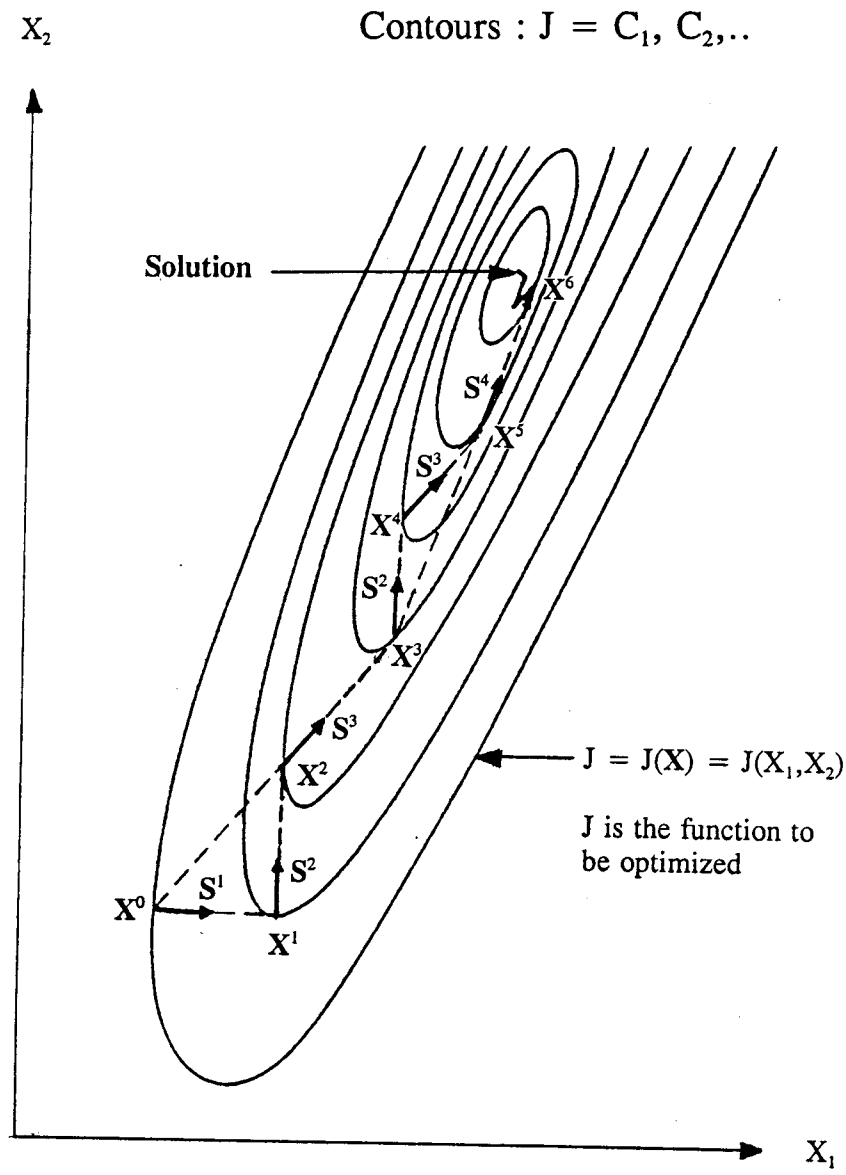


Figure 3.6 Geometric interpretation of Powell's method.

alternative interpretation for this conjugate direction is that

$$S^3 = \sum_{m=1}^{2} \alpha_m^* S^m \qquad (3.27)$$

Searching in the $\mathbf{S}^3$ direction will lead to the solution at point $\mathbf{X}^3$. Next discard one of the coordinate directions (i.e., $\mathbf{S}^1$) in favor of the conjugate direction $\mathbf{S}^3$ for inclusion in the next minimization, since this is likely to be a better direction than $\mathbf{S}^1$. Repeat the above minimization using $\mathbf{S}^2$ and $\mathbf{S}^3$ for reference directions, we can generate a new conjugate direction $\mathbf{S}^4$ and the optimum $\mathbf{X}^6$. For a quadratic function, the powell's method will arrive at the optimum on completing this step. For a general function, the whole cycles have to be repeated until a stopping criterion is satisfied.

### 3.3.1.4. Trajectory planning design algorithm for RFRA system

By adopting the algorithm of Powell's method into the proposed trajectory planning stage, the flowchart for the trajectory planning is given in Figure 3.7a and 3.7b.

Figures 3.7.a and 3.7.b summarize the step-by-step procedure to implement the open loop-loop trajectory planning suggested in this section. This procedure is described as follows:

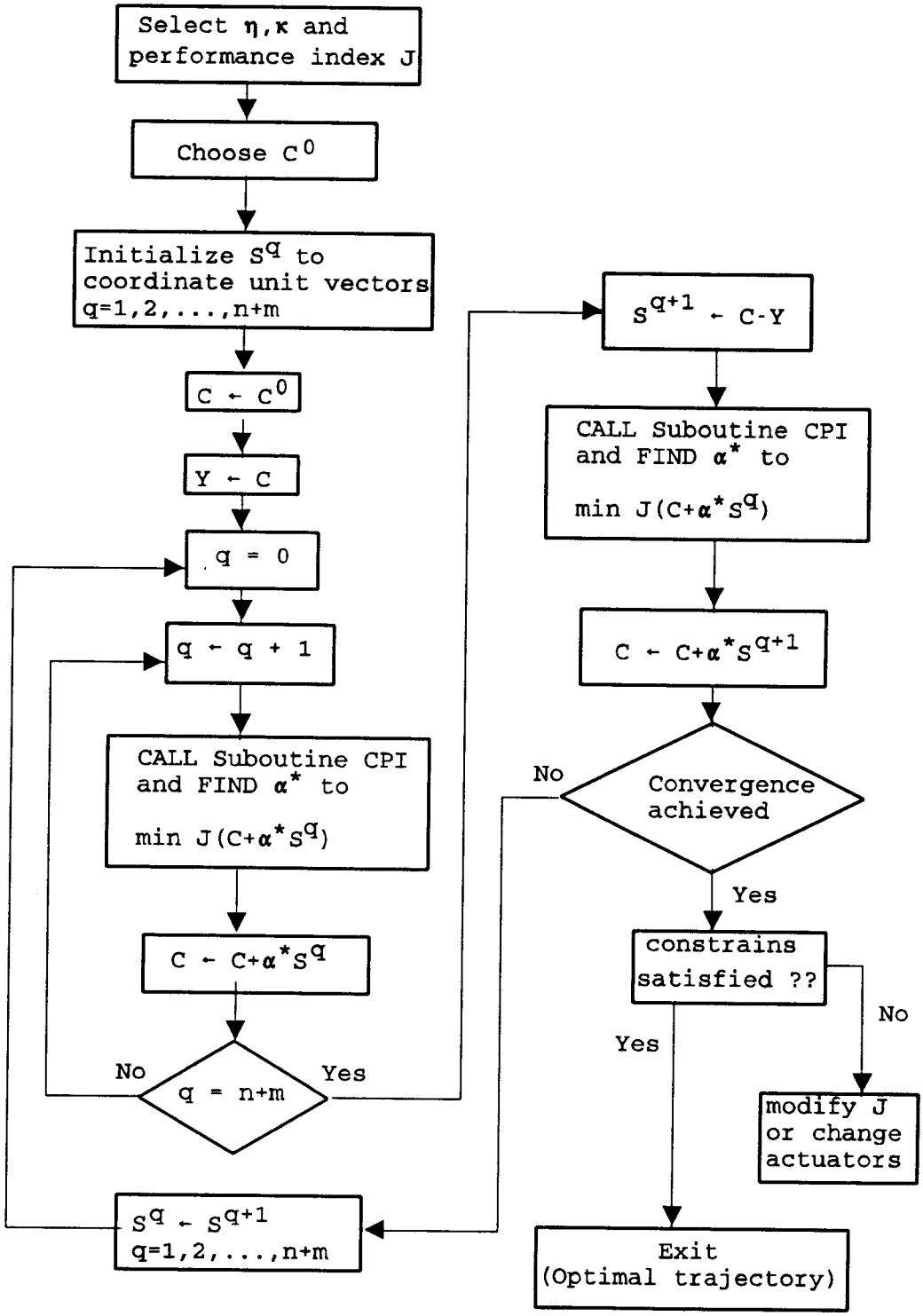


Figure 3.7a Computer algoritm using Powell's optimization search method for open-loop trajectory planning.

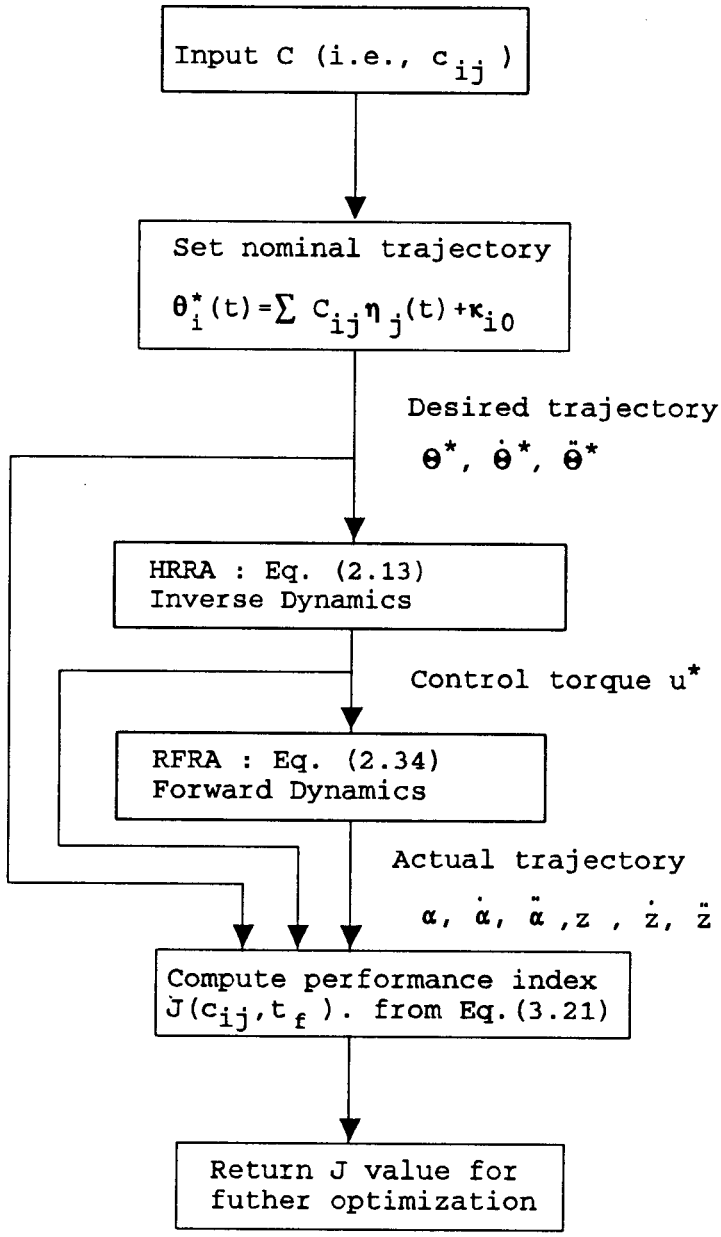


Figure 3.7b Flowchart of Subroutine CPI of computing performance index J for a given set of Ritz constants $C_{ij}$ and $t_f$.

Step 1 : Select an approximate function sets $\{\eta_j\}$ and $\{\kappa_{i0}\}$.

Step 2 : Choose initial trajectory parameters $C_{ij}$ and $t_f$.

Step 3 : Compute nominal input torque $\mathbf{u}^*(t)$ by inverse dynamic calculation using Equation (2.13) and the desired trajectories from step 1 and step 2.

Step 4 : Calculate the actual response of the flexible system (i.e., Equation (2.34)) using nominal torque $\mathbf{u}^*(t)$ from step 3, then determine the performance index value in Equation (3.1). The integration is performed by Simpson integral method with time step 0.002 second. The time step is selected on the basis of the natural frequencies of the flexible beam (clamped). For the cases run, a value $\Delta t=0.002$ seconds was appropriate.

Step 5 : Perform Powell's optimal search method for trajectory parameters $C_{ij}$ and $t_f$, and repeat step 2-5 until an optimal solution $\theta^*(t)$ is obtained.

Step 6 : Check the actuator- related inequality constraints, i.e., $|\tau_i(t)| \leq \tau_i(\max)$ , $\forall\ t \in [t_0, t_f]$, $i=1,\ldots,n$

where $\tau_i(max)$ is the maximum allowable torque at i-th joint. These constraints reflect the fact that each joint actuator is power limited and subject to saturation. If the condition is not satisfied, we cannot realize the desired trajectory by the chosen actuator and we must select another trajectory, or another actuator (i.e., choose a different performance index , or change the actuator), until the constraint is met.

In using this algorithm for this class of problem, a word of caution is necessary about the classification of the problems. This algorithm is guaranteed to have a global minimum only when the Hessian matrix is positive definite for all possible values of the design variables $C_{ij}$ and $t_f$. Generally, the problem referred to in this study is a nonconvex programming problem. This means that the algorithm may converge to a local minimum and not necessarily to the global minimum. Also due to the nature of many optimization problems, all of these procedures may find a local minimum rather than the global minimum. Thus, different starting reference points should be tried to assure that the optimal search is converging to the same minimum and this may be cautiously identified as global minimum.

### 3.3.2 Feedback Control Stage

The feedforward control scheme described above yields an open-loop optimal control strategy. Very few robots can be controlled to track the planned trajectory in an open-loop fashion because the actual trajectory may deviate substantially from the desired "optimal" trajectory due to external disturbances and system modelling error (e.g., inaccuracy of system parameters, or unknown payload). The purpose of the closed-loop feedback control scheme in the second stage is to minimize the tracking error by superimposing "correction torques" on the nominal control torques when deviation occurs.

The design of the feedback controller in this research involves computing the gains for the control of a two link rigid manipulator HRRA and applying them to the flexible model RFRA. This method was first proposed by Book et al.,[1975] with successful results. The control gains are tuned based on a linearized version of the full nonlinear rigid body equation of the motion about the planned trajectory.

There are two advantages of motion trajectory planning before the on-line feedback control, the first is that this procedure ensures that the HRRA model is "closer" to the exact RFRA model. Thus, a later, simple feedback controller based on the linearized model of HRRA model is more adequate when applied to the actual flexible model.

The second is that all the complex nonlinearities (flexibility, friction,...) can be taken into account in the off-line computation without overwhelming the on-line control computer.

Figure 3.8 shows the whole structure of the two-stage feedforward plus feedback control. First, the desired optimal trajectory $\theta^*(t)$ is calculated off-line in the motion trajectory planning stage. Then by inverse kinematics using Equation (2.13), the feedforward nominal torque $\mathbf{u}^*(t)$ is pre-calculated using $\theta^*(t)$, $\dot{\theta}^*(t)$ and $\ddot{\theta}^*(t)$ as the nominal trajectory and is fed to the actual RFRA system as the nominal driving torques. In order to compensate for the deviation between planned trajectory and the actual trajectory of the RFRA due to link flexibility and other nonlinear effects or disturbances, additional measurements $\alpha(t)$ and $\dot{\alpha}(t)$ are taken and a correction torque $\Gamma(t)$ is added to the feedforward torque $\mathbf{u}^*(t)$ to drive the actual trajectory back to the planned path. That is,

$$\mathbf{u}(t) = \mathbf{u}^*(t) + \Gamma(t) \tag{3.28}$$

Many conventional techniques have been proposed for developing the feedback controller of the linear time-invarying system. The general linear state feedback control law [Book et al., 1975, Blanck, 1988] is adopted in this research. The reason for choosing linear state

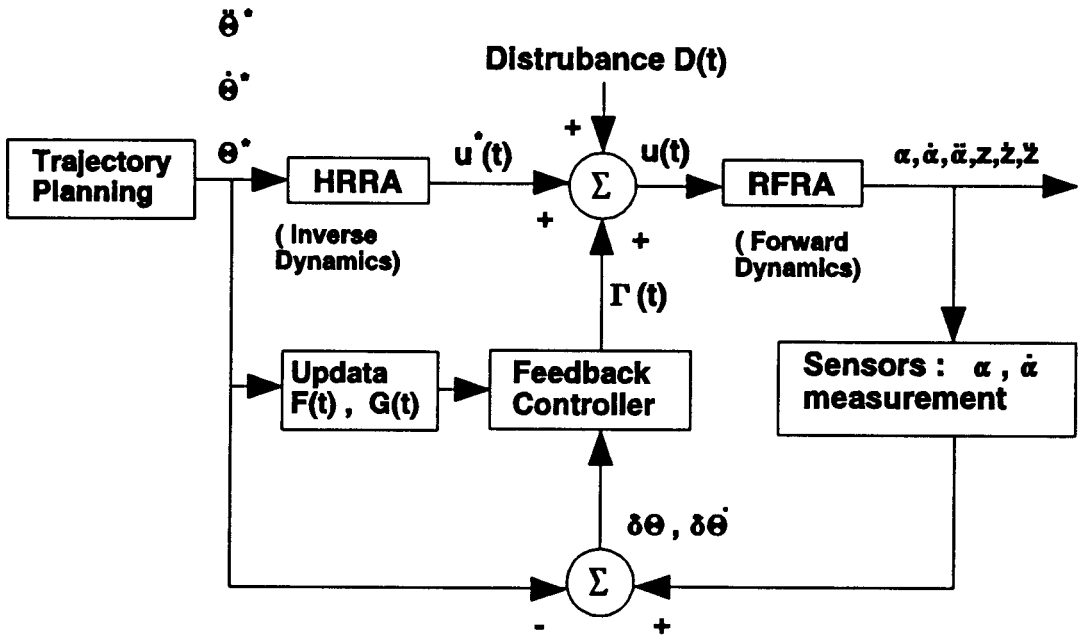


Figure 3.8 Scheme of a two-stage control of RFRA System.

feedback control law instead of conventional PD or PID control is that the closed-loop pole location of PD or PID control are restricted to lie on the root locus. Because there are more free parameters to choose in linear state feedback control than in the PD or PID controller, it may be possible to achieve a much large range of closed loop poles [Spong and Vidyasagar,1989].

The linear state control can be expressed as

$$\boldsymbol{\Gamma}(t) = -\boldsymbol{K}^T(t)\boldsymbol{x}(t) \tag{3.29}$$

where $\mathbf{K}(t)$ is a time-varying feedback gain matrix and $\mathbf{x}(t)$ is the position and velocity error vector between the desired trajectory and the measured trajectory.

The main advantage of the control scheme (i.e., Equation (3.29)) is that the feedback gains are time-varying. It has the capability of updating the feedback gains under varying conditions. Since an industrial robot is a highly nonlinear system, the inertia load, the coupling between joints and gravity effects are all either position-dependent or velocity-dependent. Furthermore, at high speeds the inertial loading term can change drastically. Thus the control scheme using constant feedback gains would not perform well under this condition.

In order to determined the time-varying feedback gain matrix $\mathbf{K}(t)$, the pole-placement method [Blanck, 1988] and

linear quadratic method [Anderson and Moore,1991] are introduced.

3.3.2.1. Pole-placement method

The time-varying pole-placement method was proposed by Blanck to determine the time-varying control gain matrix $\mathbf{K}(t)$ for the linearized time-varying system. The method can be described as follows:

Divide the feedback gain matrix $\mathbf{K}(t)$ (in Equation (3.29)) into two parts as

$$\mathbf{K}(t) = [\mathbf{K}_P(t), \mathbf{K}_D(t)] \tag{3.30}$$

where

$\mathbf{K}_P(t)$ is a 2×2 proportional gain matrix.

$\mathbf{K}_D(t)$ is a 2×2 derivational gain matrix.

By substituting Equation (3.29) and (3.30) into

$$\dot{\boldsymbol{x}}(t) = \boldsymbol{F}(t)\boldsymbol{x}(t) + \boldsymbol{G}(t)\boldsymbol{\Gamma}(t) \ , \ \boldsymbol{x}(0) \ \textit{is given} \tag{2.41}$$

the closed-loop of the linear time-varying system becomes

$$\frac{d}{dt}\begin{bmatrix} x_1 \\ x_2 \\ x_3 \\ x_4 \end{bmatrix}_{4\times1} = \begin{bmatrix} \mathbf{0}_{2\times2} & I_{2\times2} \\ -M^{-1}(Q+K_P)_{2\times2} & -M^{-1}(P+K_D)_{2\times2} \end{bmatrix}_{4\times4} \begin{bmatrix} x_1 \\ x_2 \\ x_3 \\ x_4 \end{bmatrix}_{4\times1} \tag{3.31}$$

The pole-placement method for the closed-loop system requires the matrices $\mathbf{M}^{-1}(\mathbf{P}+\mathbf{K}_D)$ and $\mathbf{M}^{-1}(\mathbf{Q}+\mathbf{K}_P)$ to be constants at every sampling time t. Additionally, if the joints are to be decoupled, these matrices are diagonal. In this case,

$$\boldsymbol{M}^{-1}(\boldsymbol{Q}+\boldsymbol{K}_P) = \begin{bmatrix} \omega_1^2 & 0 \\ 0 & \omega_2^2 \end{bmatrix} \tag{3.32}$$

and

$$\boldsymbol{M}^{-1}(\boldsymbol{P}+\boldsymbol{K}_D) = \begin{bmatrix} 2\zeta_1\omega_1 & 0 \\ 0 & 2\zeta_2\omega_2 \end{bmatrix} \tag{3.33}$$

where $\omega_1$, $\omega_2$ and $\zeta_1, \zeta_2$ are the system natural frequencies and damping ratios respectively.

Now, the i-th decoupled second order sub-system of Equation (3.31) becomes

$$\delta\ddot{\theta}_i + 2\,\zeta_i\omega_i\,\delta\dot{\theta}_i + \omega_i^2\,\delta\theta = 0, \quad i=1,2 \tag{3.34}$$

From the above Equation, we can see that this controller decouples the linearized system thus allowing us to carry out a design procedure for each axis independently. Any desired pole location to achieve the desired performance may be obtained by appropriate choice of $\omega_i$ and $\zeta_i$. It is customary in robotics applications to take $\zeta_i$=1, so that the response is critically damped to produce the fastest non-oscillatory response.

This type of control is termed general rigid control (GRC) in the original paper by Book et al. [1975].

3.3.2.2. Linear quadratic method

In the pole placement method, most of the difficulty lies in choosing the appropriate set of closed loop poles based on the desired performance, the limits of the available torque,.. etc. Usually, it involves lots of trial and error. One systematic way to design the linear feedback gains is through an optimization procedure.

The procedure of finding an optimal feedback control gain is to form a quadratic performance index $J(\Gamma)$ defined as

$$J(\Gamma) = \frac{1}{2}\boldsymbol{x}^T(t_f)\, \boldsymbol{S}\, \boldsymbol{x}(t_f) + \frac{1}{2}\int_{t_0}^{t_f}[\Gamma^T(t)\, \boldsymbol{R}(t)\, \Gamma(t) + \boldsymbol{x}^T(t)\, \boldsymbol{Q}(t)\, \boldsymbol{x}(t)]\, dt \tag{3.35}$$

with weighting matrices

$$\boldsymbol{R}(t) = \boldsymbol{R}^T(t) > 0, \quad \boldsymbol{Q}(t) = \boldsymbol{Q}^T(t) \geq 0, \quad \boldsymbol{S} \geq 0 \tag{3.36}$$

Note that the restrictions on the weighting matrices are required for a minimum of J to exist [Palm, 1983].

With the final time $t_f$ fixed, the objective is to find an optimal control $\Gamma(t)$ to move the system from an arbitrary initial state $\mathbf{x}(t_0)$ to the origin of the error-space while minimizing $J(\Gamma)$.

It is assumed that the states $\mathbf{x}(t)$ and controls $\Gamma(t)$ are not bounded, and $\mathbf{x}(t_f)$ is free.

To drive the optimal control, we rewrite the linear time-varying Equation (2.41)

$$\dot{\boldsymbol{x}}(t) = \boldsymbol{F}(t)\,\boldsymbol{x}(t) + \boldsymbol{G}(t)\,\Gamma(t) \tag{2.41}$$

the Hamiltonian can be written as

$$\begin{aligned} H[\boldsymbol{x}(t),\Gamma(t),\lambda(t),t] &= \frac{1}{2}\boldsymbol{x}^T(t)\boldsymbol{Q}(t)\boldsymbol{x}(t) \\ &+ \frac{1}{2}\Gamma^T(t)\boldsymbol{R}(t)\Gamma(t) + \lambda^T(t)\boldsymbol{F}(t)\boldsymbol{x}(t) + \lambda^T(t)\boldsymbol{G}(t)\Gamma(t) \end{aligned} \tag{3.37}$$

where $\lambda(t)$ is the vector of Lagrange multipliers.

Again, the necessary conditions (Equation (3.7)-(3.9)) for optimality are applied. These become

$$\dot{\boldsymbol{x}}(t) = \frac{\partial H}{\partial \lambda} = \boldsymbol{F}(t)\boldsymbol{x}(t) + \boldsymbol{G}(t)\Gamma(t) \tag{3.38.1}$$

$$\dot{\lambda}(t) = -\frac{\partial H}{\partial \boldsymbol{x}} = -\boldsymbol{Q}(t)\boldsymbol{x}(t) - \boldsymbol{F}^T(t)\lambda(t) \tag{3.38.2}$$

$$\mathbf{0} = \frac{\partial H}{\partial \Gamma} = \boldsymbol{R}^T(t)\lambda(t) \tag{3.38.3}$$

Equation (3.38.1)-(3.38.3) can be solved for $\Gamma(t)$, and the result is given by the same linear state feedback form as Equation (3.29) (For proof see Kirk [1970], and Anderson [1990]).

$$\Gamma(t) = -\,\mathbf{K}(t)\mathbf{x}(t) \tag{3.29}$$

with

$$\mathbf{K}(t) = \mathbf{R}^{-1}(t)\mathbf{G}^{T}(t)\mathbf{P}(t) \tag{3.39}$$

where $\mathbf{P}(t)$ denotes the symmetric positive definite solution of the matrix Riccati Equation

$$-\dot{\mathbf{P}}(t) = \mathbf{P}(t)\mathbf{F}(t)+\mathbf{F}^{T}(t)\mathbf{P}(t)-\mathbf{P}(t)\mathbf{G}(t)\mathbf{R}^{-1}(t)\mathbf{G}^{T}(t)\mathbf{P}(t)+\mathbf{Q}(t) \tag{3.40}$$

with terminal condition

$$\mathbf{P}(t_f) = \mathbf{S}. \tag{3.41}$$

Note that the existence of $\mathbf{R}^{-1}$ is assured, since $\mathbf{R}$ is a positive definite matrix.

In order to select the feedback gains $\mathbf{K}(t)$, we confront solving the differential matrix type of Riccati Equation (3.40). Techniques aimed at solving the matrix type of Riccati Equation analytically have been given in several ways [Anderson and Moore,1990], but these are only applicable for low order systems ($n \leq 2$). For more complex systems, such as robots, numerical integration using a digital computer is required to solve the differential Equation (3.40) [Melsa and Jones, 1973, Palm, 1983]. The integration is started at $t=t_f$ with initial conditions (3.41) and proceeds backward in time to $t=t_0$. Then, the feedback gain matrix is determined from Equation (3.39).

Since it is so difficult to calculate these feedback gains by solving Equation (3.39) and (3.40) on the real time control, they might be calculated in advance for all possible configurations along the given trajectory $\theta^*(t)$ and the corresponding time-varying gains stored in the computer.

One disadvantage of tabular gain values $\mathbf{K}(t)$ is that for high degree-of-freedom robotic systems, this will require a lot of memory in the computer to save these gain values $\mathbf{K}(t)$ at every sampling time.

To avoid this computational difficulty, a "one-step" optimal control algorithm based on dynamic programming techniques is used [Dick, 1986, Fu et al, 1987, Singh and Leu, 1987]. Such a control is obtained by reducing a so-called "N-stage decision process" [Jacquot,1981, Owens, D.H., 1988] to one step. This algorithm can be partially solved analytically, hence reducing the need to store large tables for look-up and making application to high order system feasible.

For implementation of the one-step optimization control, the associated linearized perturbation Equation (2.41) is discretized to obtain the appropriate discrete-time linear Equation.

$$x(k+1) = \Delta(k)x(k) + \Omega(k)\Gamma(k) \qquad (3.42)$$

where

$$\Delta = exp(FT) \quad \textit{is the } 4\times4 \textit{ state transition matrix} \tag{3.43.1}$$

$$\Omega = \left[\int_0^T \exp(F\nu)\, d\nu\right] G \quad \textit{is the } 4\times2 \textit{ input gain matrix} \tag{3.43.2}$$

T is the sampling period, and $\Gamma(kT)$ (or $\Gamma(k)$ for simplification) is a 2-dimensional piecewise constant control input vector over the time interval between any two consecutive sampling instants $kT \le t \le (kT+1)$, and $\mathbf{x}(k)$ is a 4-dimensional perturbed state vector.

For high sampling rate the discrete system parameters $\Delta(k)$ and $\Omega(k)$ may be approximated by

$$\Delta \approx I + FT = \begin{bmatrix} I & IT \\ -M^{-1}QT & I - M^{-1}PT \end{bmatrix} \tag{3.44.1}$$

$$\Omega \approx GT = \begin{bmatrix} 0 \\ M^{-1}T \end{bmatrix} \tag{3.44.2}$$

Define the performance index at (K+1)T to be

$$J(K+1,K+1) = \frac{1}{2}\, x^T(K+1)\, Q\, x(K+1) \tag{3.45}$$

Then, the performance index over KT and (K+1)T is

$$J(K+1,K) = 1/2[\ \mathbf{x}^T(k+1)\ \mathbf{Q}\ \mathbf{x}(k+1) + \Gamma^T(k)\ \mathbf{R}\ \Gamma(k)\ ] \tag{3.46}$$

where

$$\mathbf{Q} = \mathbf{Q}^T \ge \mathbf{0} \quad \text{and} \quad \mathbf{R} = \mathbf{R}^T > \mathbf{0}. \tag{3.47}$$

The objective is to find an optimal control $\Gamma(k)$, which minimizes the performance index J (Equation (3.46))

and satisfies the constraint Equation (3.42) at every time instant kT.

$$J_{min}(k+1,k) = \min_{\Gamma(k)} J(k+1,k) \tag{3.48}$$

Now, substitution of the state Equation (3.42) into (3.48) yields

$$\begin{aligned} J_{min}(K+1,K) = \min_{\Gamma(K)}\{&\frac{1}{2}\Gamma(K)^T R\Gamma(K) + \frac{1}{2}[\Delta(K)\,x(K) \\ &+ \Omega(K)\,\Gamma(K)]^T Q\,[\Delta(K)\,x(K) + \Omega(K)\,\Gamma(K)]\} \end{aligned} \tag{3.49}$$

Minimizing Equation (3.49) with respect to $\Gamma(k)$ yields

$$\frac{\partial J(K+1,K)}{\partial \Gamma(K)} = \Gamma^T(K)\,R + [\Delta(K)\,x(K) + \Omega(K)\,\Gamma(K)]^T Q\,\Omega(K) = 0 \tag{3.50}$$

The resulting optimal control effort of the one-step linear optimal regulator becomes

$$\Gamma(K) = -P(K)x(K) \tag{3.51}$$

where

$$P(K) = [\,R + \Omega^T(K)\,Q\,\Omega(K)\,]^{-1}\,\Omega^T(K)\,Q\,\Delta(K)\,x(K) \tag{3.52}$$

Note that Equation (3.51) also forms a linear state feedback control.

# CHAPTER 4. APPLICATION AND RESULT

The purpose of this chapter is to present the results of application of the mathematical techniques and the several general control methods to the robot illustrated in Figure 2.1. The design principles of both open-loop trajectory planning and closed-loop feedback trajectory control will be demonstrated in this chapter. Although the example has two degrees of freedom, the procedures can be extended to systems with an arbitrary number of degrees of freedom. The mass of the payload is also varied to demonstrate the robustness of the control system under various loading conditions. Disturbances are purposely introduced to the system to see how the entire system reacts to the external disturbances. The numerical integration routine is based on the fourth-order Runge-Kutta method.

## 4.1. System Dimensions

The physical model of the two-link manipulator (before deformation) is shown in Figure 4.1 and the main geometric characteristics are presented in Table 1. Note that both links have different radii and were chosen so that the stiffness EI for the first beam is approximately equal to ten times the value for the second beam. The motions were assumed to be in the plane of the beam, no structural or

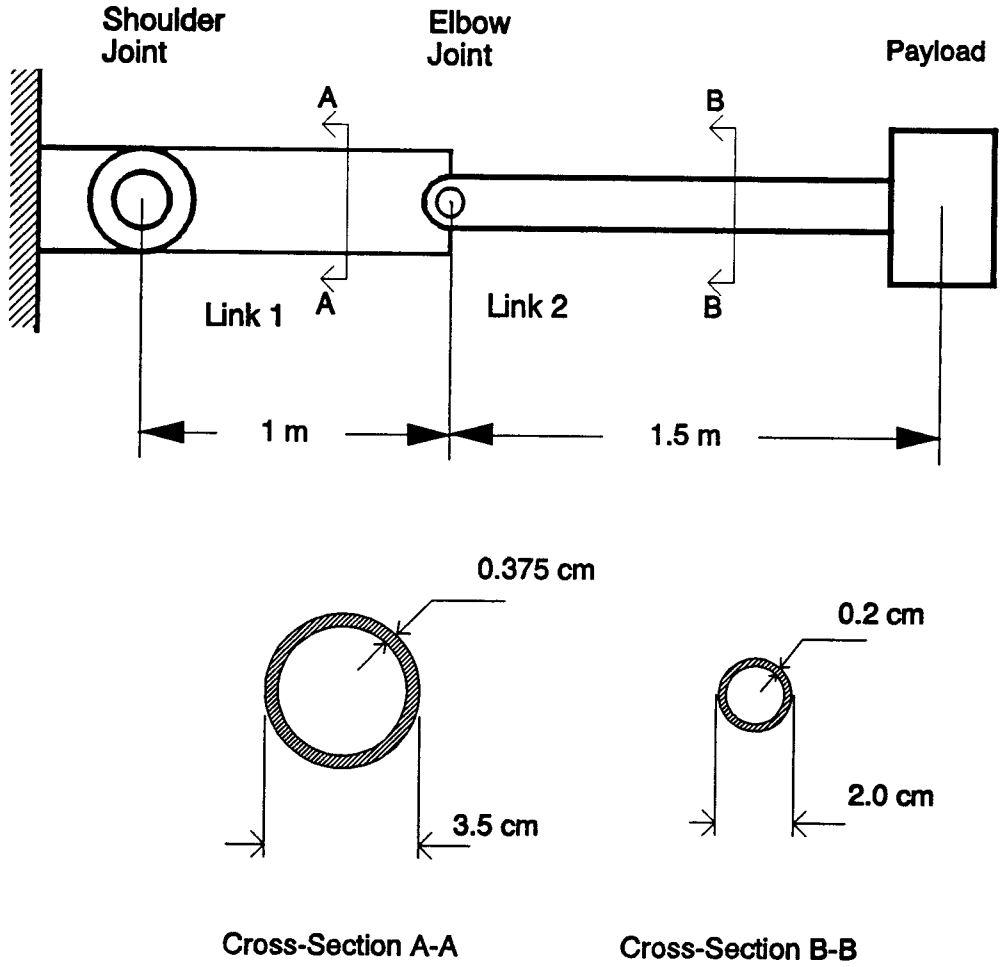


Physical Model

Figure 4.1 Physical model of RFRA system with cross-section view.

joint damping were considered and gravity was neglected. However, the computer program presented can accommodate both structural and joint damping.

Table 1. System parameters of two-link manipulator

| | | |
|---|---|---|
| material of beam 1 | | aluminum |
| material of beam 2 | | aluminum |
| Young's modulus E | $6.895\times10^{10}$ | $N/m^2$ |
| length of beam 1 | 1.000 | m |
| length of beam 2 | 1.500 | m |
| maximum payload mass | 1.000 | kg |
| elbow joint lump mass | 0.500 | kg |
| internal diameter of beam 1 | $2.750\times10^{-2}$ | m |
| internal diameter of beam 2 | $1.600\times10^{-2}$ | m |
| external diameter of beam 1 | $3.500\times10^{-2}$ | m |
| external diameter of beam 2 | $2.000\times10^{-2}$ | m |
| mass per unit length: beam 1 | $9.988\times10^{-1}$ | kg/m |
| mass per unit length: beam 2 | $3.068\times10^{-1}$ | kg/m |

The desired trajectory is designed for pick-and-place motion; the object is picked from the initial positions $(\theta_1,\theta_2)=(15°,15°)$ and placed to the final positions $(\theta_1(T),\theta_2(T))=(75°,75°)$ in 3 seconds. Both initial and final velocities of the motion are required to remain

zero.

## 4.2. Open-Loop Trajectory Approximation

In this section, the trajectory planning problem is converted to an optimization problem using the parameter-optimization approach discussed in chapter 3. The desired path is expressed in terms of a series of shape functions with arbitrary coefficients which need to be determined. The selection of the shape function have been presented in many ways. Schmitt et al. [1985] suggested a sum of a cubic polynomial and a versine series which can be expressed as

$$\theta_i(t) = \sum_{j=0}^{3} a_{ij} t^j + \sum_{j=1} b_{ij} \left(1 - \cos \frac{2\pi j t}{T}\right) \qquad (4.1)$$

*where*

$$a_{i0} = \theta_i(0)$$

$$a_{i1} = \dot{\theta}_i(0)$$

$$a_{i2} = \frac{3}{T^2}\left[\theta_i(T) - \theta_i(0)\right] - \frac{2}{T}\dot{\theta}_i(0) - \frac{1}{T}\dot{\theta}_i(T)$$

$$a_{i3} = -\frac{2}{T^3}\left[\theta_i(T) - \theta_i(0)\right] + \left[\dot{\theta}_i(T) + \dot{\theta}_i(0)\right]$$

Nagurka and Yen [1987] approximated the joint angular displacements by the sum of a fifth order polynomial and a finite Fourier-type series. This is

$$\theta_i(t) = \sum_{j=0}^{5} c_{ij} t^j + \sum_{j=1} \left( d_{ij} \cos \frac{2\pi j t}{T} + e_{ij} \sin \frac{2\pi j t}{T} \right) \qquad (4.2)$$

*where*

$$c_{i0} = \theta_i(0)$$

$$c_{i1} = \dot{\theta}_i(0)$$

$$c_{i2} = \frac{\ddot{\theta}_i(0)}{2}$$

$$c_{i3} = \frac{20\theta_i(T) - 20\theta_i(0) - [8\dot{\theta}_i(T) + 12\dot{\theta}_i(0)]T - [3\ddot{\theta}_i(0) - \ddot{\theta}_i(T)]T^2}{2T^3}$$

$$c_{i4} = \frac{30\theta_i(0) - 30\theta_i(T) + [14\dot{\theta}_i(T) + 16\dot{\theta}_i(0)]T + [3\ddot{\theta}_i(0) - 2\ddot{\theta}_i(T)]T^2}{2T^4}$$

$$c_{i5} = \frac{12\theta_i(T) - 12\theta_i(0) - [6\dot{\theta}_i(T) + 6\dot{\theta}_i(0)]T - [\ddot{\theta}_i(0) - \ddot{\theta}_i(T)]T^2}{2T^5}$$

$\theta_i(0), \dot{\theta}_i(0), \ddot{\theta}_i(0)$ and $\theta_i(T), \dot{\theta}_i(T), \ddot{\theta}_i(T)$ are prescribed values of displacements, velocities and accelerations at time t=0 and t=T, respectively. The difference between Schmitt's and Nagurka's approximations can lead to a very significant difference in dynamic effect of controlling the flexible manipulator; this will be discussed later in this chapter.

## 4.3. Selection of Performance Index

The performance index considered in this study is based on the following considerations:

1. Transverse vibrations during the motion period should be suppressed in order to produce better trajectory tracing and smaller settling time.
2. The position and velocity error between planned trajectory of HRRA model and actual trajectory of RFRA system should be minimized in order to implement the linear state feedback control about the planned trajectory.
3. The deflection of the flexible link and the vibration velocity at the final time must be zero.
4. The control effort is minimum.

To meet these requirements, the performance index is chosen in terms of the joint angular velocities and displacements, and the transverse displacement and vibration velocity of the flexible forelink and can be expressed as

$$J(t) = \frac{\mu_1}{2}\sum_{i=1}^{2}\left|\alpha_i(T) - \theta_i(T)\right|^2 + \frac{\mu_2}{2}\sum_{i=1}^{2}\left|\dot{\alpha}_i(T) - \dot{\theta}_i(T)\right|^2 + \frac{\mu_3}{2}\sum_{i=1}^{2}\int_0^T\left|\tau_i(t)\right|^2 dt$$

$$+ \frac{\mu_4}{2}\sum_{i=1}^{2}\int_0^T\left|\alpha_i(t) - \theta_i(t)\right|^2 dt + \frac{\mu_5}{2}\sum_{i=1}^{2}\int_0^T\left|\dot{\alpha}_i(t) - \dot{\theta}_i(t)\right|^2 dt$$

$$+ \frac{\mu_6}{2}\int_0^{L_2}|w(\xi,T)|^2 d\xi + \frac{\mu_7}{2}\int_0^{L_2}\left|\frac{\partial w(\xi,T)}{\partial t}\right|^2 d\xi$$

$$+ \frac{\mu_8}{2}\int_0^T\left\{\int_0^{L_2}\left[\rho\left|\frac{\partial w(\xi,t)}{\partial t}\right|^2 + EI_z\left|\frac{\partial^2 w(\xi,t)}{\partial t^2}\right|^2\right] d\xi + m_p\left|\frac{\partial w(L_2,t)}{\partial t}\right|^2\right\} dt$$

$$+ \frac{\mu_9}{2}|w(L_2,T)|^2 \qquad (4.3)$$

The first two terms describe accuracy near the target point. The sum of square of joint torques in the third term is selected to minimize the driving energy and also to prevent control instability problem. The sixth and seventh terms represent deflections and vibration velocity of the flexible link at the final time. The eighth term indicates the structural vibration energy of the flexible link over the entire length throughout the period of operation, and the last term is the tip deflection at the end of the operation. Note that the final time $t_f$ can be included in Equation (4.3) if the final time is not fixed and the optimal time control is required to move the object from one station to another station in a minimum time.

## 4.4. Off-Line Control Simulation Results

On the basis of the parameter-optimization method proposed in chapter 3 and the selected performance index, a computer program OPPATH has been developed to search the optimal trajectory for controlling the flexible manipulator. The program based on Powell' optimal search method is coded in FORTRAN 77 with double precision via routines taken from other sources [Press,et.al.,1989] and is implemented on the FPS (Floating Point System) with VAX 780 at Oregon State University.

To carry out the numerical integration, the fourth-order Runge-Kutta method has been used, and the integration time interval was selected to be 2 ms based on the natural frequencies of the flexible beam (clamped). The integration in Equation (4.3) is performed by Simpson integral method with time step 0.002 seconds. The weighing factors (i.e., $\mu_i$, i=1,...,9) in performance index are adjustable in order to obtain the best performance.

In order to analyze the effect of the payload in the design of the open-loop control, a comparison was made between three different payloads for the example presented in Table 1. The payloads were assumed to be lumped masses at the end of the second link with values indicated in Table 2.

Table 2. Varying loading conditions for the two-link flexible/rigid manipulator

| loading conditions | payload (kgs) |
|---|---|
| case 1 | 0 |
| case 2 | 0.5 |
| case 3 | 1.0 |

In general, the optimization problem is a nonconvex optimization problem. To guarantee that the optimization algorithm will obtain the global minimum value of the performance index, it is necessary to restart the optimization process from several different starting points to provide reasonable assurance of obtaining the global minimum. Three starting points were selected for each loading condition and the resulting smallest value of the performance index is carefully identified to be the global minimum.

A normal control, which used the cubic polynomial path, was chosen for comparison, and the results of the optimization are showed in Table 3 and Table 4.

The trajectories resulting from the different schemes are shown in Figure 4.2-4.4 for three different cases. Figure 4.2(a) represents the normal cubic polynomial path which is commonly used by industry. Figure 4.2(b) shows the result of the Schmitt approximation, and shows that in order to avoid unnecessary vibration, the flexible second

Table 3. Determination of optimal trajecrories with cubic polynomial plus version function approximation

| Cubic Polynomial plus Versine Function | | | | |
|---|---|---|---|---|
| | start point | | convergence point | J(cij) |
| case 1 | c11=1.0 c12=0.0 c13=0.0<br>c21=1.0 c22=0.0 c23=0.0 | | c11=-0.8100 c12=-14.0608 c13=0.7016<br>c21=-11.6705 c22=20.9038 c23=-0.1379 | 0.000620 |
| | c11=0.0 c12=1.0 c13=0.0<br>c21=0.0 c22=1.0 c23=0.0 | | c11=-7.9915 c12=-12.1109 c13=0.8628<br>c21=-0.8741 c22=17.0382 c23=0.0016 | 0.000578 |
| | c11=0.0 c12=0.0 c13=1.0<br>c21=0.0 c22=0.0 c23=1.0 | | c11=-7.8673 c12=-11.8003 c13=0.6351<br>c21=-0.8741 c22=16.6510 c23=0.3119 | 0.00562 |
| case 2 | c11=1.0 c12=0.0 c13=0.0<br>c21=1.0 c22=0.0 c23=0.0 | | c11=-57.4363 c12=-3.0073 c13=-0.9110<br>c21=47.7705 c22=10.8498 c23=1.7512 | 0.002439 |
| | c11=0.0 c12=1.0 c13=0.0<br>c21=0.0 c22=1.0 c23=0.0 | | c11=-59.2461 c12=-1.7996 c13=-0.2157<br>c21=-0.2157 c22=10.7895 c23=0.0253 | 0.006577 |
| | c11=0.0 c12=0.0 c13=1.0<br>c21=0.0 c22=0.0 c23=1.0 | | c11=-56.6630 c12=-3.7791 c13=-0.0111<br>c21=47.5164 c22=11.5109 c23=0.4435 | 0.005206 |
| case 3 | c11=1.0 c12=0.0 c13=0.0<br>c21=1.0 c22=0.0 c23=0.0 | | c11=4.9345 c12=-17.1911 c13=0.0621<br>c21=-12.7870 c22=23.4878 c23=0.0759 | 0.044392 |
| | c11=0.0 c12=1.0 c13=0.0<br>c21=0.0 c22=1.0 c23=0.0 | | c11=-66.5156 c12=1.7425 c13=-1.0313<br>c21=53.0765 c22=9.5397 c23=-0.0091 | 0.022988 |
| | c11=0.0 c12=0.0 c13=1.0<br>c21=0.0 c22=0.0 c23=1.0 | | c11=-66.2431 c12=-0.2624 c13=-0.9478<br>c21=52.4733 c22=10.3662 c23=0.9616 | 0.013179 |

Table 4. Determination of optimal trajectory with fifth polynomial plus fourier-type-based approximation

| Fifth Polynomial plus Fourier Series | | | | | |
|---|---|---|---|---|---|
| | start point | | convergence point | | J(cij) |
| case 1 | c11=1.0 c12=0.0 c13=0.0<br>c21=1.0 c22=0.0 c23=0.0 | | c11=2.3759 c12=6.4451 c13=-0.1670<br>c21=-4.0645 c22=-7.7541 c23=-0.4315 | | 0.000252 |
| | c11=0.0 c12=1.0 c13=0.0<br>c21=0.0 c22=1.0 c23=0.0 | | c11=2.3685 c12=6.0315 c13=-0.1497<br>c21=-4.0243 c22=-7.0851 c23=-0.4581 | | 0.000253 |
| | c11=0.0 c12=0.0 c13=1.0<br>c21=0.0 c22=0.0 c23=1.0 | | c11=2.2982 c12=6.3787 c13=-0.1365<br>c21=-3.9482 c22=-7.5267 c23=-0.5288 | | 0.000253 |
| case 2 | c11=1.0 c12=0.0 c13=0.0<br>c21=1.0 c22=0.0 c23=0.0 | | c11=3.1635 c12=5.8004 c13=-0.0250<br>c21=-4.8075 c22=-6.9905 c23=-0.3355 | | 0.005589 |
| | c11=0.0 c12=1.0 c13=0.0<br>c21=0.0 c22=1.0 c23=0.0 | | c11=3.0788 c12=5.7113 c13=-0.0729<br>c21=-4.6831 c22=-6.7883 c23=-0.3004 | | 0.005586 |
| | c11=0.0 c12=0.0 c13=1.0<br>c21=0.0 c22=0.0 c23=1.0 | | c11=3.1351 c12=5.5417 c13=-0.0930<br>c21=-4.7520 c22=-6.6329 c23=-0.2253 | | 0.005581 |
| case 3 | c11=1.0 c12=0.0 c13=0.0<br>c21=1.0 c22=0.0 c23=0.0 | | c11=3.2033 c12=3.9408 c13=-0.0282<br>c21=-4.7594 c22=-4.1634 c23=-0.2876 | | 0.018372 |
| | c11=0.0 c12=1.0 c13=0.0<br>c21=0.0 c22=1.0 c23=0.0 | | c11=2.9510 c12=4.2205 c13=-0.0214<br>c21=-4.4240 c22=-4.3547 c23=-0.4052 | | 0.018392 |
| | c11=0.0 c12=0.0 c13=1.0<br>c21=0.0 c22=0.0 c23=1.0 | | c11=3.2412 c12=4.7589 c13=-0.2623<br>c21=-4.8139 c22=-5.4767 c23=0.0652 | | 0.018311 |

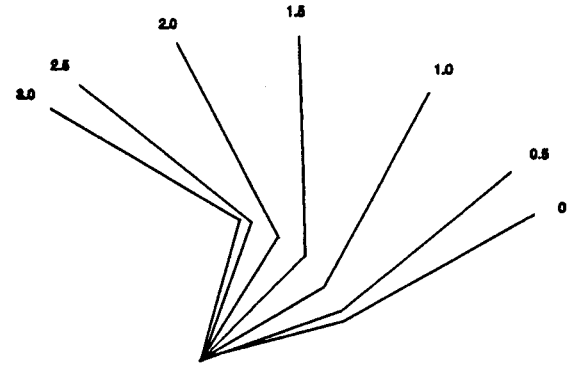


(a) Cubic Ploynomial path

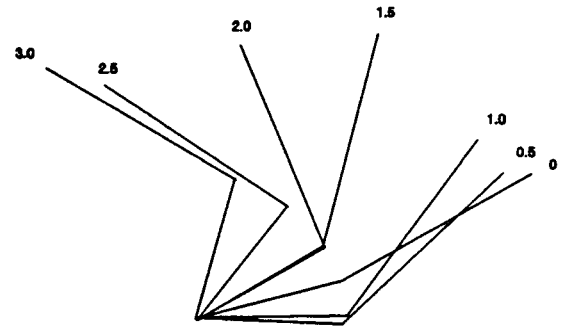


(b) Planned Cubic Polynomial + Versine Function path

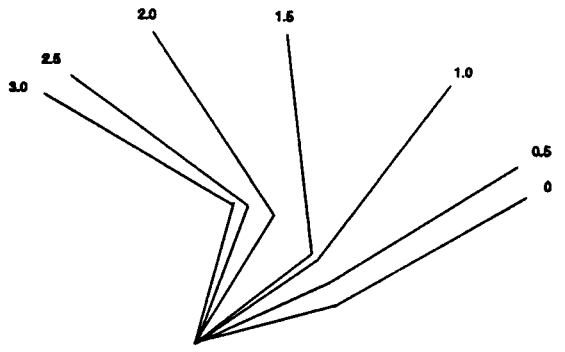


(c) Planned Fifth polynomial + Fourier series path

Figure 4.2 Motion trajectories of planned paths for case 1 ($m_p$=0 kg): (a) cubic path. (b) cubic poly. + versine path (c) fifth poly. + Fourier type path.

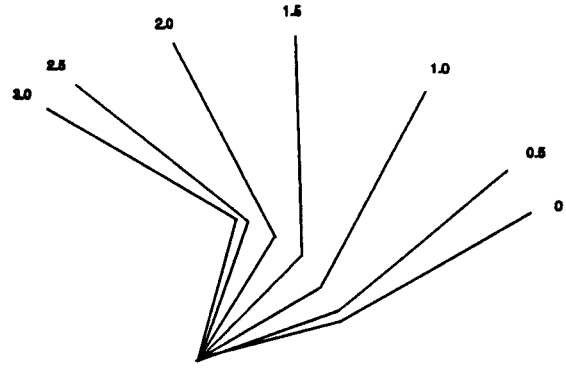


(a) Cubic Ploynomial path

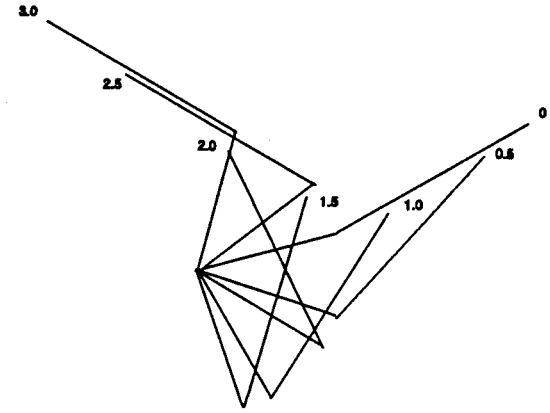


(b) Planned Cubic Polynomial + Versine Function path

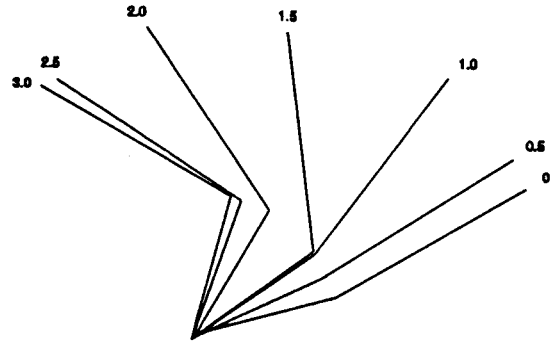


(c) Planned Fifth Polynomial + Fourier Series path

Figure 4.3 Motion trajectories of planned paths for case 2 ($m_p$=0.5 kg): (a) cubic path. (b) cubic poly. + versine path. (c) fifth poly. + Fourier type path.

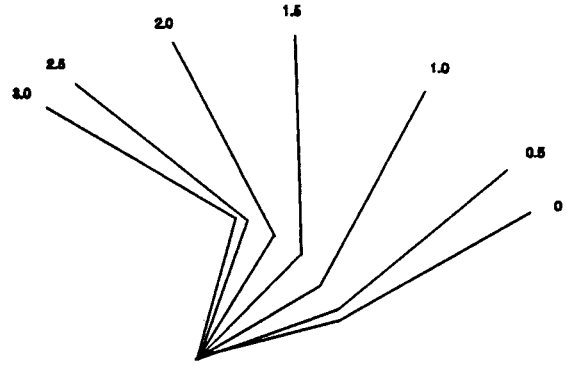


(a) Cubic Ploynomial path

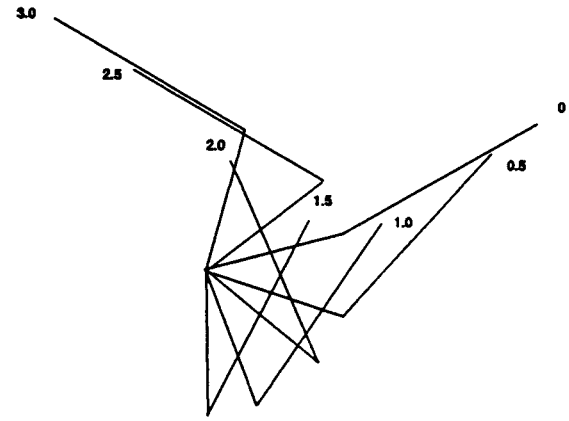


(b) Planned Cubic Polynomial + Versine Function path

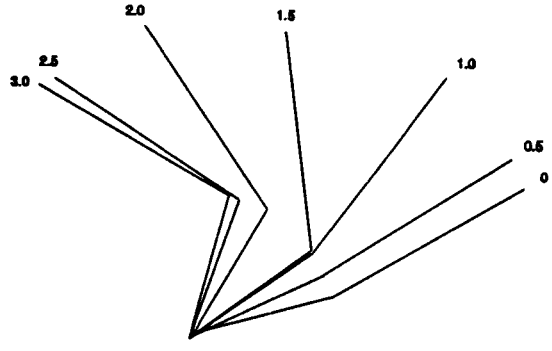


(c) Planned Fifth Polynomial + Fourier Series path

Figure 4.4 Motion trajectories of planned path for case 3 (mp = 1 kg): (a) cubic path (b) cubic poly. + versine path. (c) fifth poly. + Fourier type path.

link must move quickly to reach an orientation perpendicular position to the first rigid link, and move with the first link in its axial direction thereafter to avoid transverse excitation. Figure 4.2(c) indicates the result of a fifth polynomial plus Fourier series type approximation, and the profile is about the same as the normal cubic polynomial path in Figure 4.2(a). Figure 4.3 and 4.4 explain the motion profile for case 2 and case 3.

Once the optimal trajectories have been found, the desired optimal control torques can be calculated using Equation (2.13), which is the inverse dynamics of the corresponding HRRA model. The simulation of the open-loop control using the optimal control torques is coded in program SIMUL.

The results of the numerical simulation are presented in Figure 4.5-4.15 for no loading condition (i.e., case 1). In Figure 4.5-4.7, it is observed that both elbow and shoulder displacements for the proposed and normal control are essentially the same. This is to be expected since displacement is the integrated effect of the angular velocity. On the other hand, Figure 4.8-4.10 clearly depicts the effects of link vibrations on the joint angular velocity of the actual flexible manipulator. In Figure 4.8 small amplitude oscillations (dotted line) superimposed on the normal planned velocity trajectories (solid line) are essentially due to vibrations of the

flexible link. With the application of the optimal trajectory planning, however, Figure 4.9 and 4.10 show much improvement in reducing the link vibrations using the proposed parameter-optimization approach.

The angular displacement error between the planned path and the joint displacement of the actual flexible/rigid system are shown in Figure 4.11. Significant drops in the dynamic errors of $\theta_1$ and $\theta_2$ are revealed with the Fourier-type shape functions. The maximum errors obtained with Fourier type approach are of 0.0031 degree and 0.0559 degree for $\theta_1$ and $\theta_2$ respectively while the maximum errors corresponding to the normal and versine function approach are of 0.0050 degree and 0.0146 degree for $\theta_1$ and 0.0814 degree and 0.0745 degree for $\theta_2$. Table 5 summarizes the open-loop trajectory planning results for three loading conditions.

Although the Schmitt's approximation yields very small deviation from the planned trajectory during operation, large displacement errors (i.e., 0.0146 degree and 0.0425 degree for $\theta 1$ and $\theta 2$ respectively, while Fourier-type approximation remains 0.0015 degree and 0.0016 degree in final position errors) are detected near the target point. This is due to the fact that both normal and Schmitt's planned path failed to consider the inertia effect of the flexible manipulator. This will induce high accelerations in the distal joints which induce a whipping action that

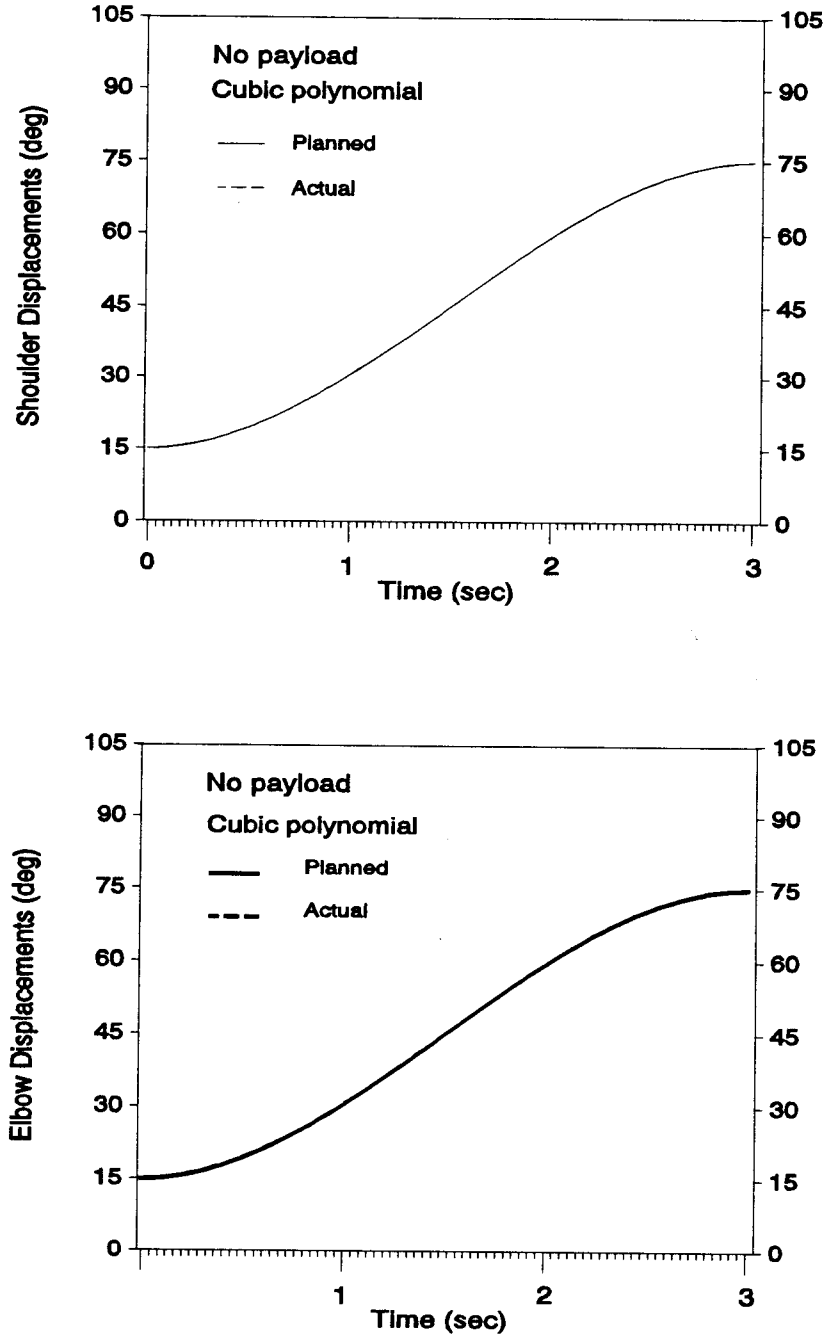


Figure 4.5 Actual joint displacements and planned joint displacements using cubic polynomial path for case 1.

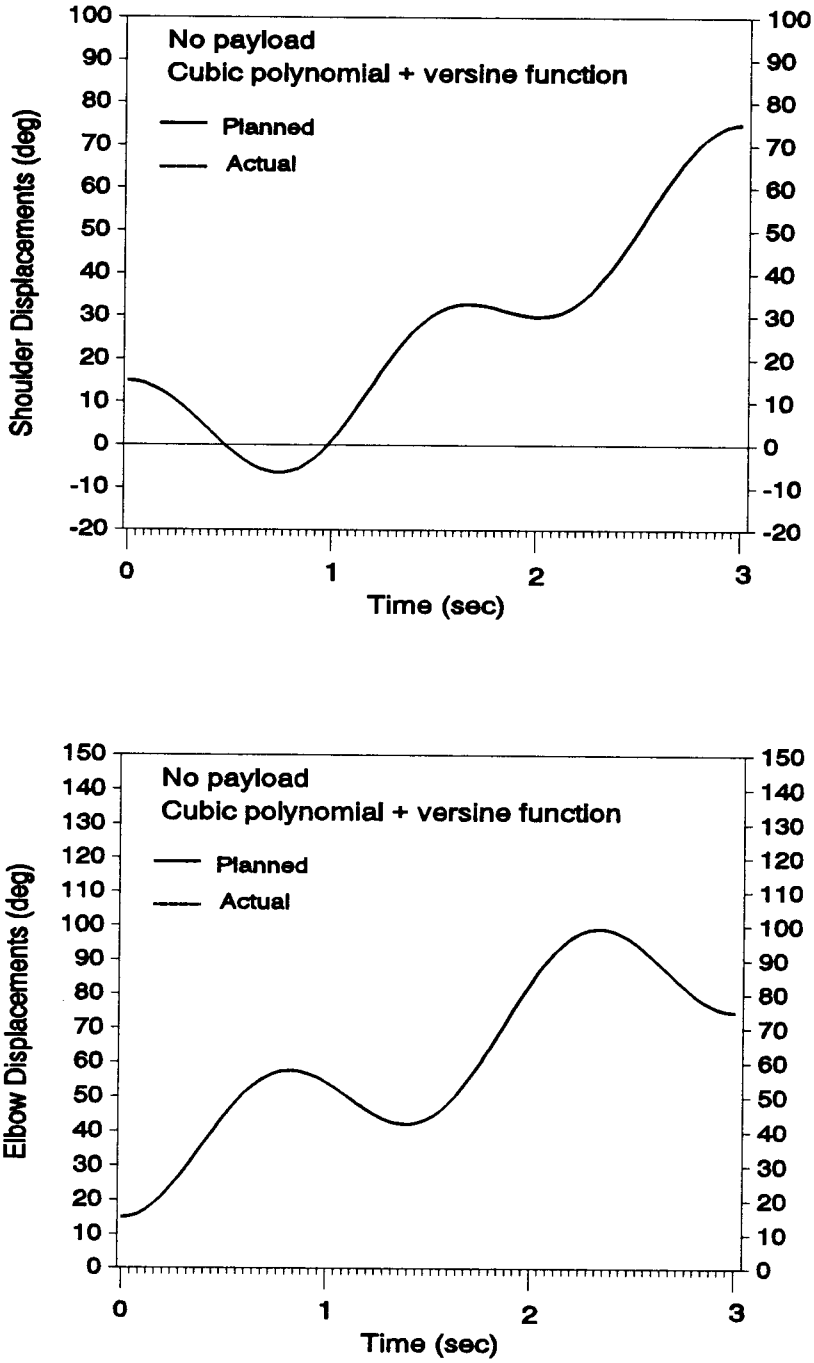


Figure 4.6 Actual joint displacements and planned joint displacements using cubic polynomial + versine function path for case 1.

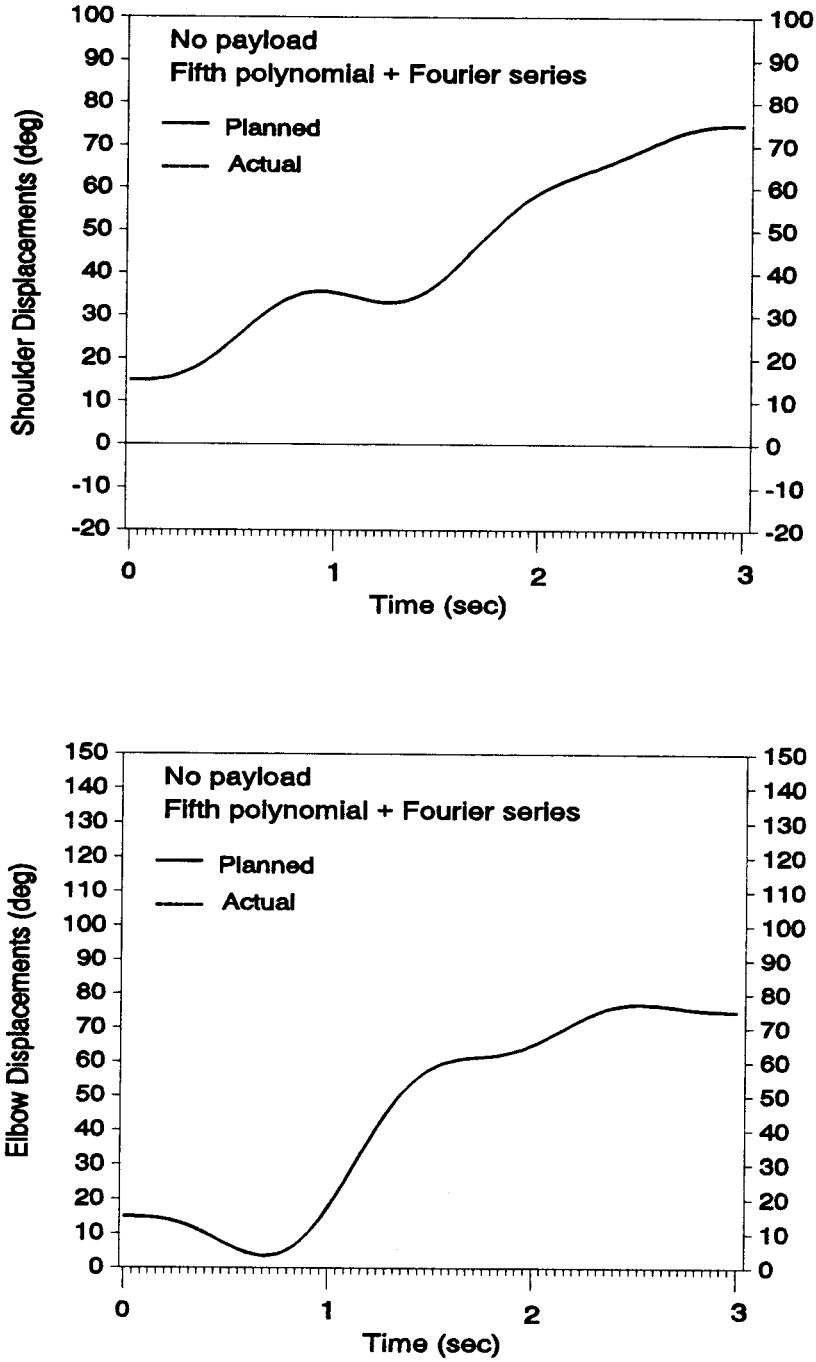


Figure 4.7 Actual joint displacements and planned joint displacements using fifth polynomial + fourier series path for case 1.

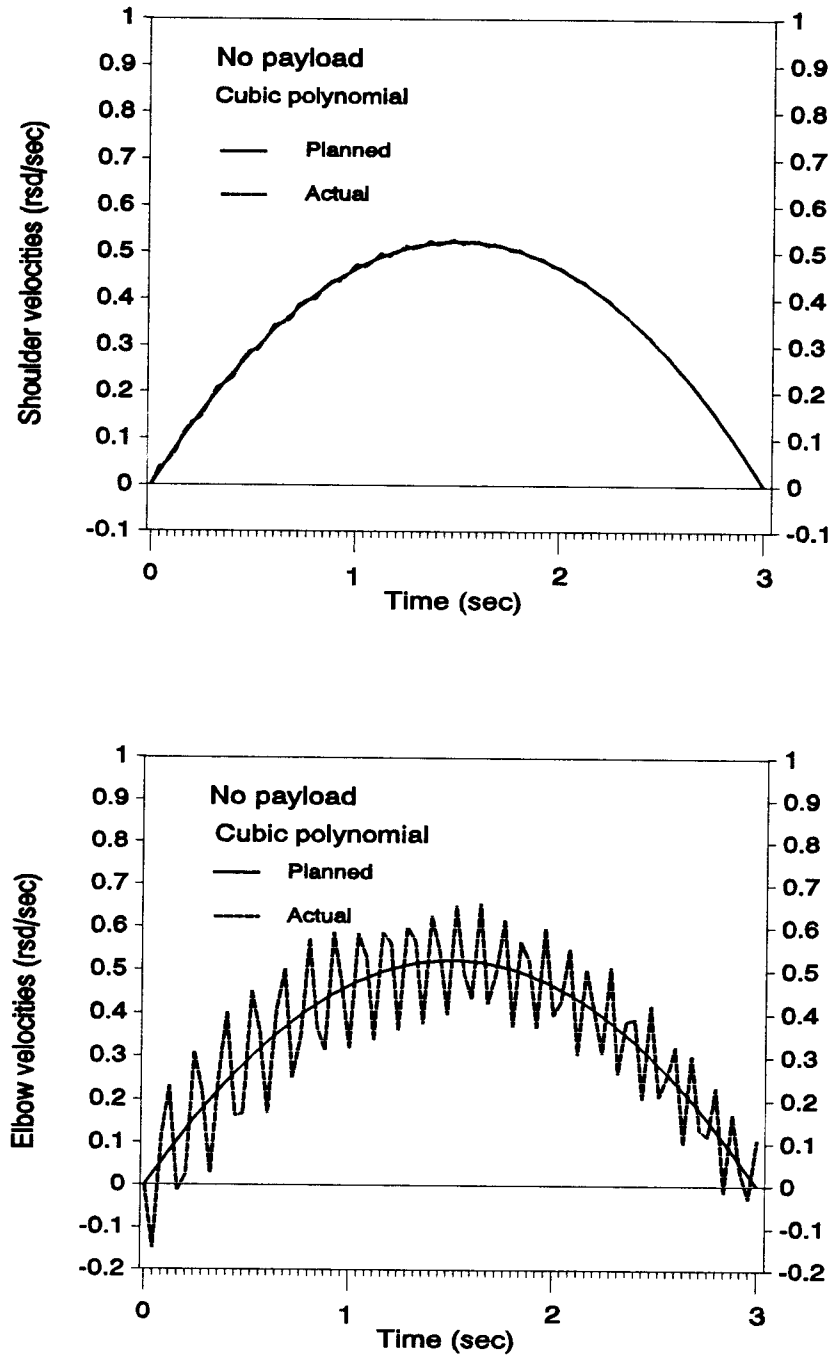


Figure 4.8 Actual joint velocities and planned joint velocities using cubic ploynomial + versine function path for case 1.

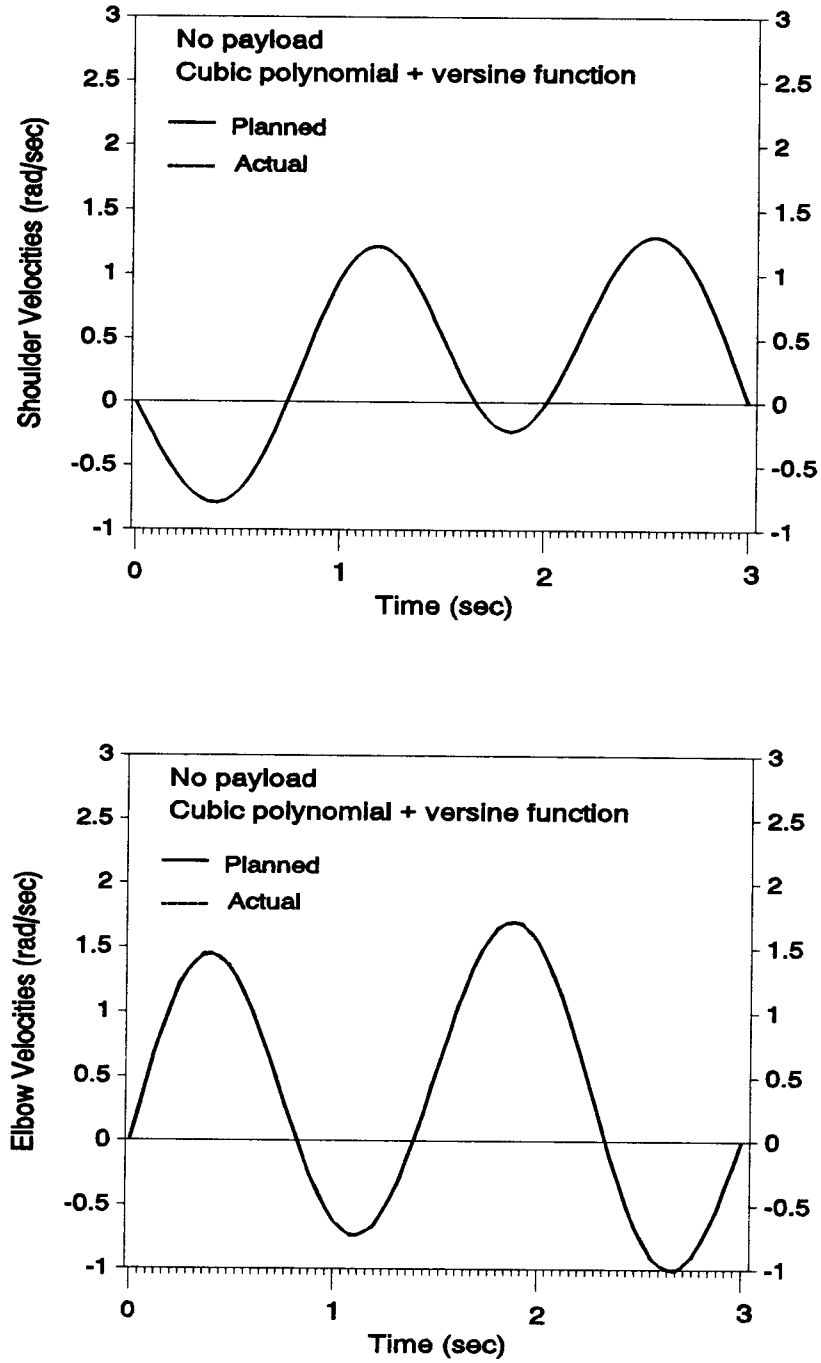


Figure 4.9 Actual joint velocities and planned joint velocities using cubic polynomial + versine function path for case 1.

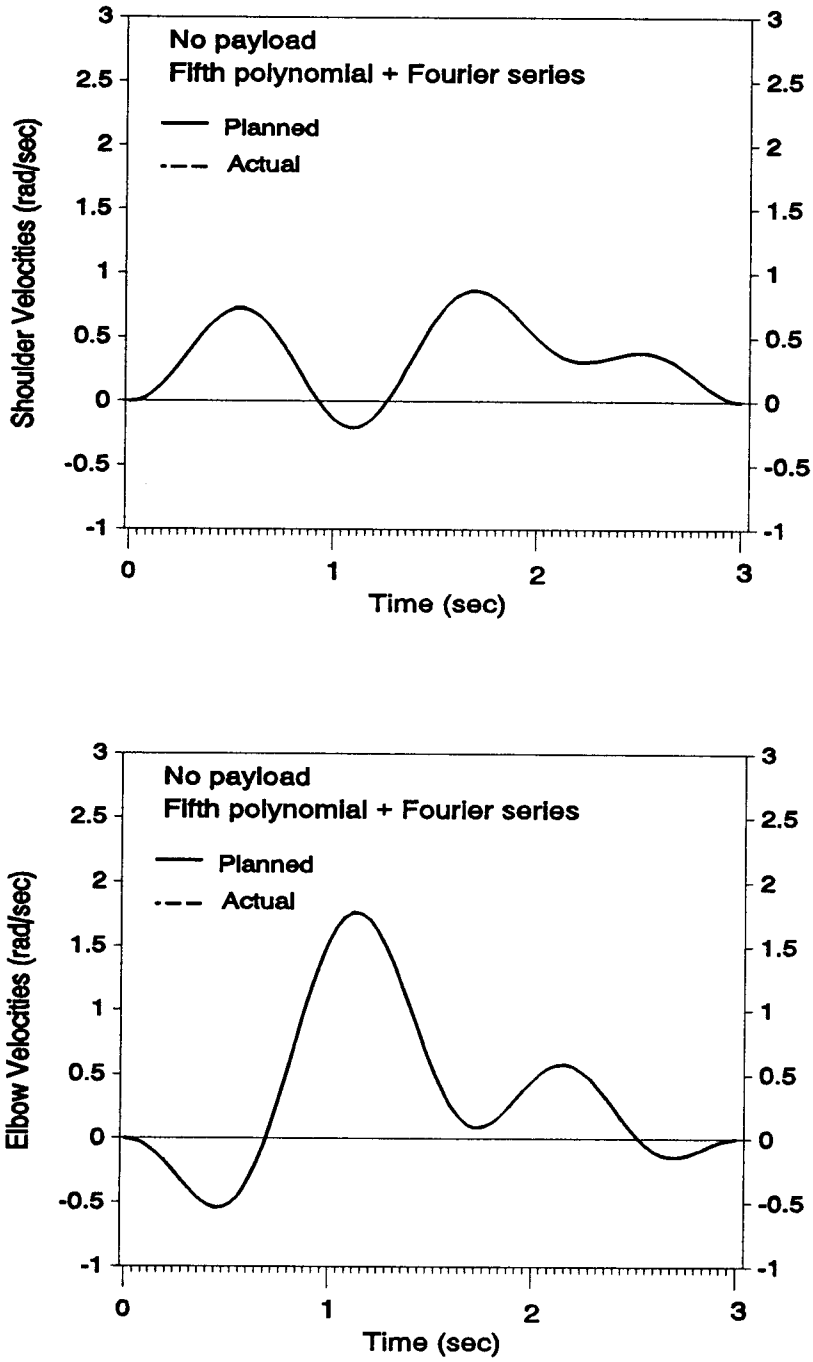


Figure 4.10 Actual joint velocities and planned joint velocities using fifth polynomial + Fourier series path for case 1.

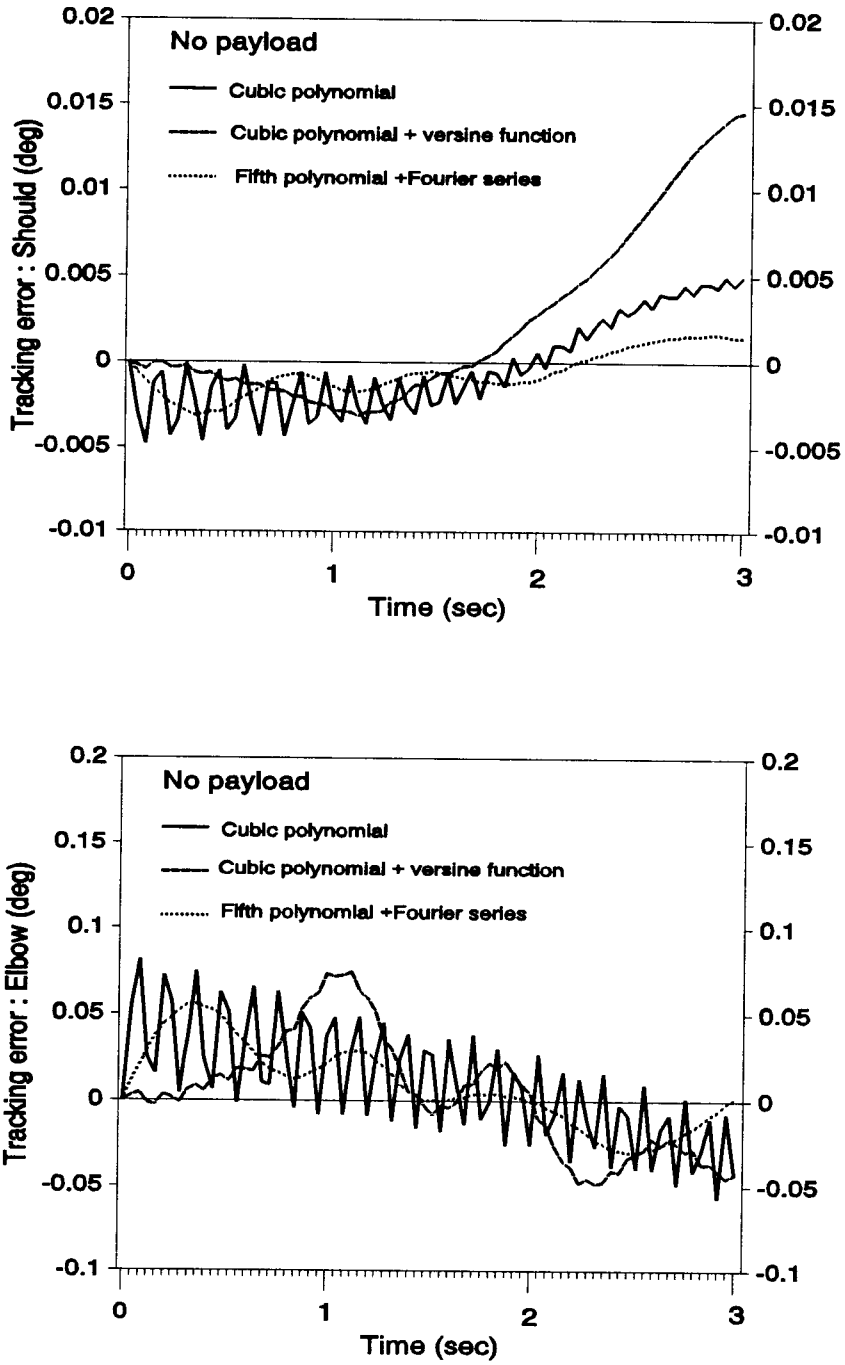


Figure 4.11 Tracking errors with three types of planned trajectories under no payload condition.

Table 5. Summary of Open-loop Trajectories Planning Results

| | | Cubic polynomial path | | | Cubic polynomial plus versine function path | | | Fifth polynomial plus Fourier series path | | |
|---|---|---|---|---|---|---|---|---|---|---|
| Various loading Conditions | Joint | Max. Error (degree) | Final Position Error (degree) | Max. Torque (N·m) | Max. Error (degree) | Final Position Error (degree) | Max. Torque (N·m) | Max. Error (degree) | Final Position Error (degree) | Max. Torque (N·m) |
| Case 1: 0 kg No load | 1<br>2 | 0.0050<br>0.0814 | 0.0050<br>0.0432 | 1.6874<br>0.6957 | 0.0146<br>0.0745 | 0.0146<br>0.0425 | 3.9193<br>1.0986 | 0.0031<br>0.0559 | 0.0015<br>0.0016 | 2.6264<br>0.8507 |
| Case 2: 0.5 kg 1/2 max. load | 1<br>2 | 0.0322<br>0.4056 | 0.0206<br>0.1980 | 5.1766<br>2.8013 | 0.0176<br>0.1630 | 0.0176<br>0.0434 | 8.9922<br>2.0206 | 0.0201<br>0.2806 | 0.0093<br>0.0023 | 6.2596<br>3.0574 |
| Case 3: 1.0 kg max.load | 1<br>2 | 0.0627<br>0.6262 | 0.0627<br>0.5861 | 8.6258<br>4.8769 | 0.0313<br>0.3408 | 0.0313<br>0.1154 | 12.7558<br>4.1042 | 0.0359<br>0.4955 | 0.0242<br>0.0083 | 9.8100<br>5.2288 |

strongly thrusts the endpoint off the path near the target point. Substantial torques are required to overcome these natural movement dynamics and to maintain the planned endpoint trajectory. In Figure 4.11, trajectories with planned fifth order polynomial plus Fourier-type based series which reach zero accelerations at the final position shows that good accuracy can be obtained while maintain small tracking error during operation.

The tip vibration and the corresponding velocity of the flexible link are shown in Figure 4.12 and 4.13, respectively. It is clear that the normal cubic polynomial path induces transverse vibrations of the flexible link, large vibration amplitude of the link at the free end. The amplitude of link vibrations are greatly attenuated and the higher-frequency eigenvibrations of the flexible link are eliminated by the action of selecting the optimal path. This is due to the fact that higher-frequency eigenvibrations need a great amount of energy for excitation. However, the open-loop trajectory planning is unable to completely eliminate the lower-frequency vibrations. That is because of the fact that the only control that is applied to the system is the motor torques. For complete elimination of vibrations, it would be necessary to apply additional controls to the system.

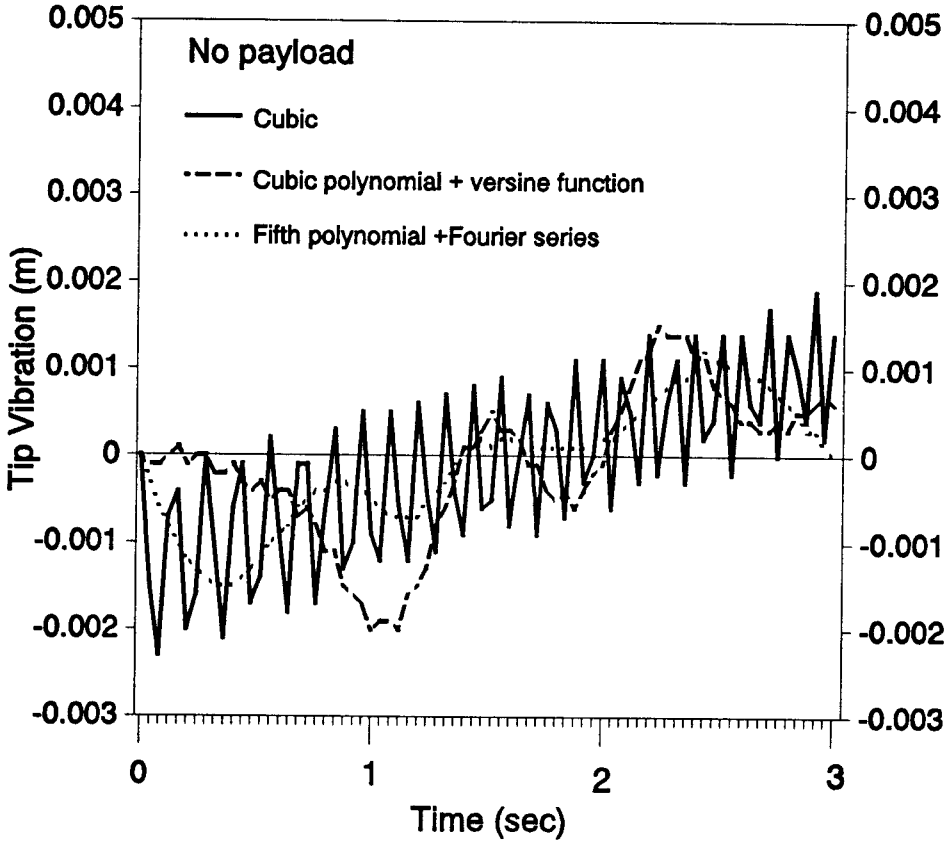


Figure 4.12 Tip vibrations with three types of planned trajectories under no payload condition.

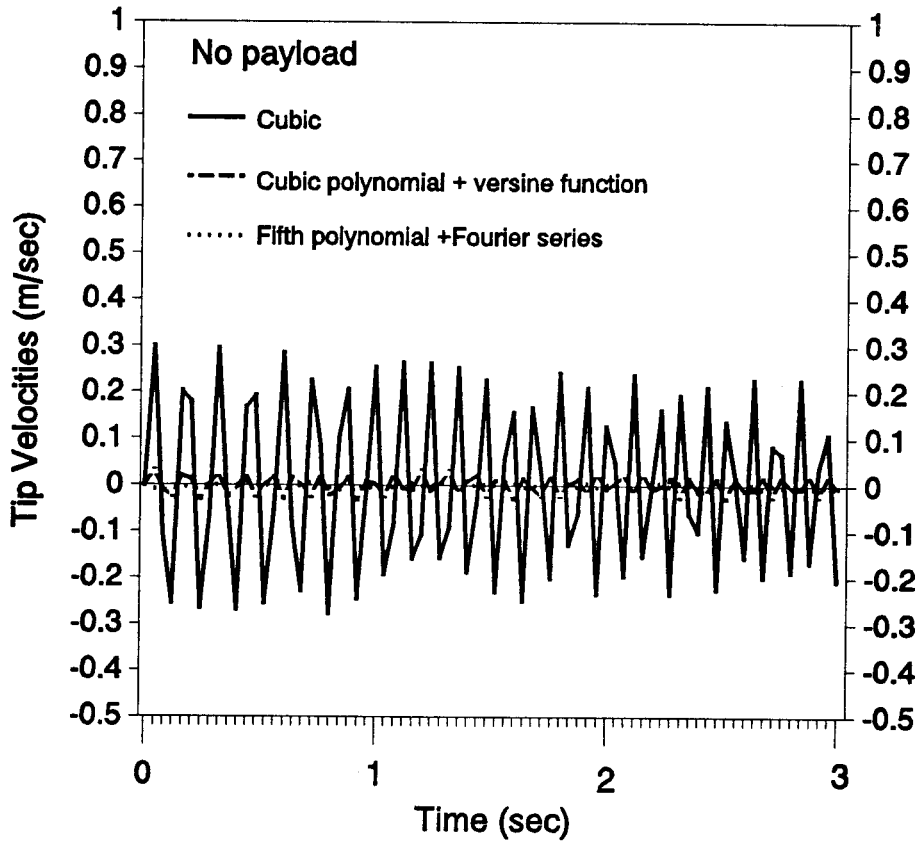


Figure 4.13 Tip vibrational velocities with three types of planned trajectories under no payload condition.

Figure 4.14 exhibits the vibration energy for different planned schemes with no payload. Both Schmitt's approximation and Nagurka's approximation generate very small vibration energy compared to the normal cubic polynomial planned path.

The integrand of the control effort (i.e., $\tau_1^2+\tau_2^2$) is displayed in Figure 4.15, it shows that high accuracy can be achieve with the proposed Fourier-type shape function approach while the required control effort remains small.

The remainder of the figures (Figure 4.16-4.37) show the simulation results of loading case 2 ($m_p$ = 0.5 kg) and case 3 ($m_p$ = 1.0 kg), which lead to the same conclusions as for the unloaded case.

Comparison of Figure 4.12, 4.23 and 4.34 shows that the smaller the payload the more the higher frequency tip vibrations were eliminated. Increase in the payload will result in a decrease in the fundamental natural frequency of the system. For a manipulator arm system with low fundamental natural frequency, the simulation result in Figure 4.34 indicated that the open-loop control will not obtain significant reduction of tracking error during operation although the finial positioning error can remain in an acceptable range. This large-motion tracking error makes it unsuitable for applying a feedback control algorithm based on the linearizied model around the operating trajectories for heavy loading case. Thus,

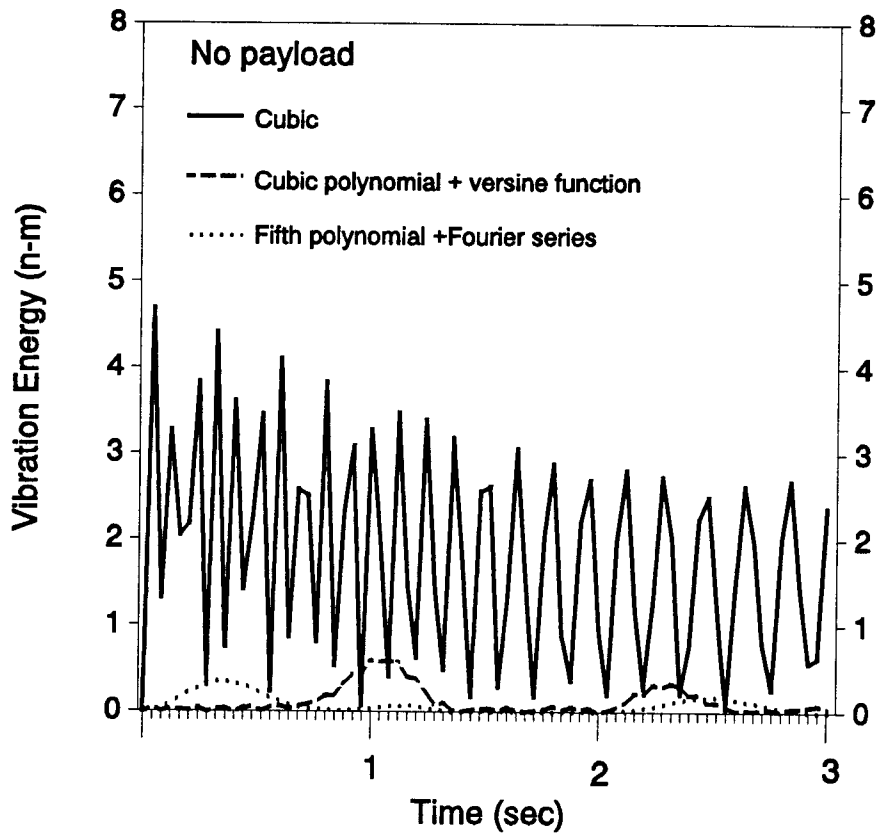


Figure 4.14 Vibrational energy for proposed trajectories with no payload.

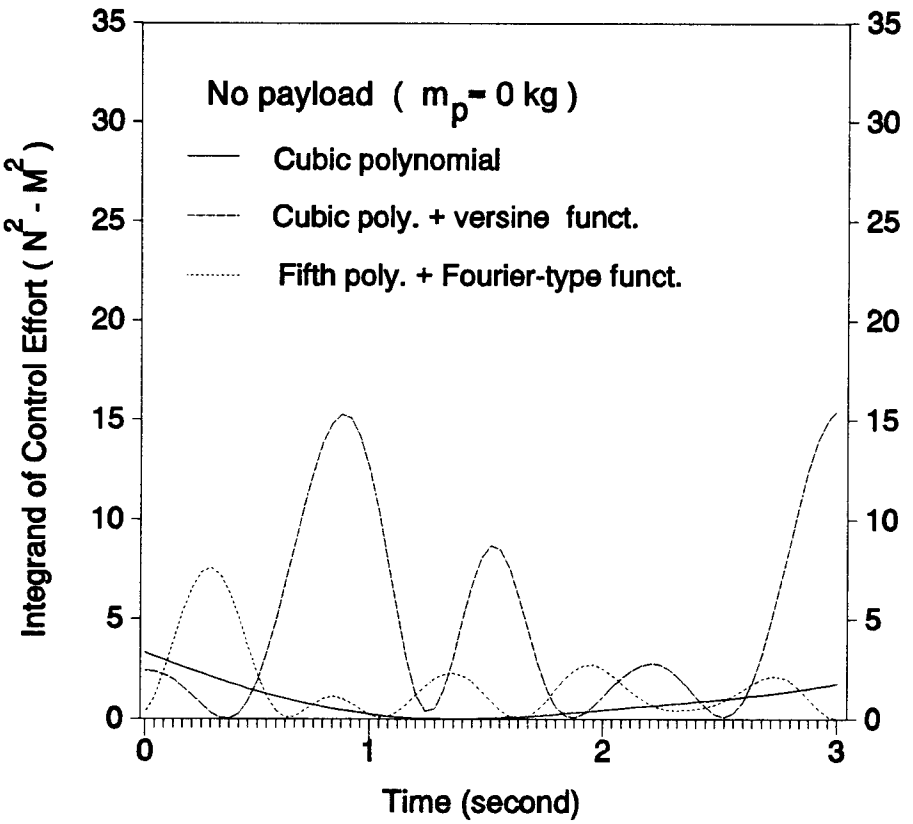


Figure 4.15 Integrand of control effort ($\tau_1^2+\tau_2^2$) with no payload.

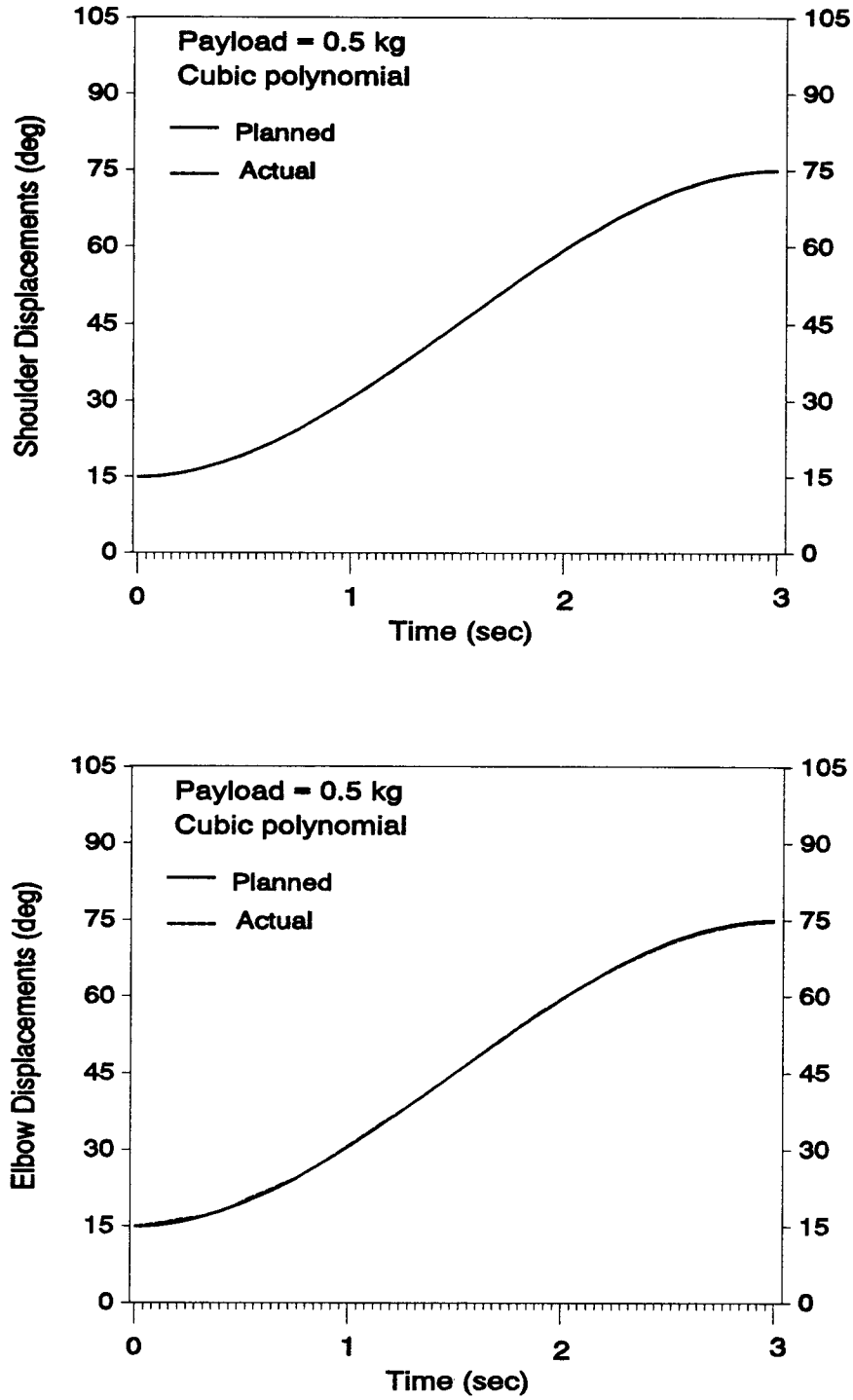


Figure 4.16 Actual joint displacements and planned joint displacements using cubic polynomial path for case 2.

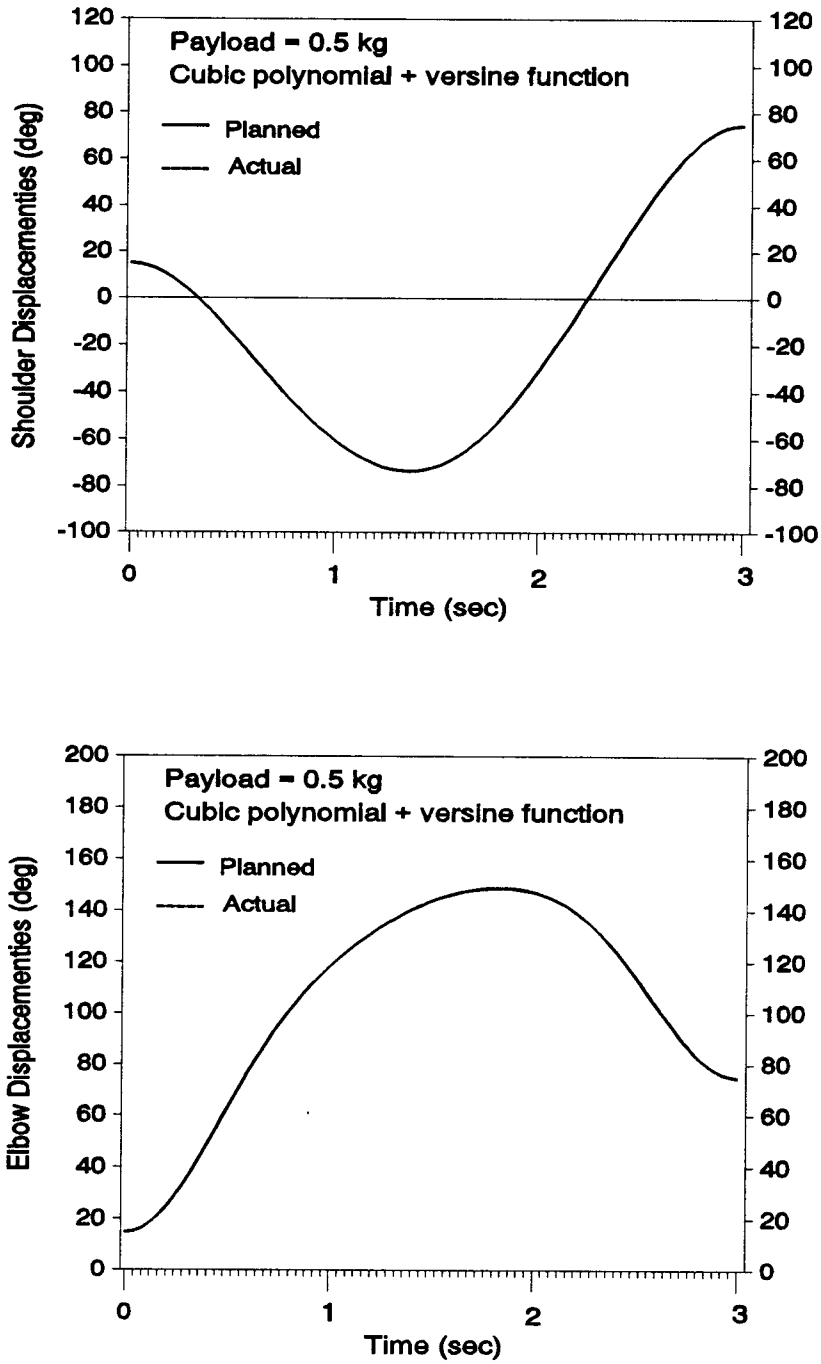


Figure 4.17 Actual joint displacements and planed joint displacements using cubic polynomial + versine function path for case 2.

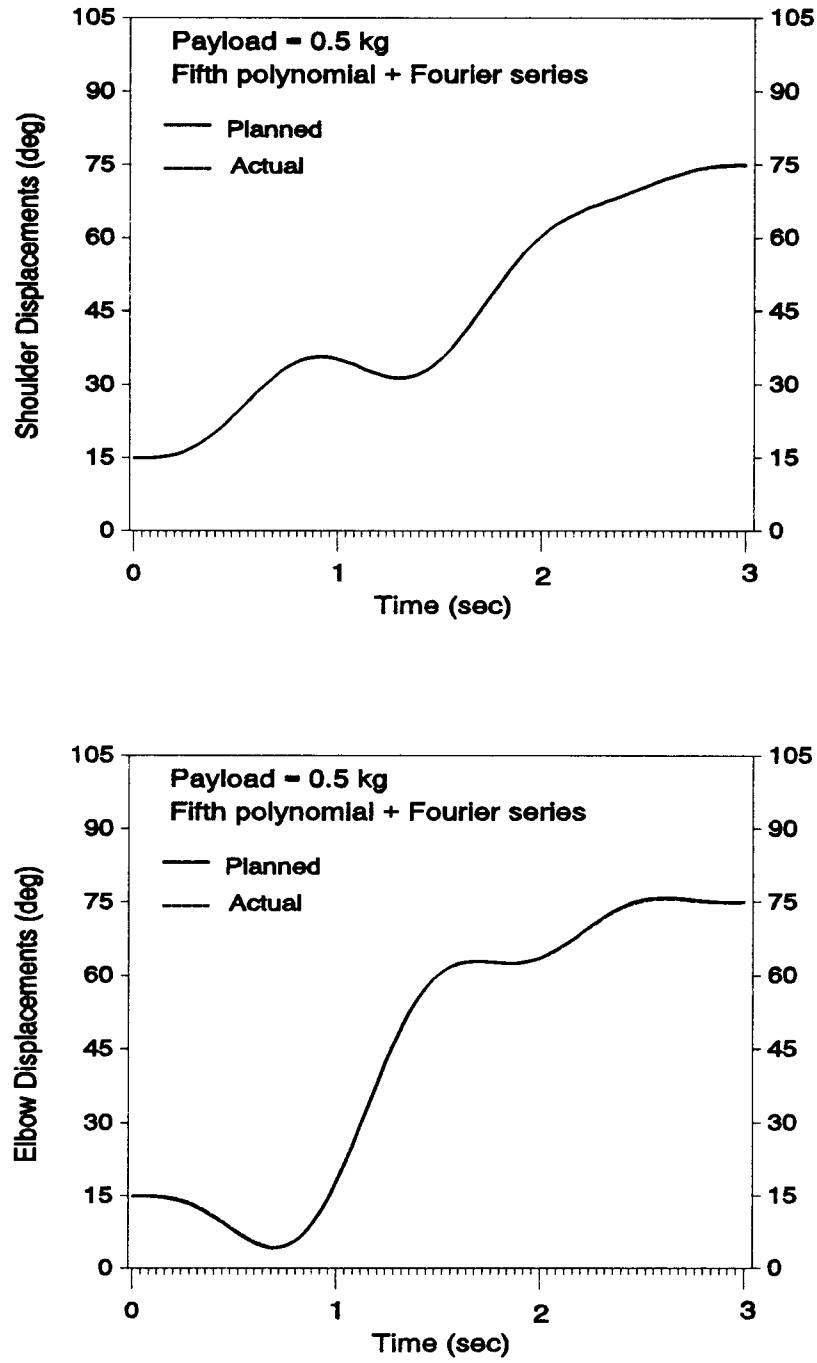


Figure 4.18 Actual joint displacements and planned joint displacements using fifth polynomial + Fourier series path for case 2.

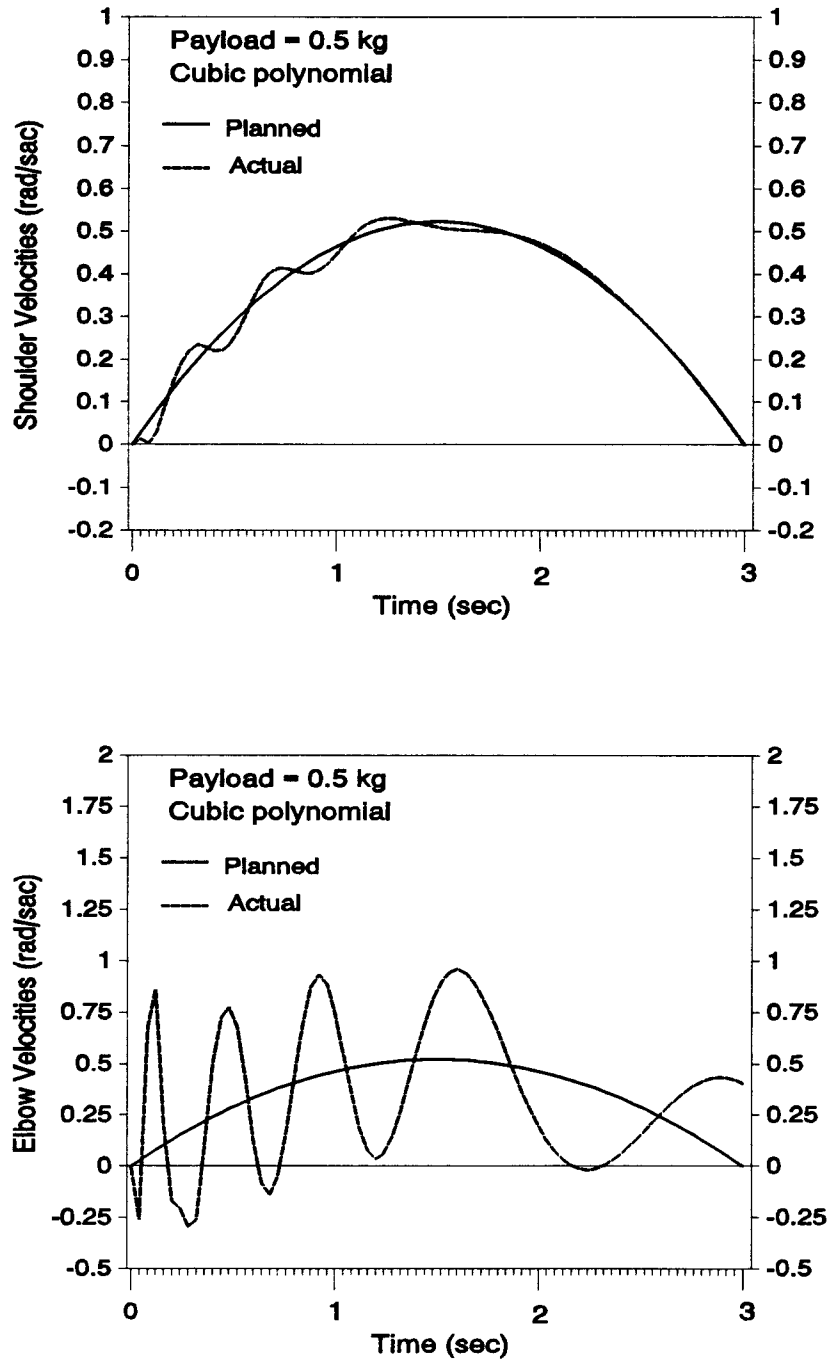


Figure 4.19 Actual joint velocities and planned joint velocities using cubic polynomial for case 2.

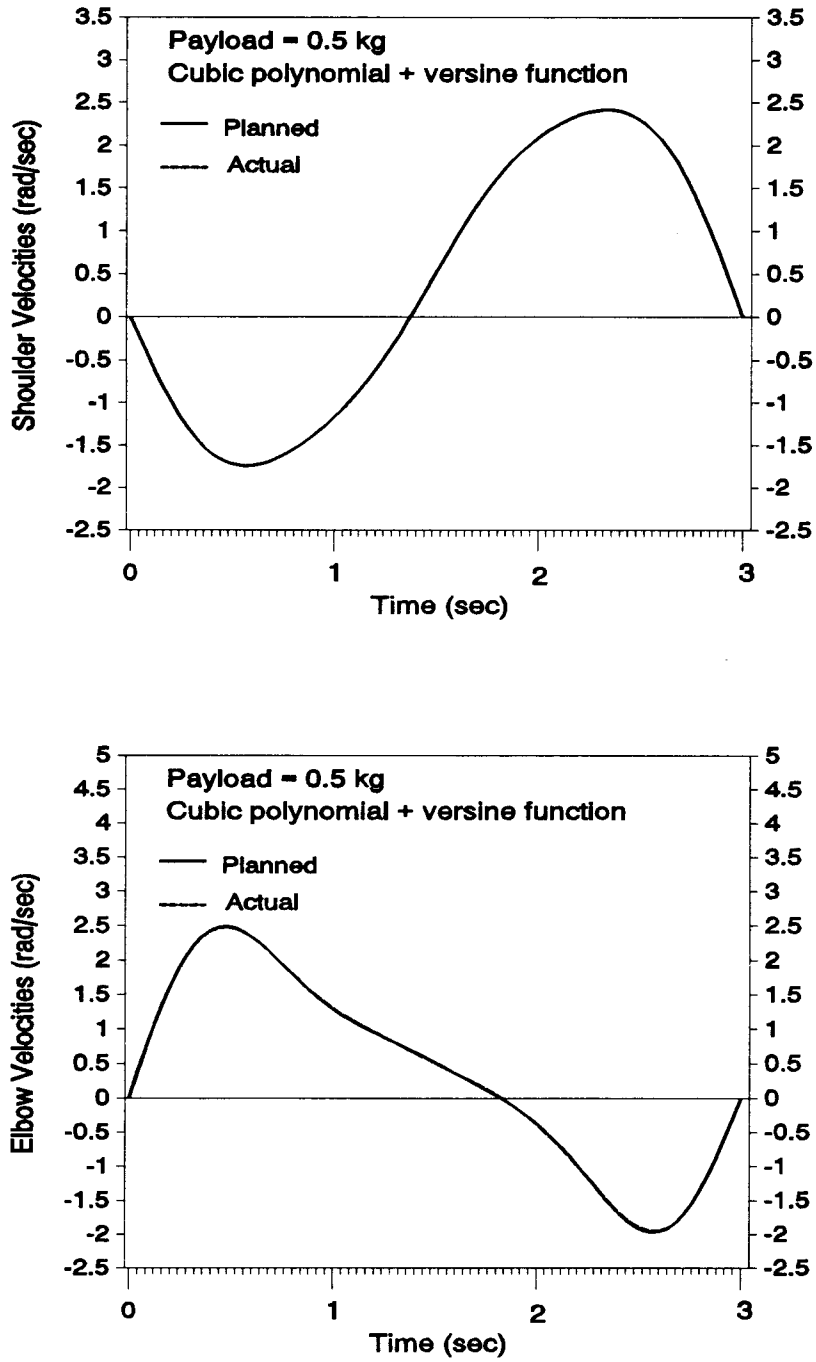


Figure 4.20 Actual joint velocities and planned joint velocities using cubic polynomial + versine function path for case 2.

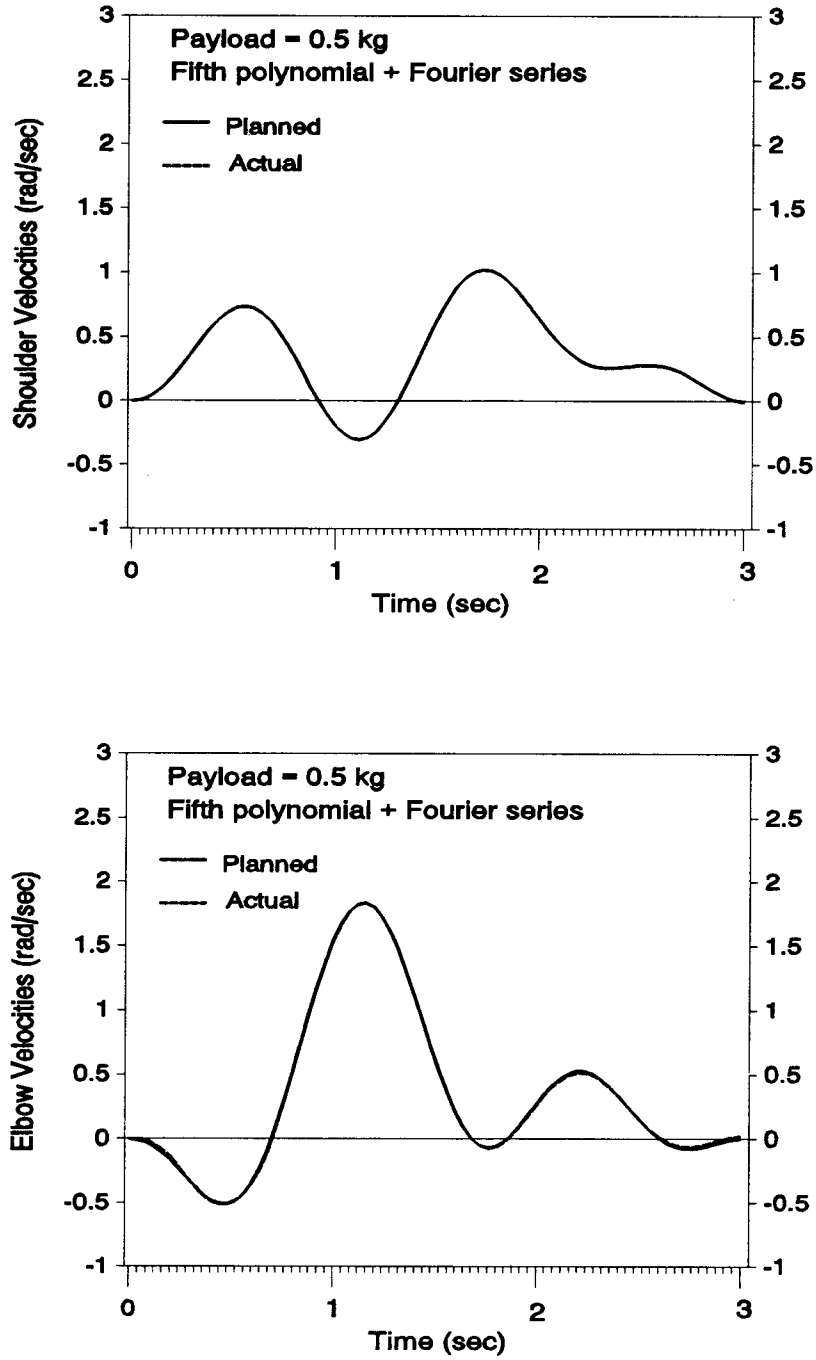


Figure 4.21 Actual joint velocities and planned joint velocities using fifth polynomial + Fourier series path for case 2.

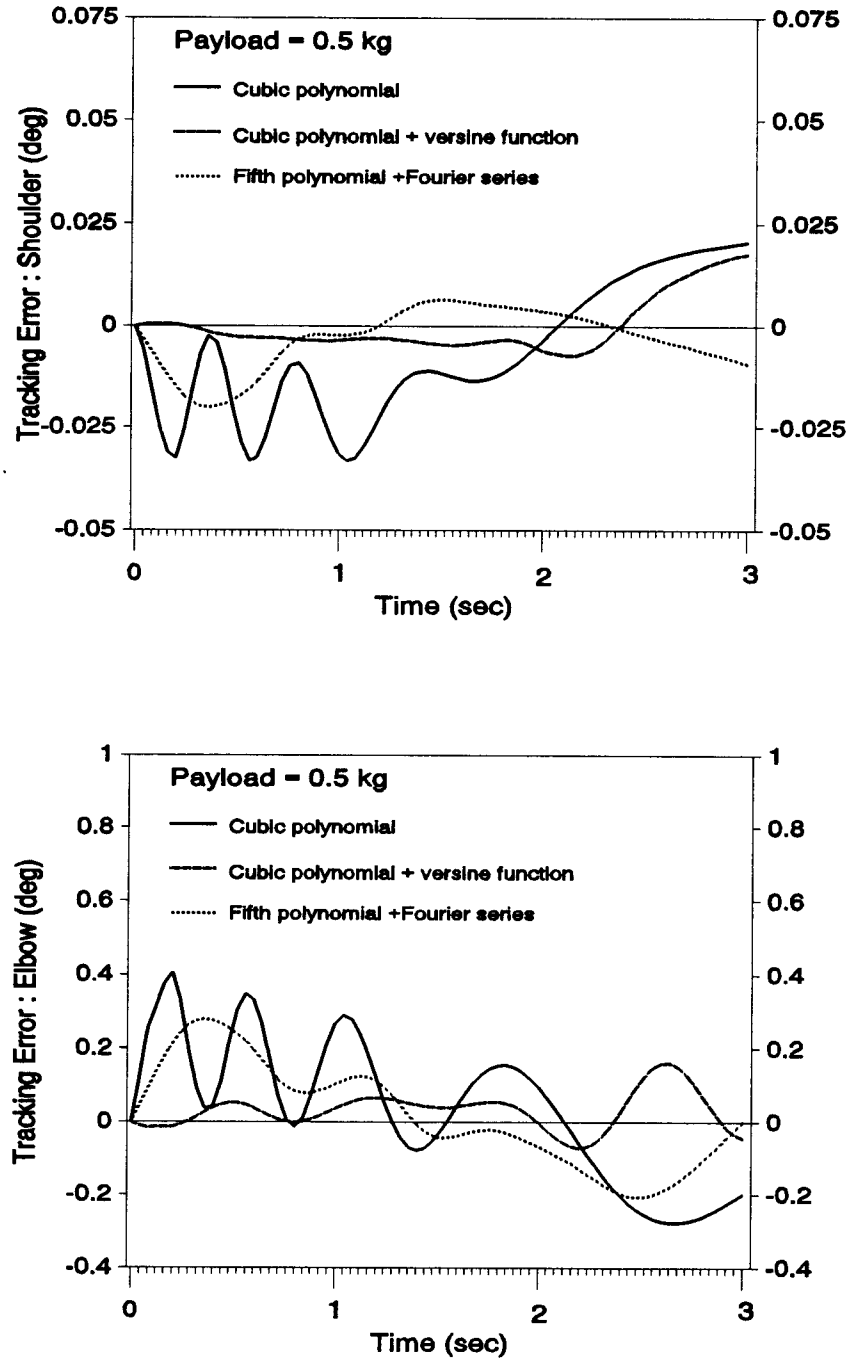


Figure 4.22 Tracking errors for proposed trajectories with payload = 0.5 kg.

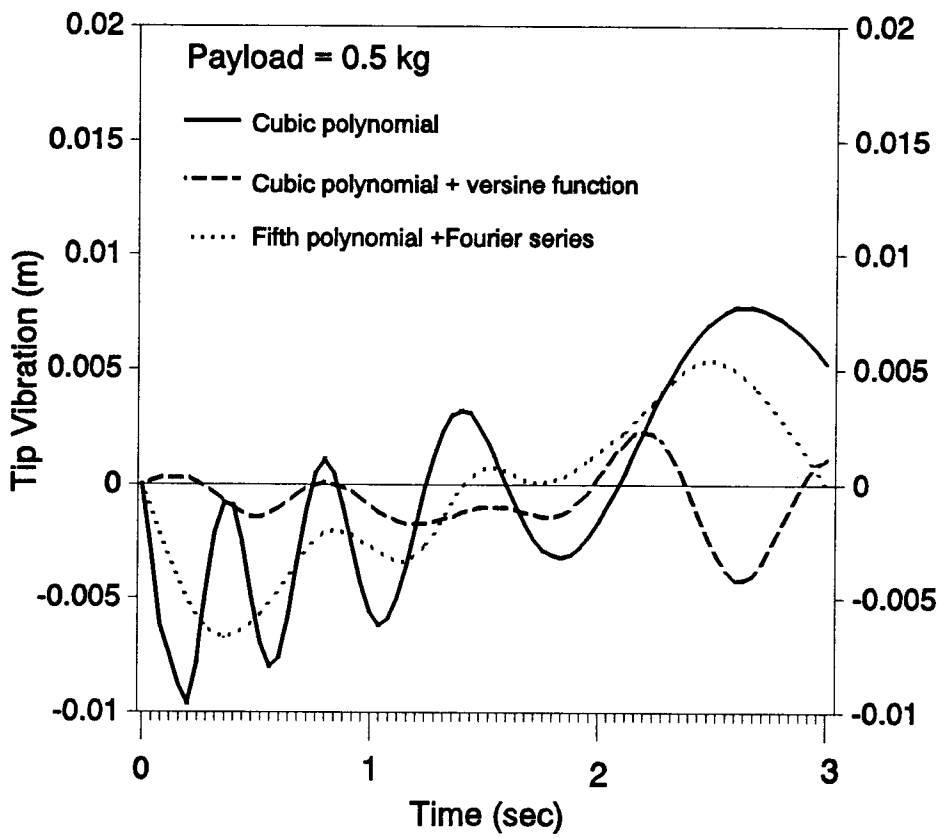


Figure 4.23 Tip vibrations for proposed trajectories with payload = 0.5 kg.

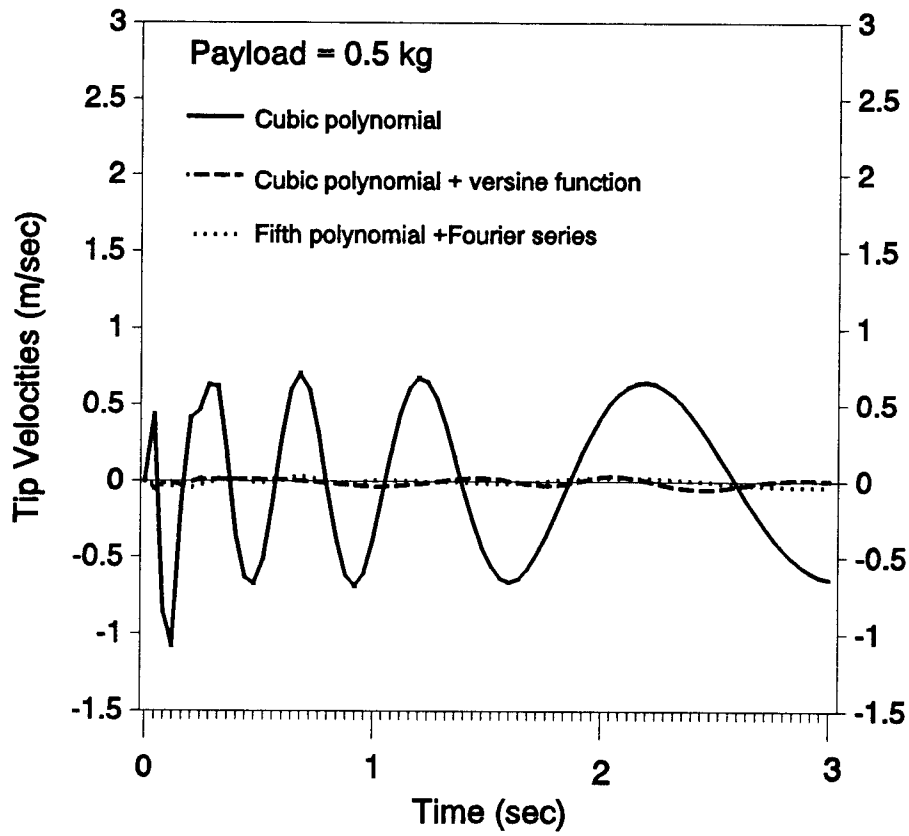


Figure 4.24 Tip vibrational velocities for proposed trajectories with payload = 0.5 kg.

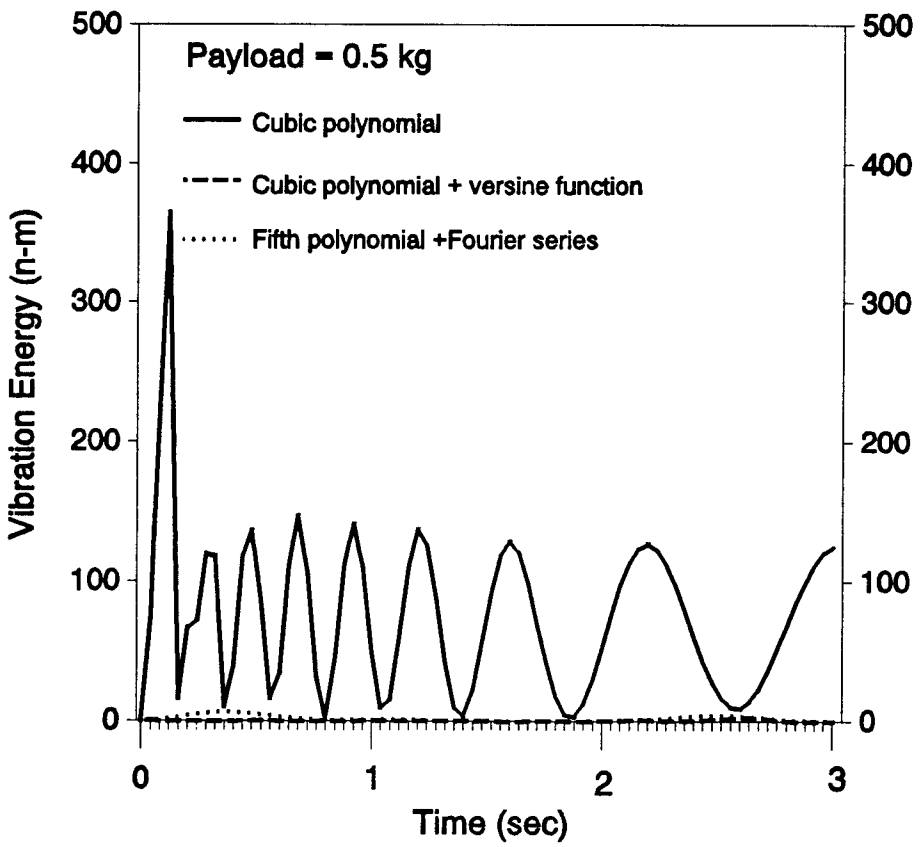


Figure 4.25 Vibrational energy for proposed trajectories with payload = 0.5 kg.

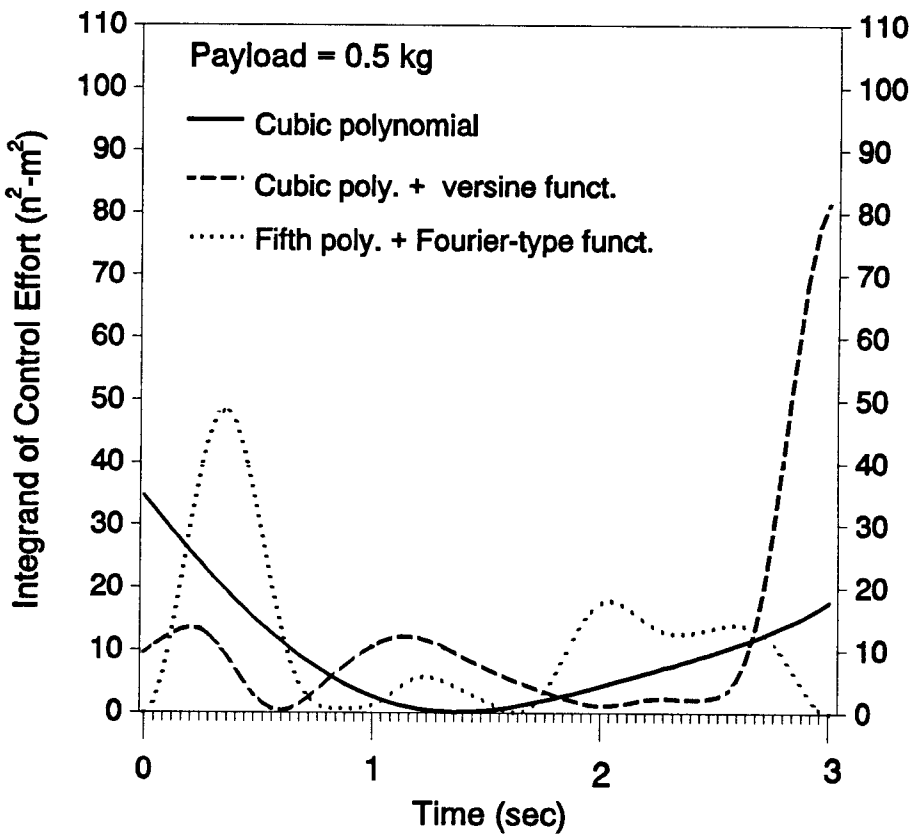


Figure 4.26 Integrand of control effort $(\tau_1^2+\tau_2^2)$ with payload = 0.5kg.

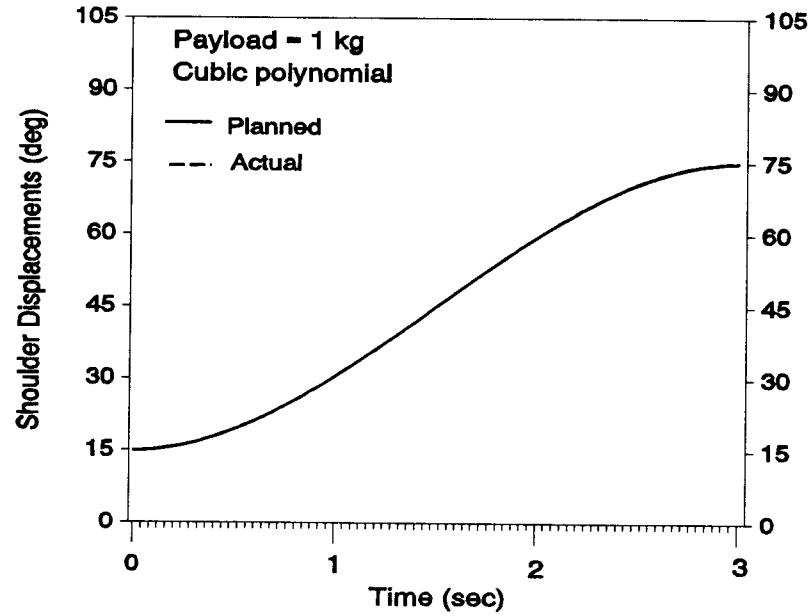


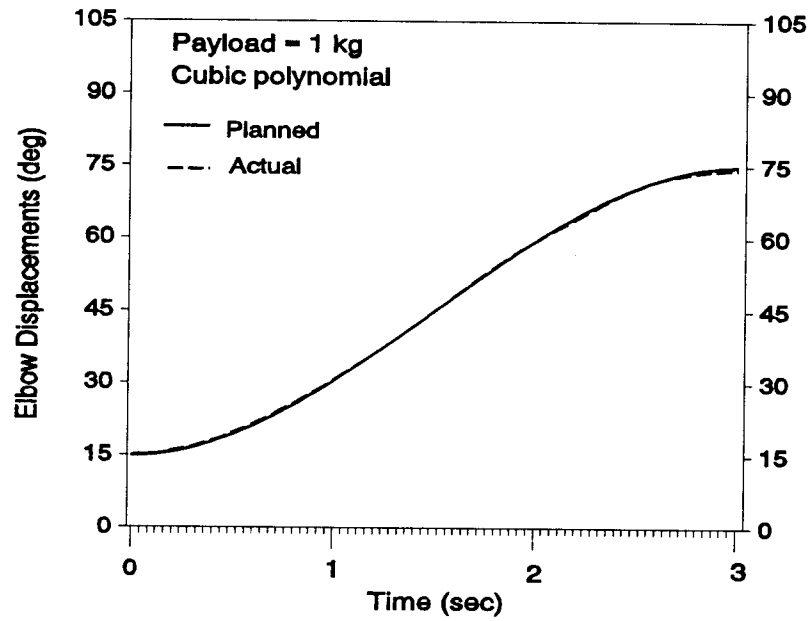


Figure 4.27 Actual joint displacements and planned joint displacements using cubic polynomial path for case 3.

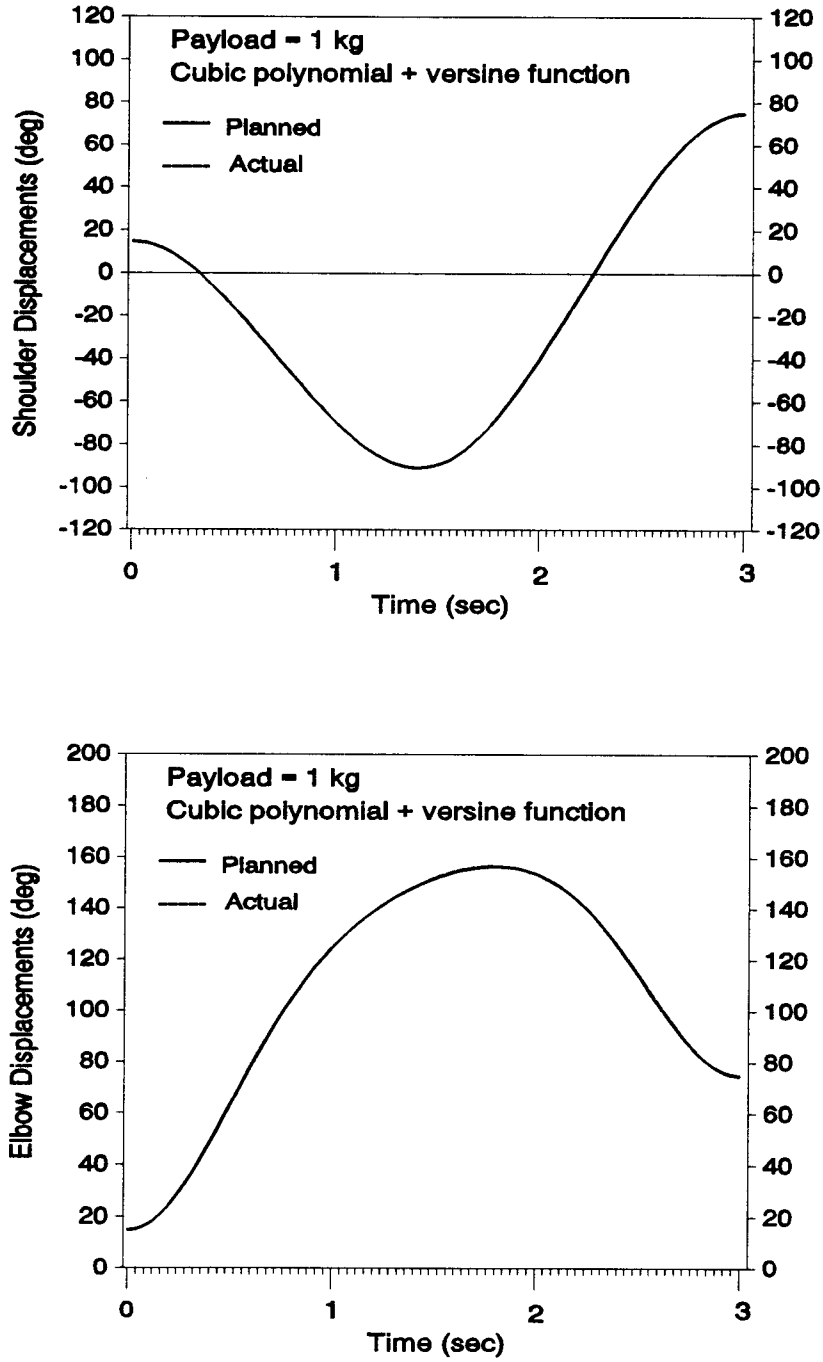


Figure 4.28 Actual joint displacements and planned joint velocities using cubic polynomial + versine function path for case 3.

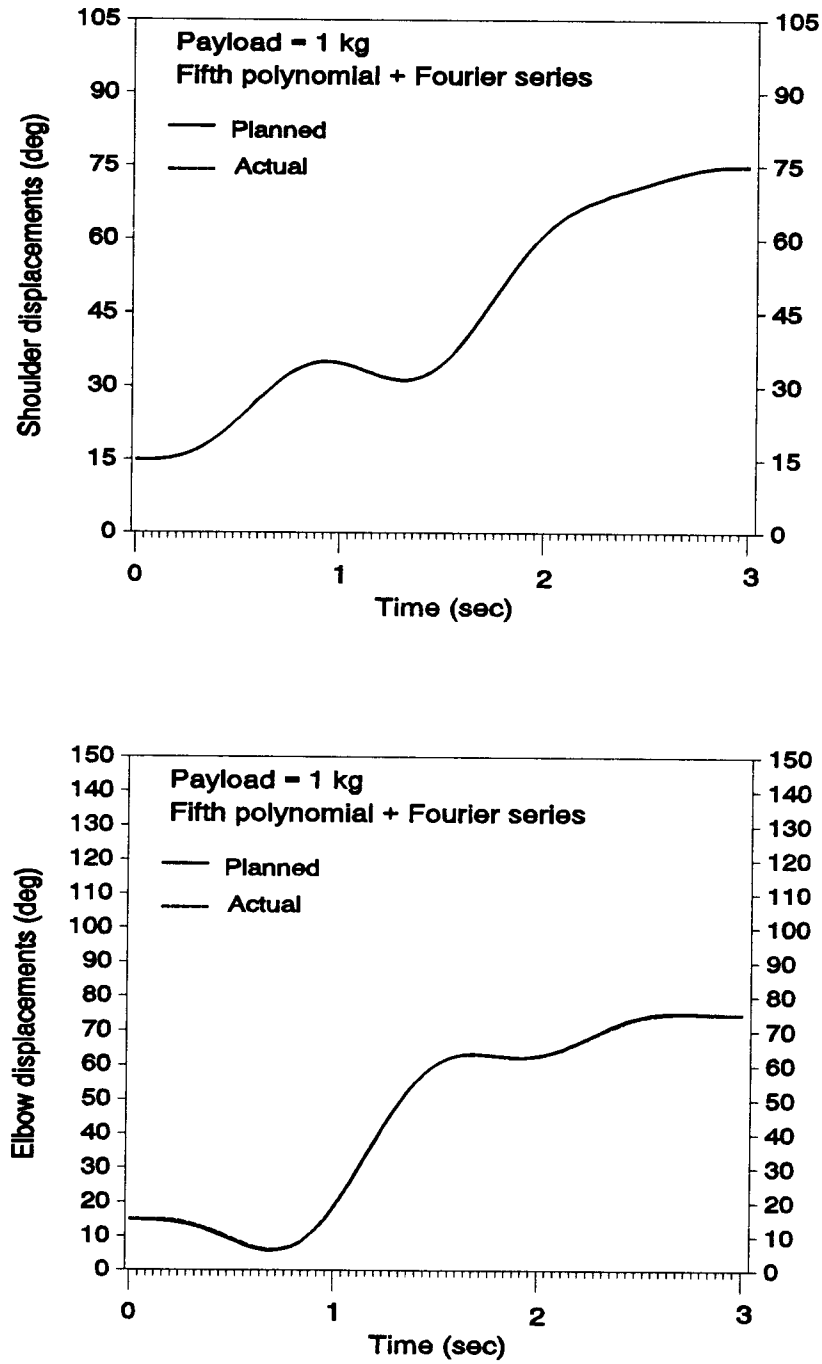


Figure 4.29 Actual joint displacements and planned joint displacements using fifth polynomial + Fourier series path for case 3.

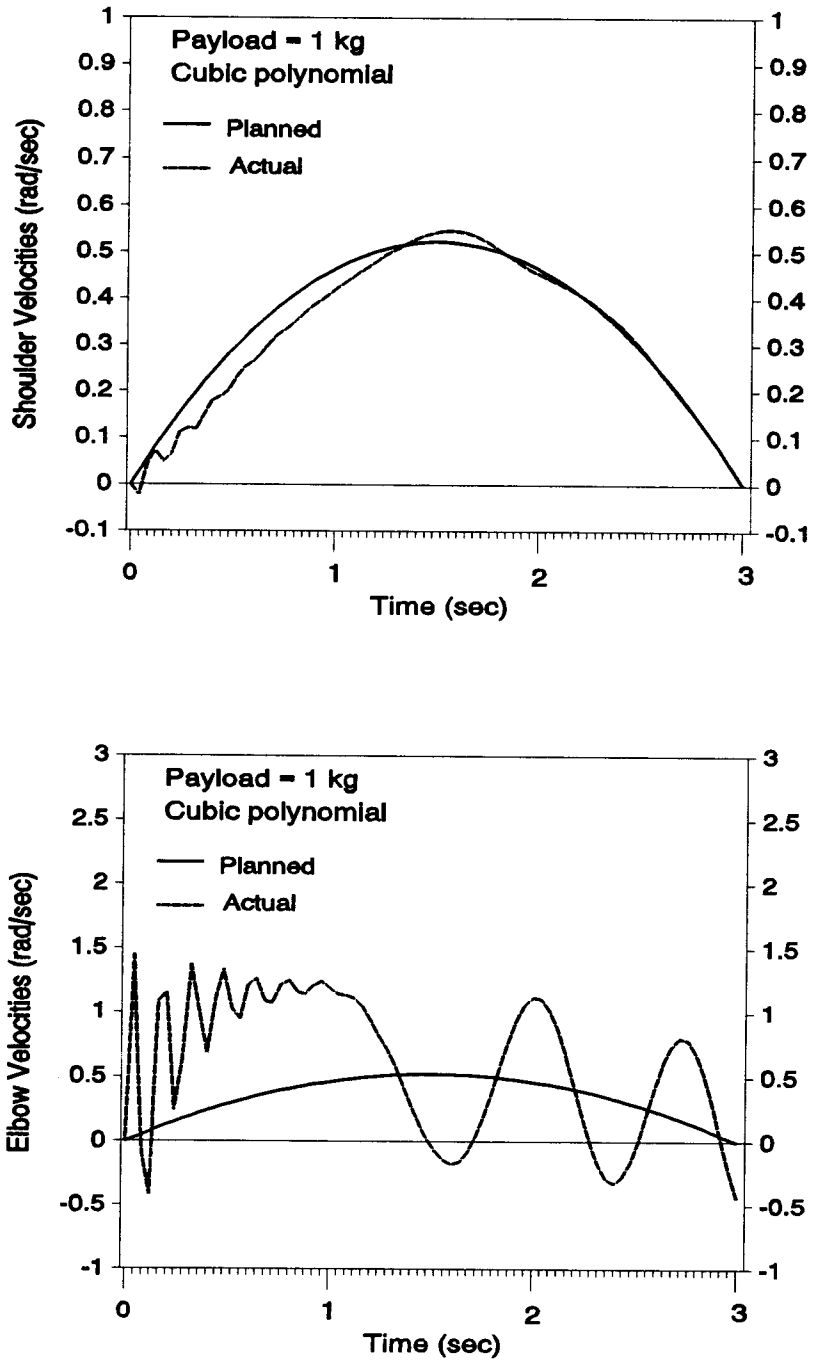


Figure 4.30 Actual joint velocities and planned joint velocities using cubic polynomial path for case 3.

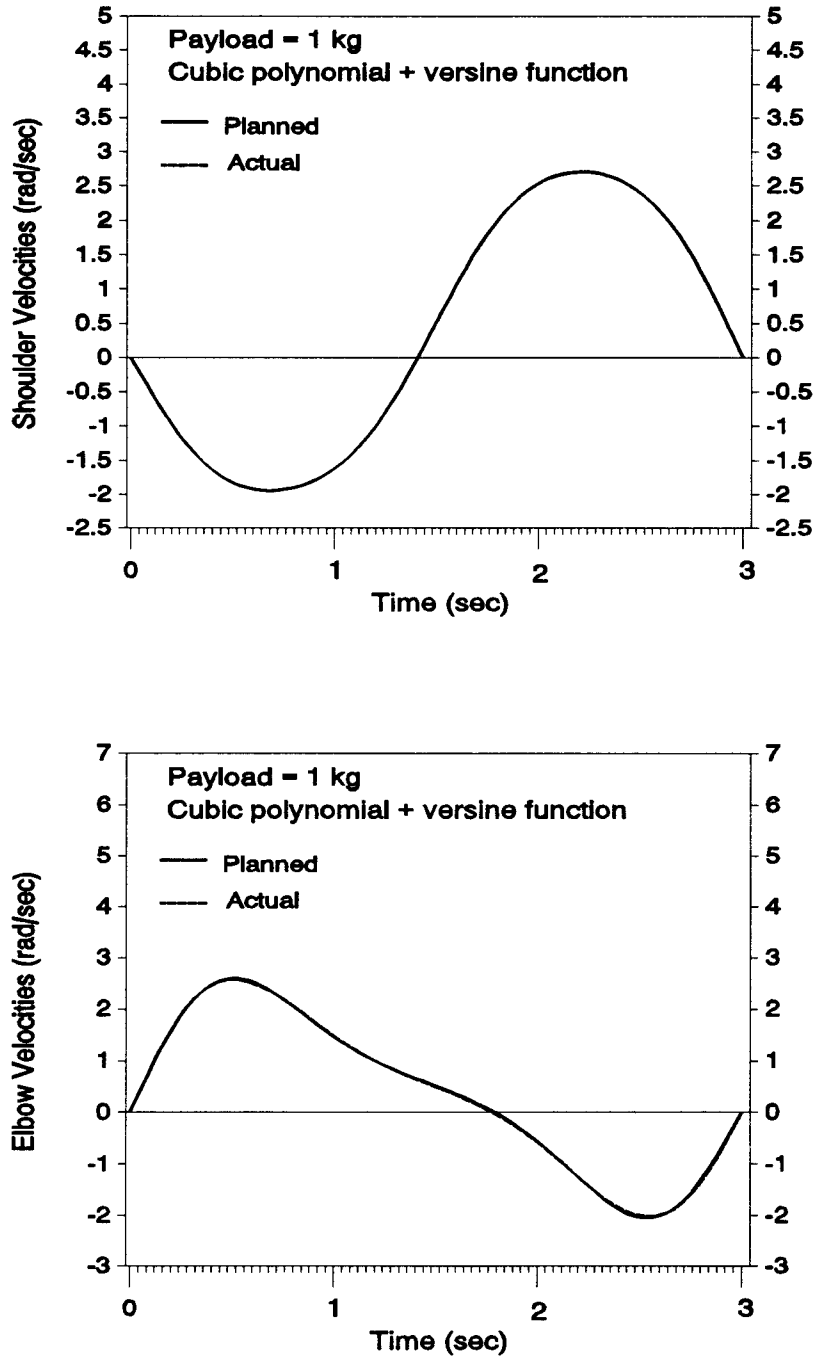


Figure 4.31 Actual joint velocities and planned joint velocities using cubic polynomial + versine function path for case 3.

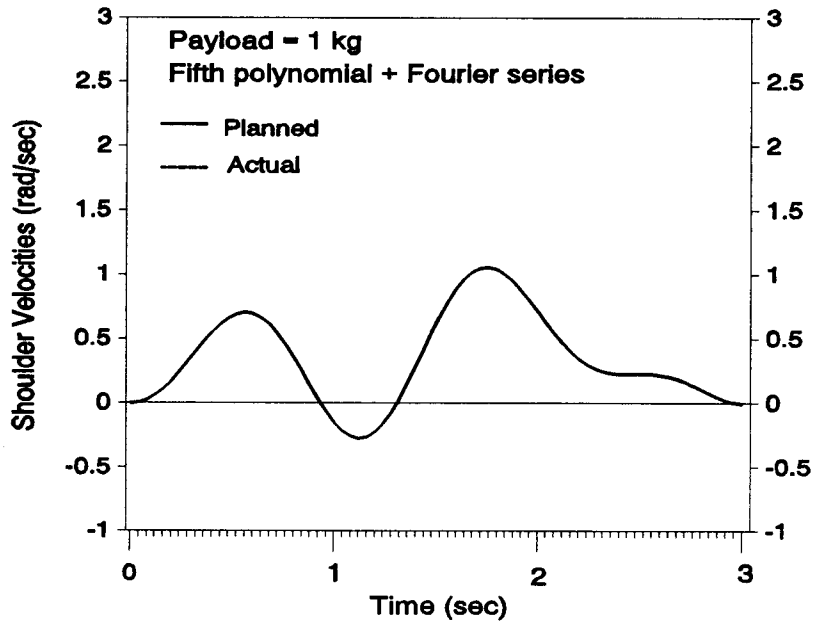


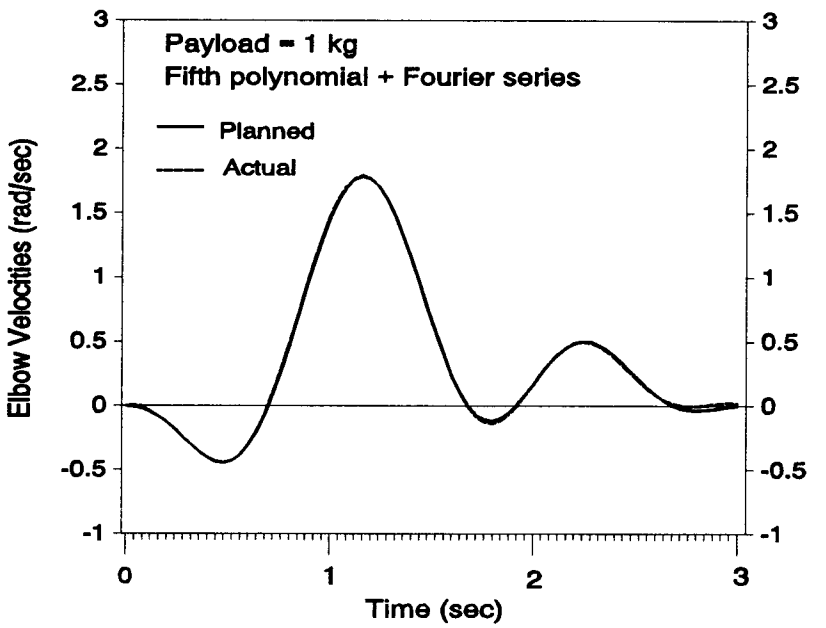


Figure 4.32 Actual joint velocities and planned joint velocities using fifth polynomial + Fourier series path for case 3.

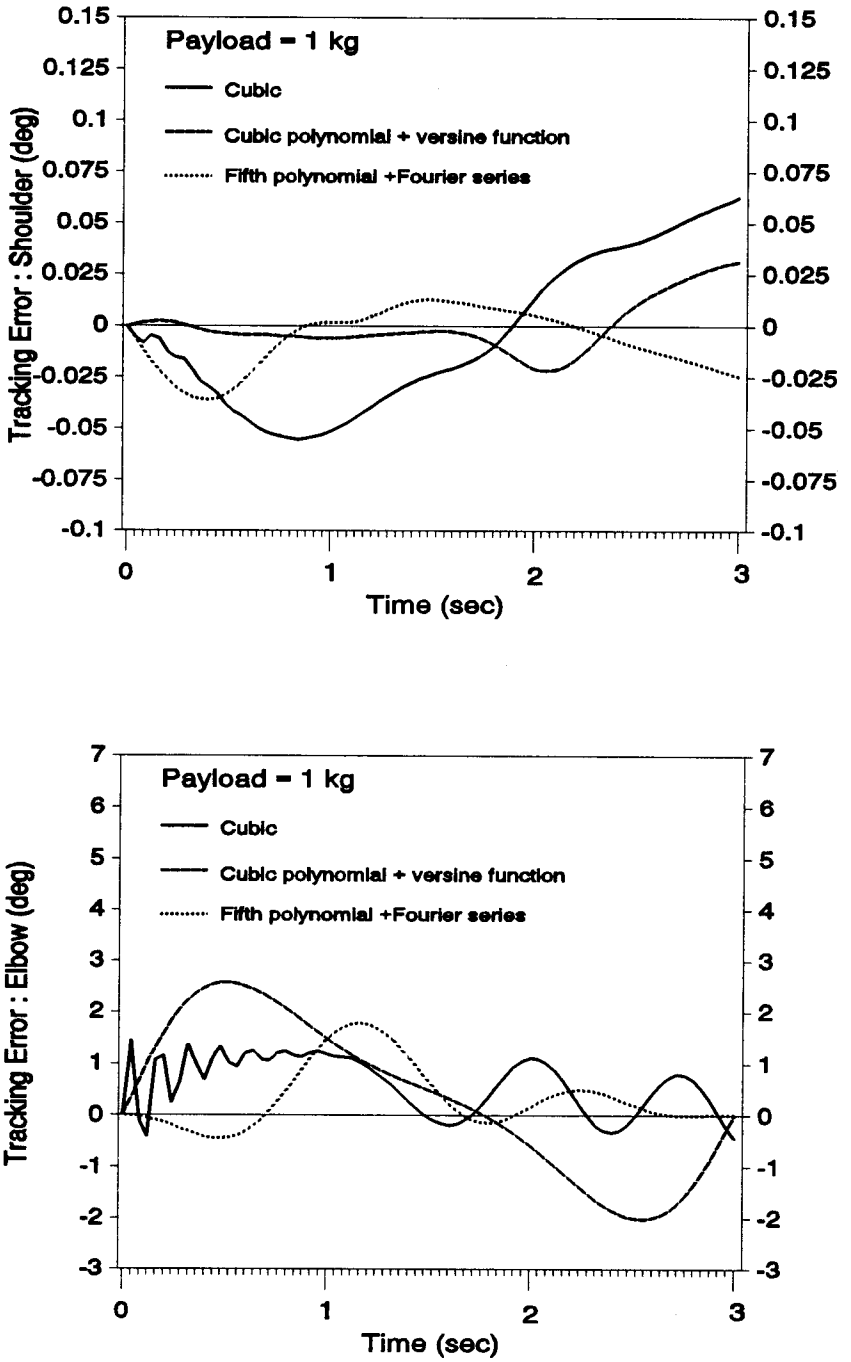


Figure 4.33 Tracking errors for proposed trajectories with payload = 1 kg.

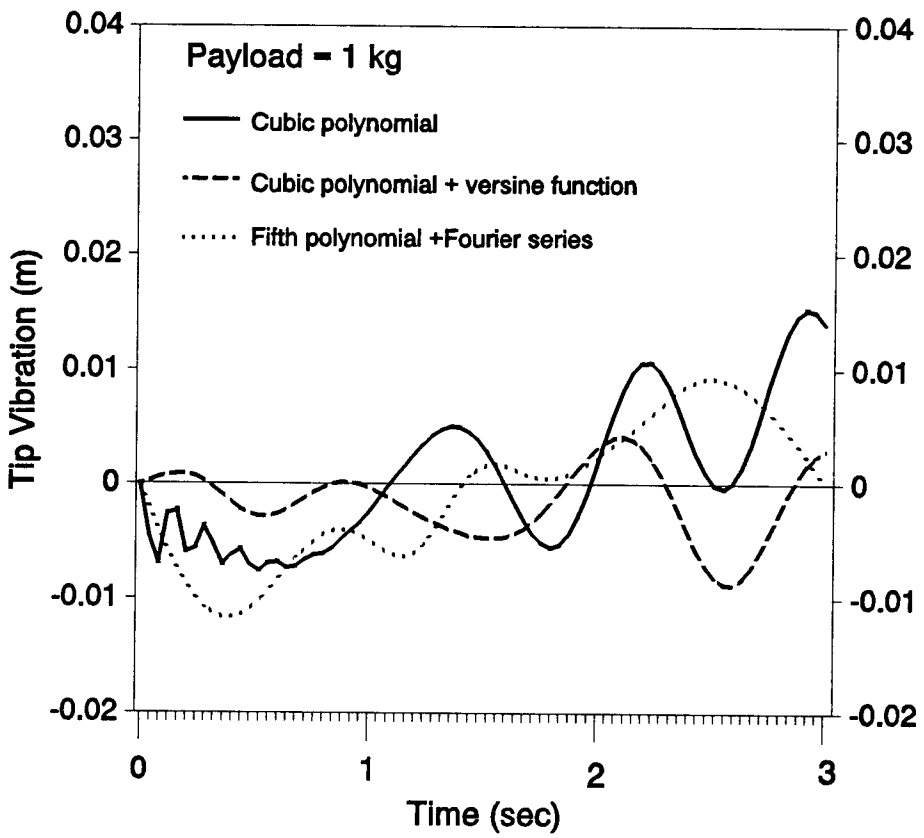


Figure 4.34 Tip vibration for proposed trajectories with payload = 1 kg.

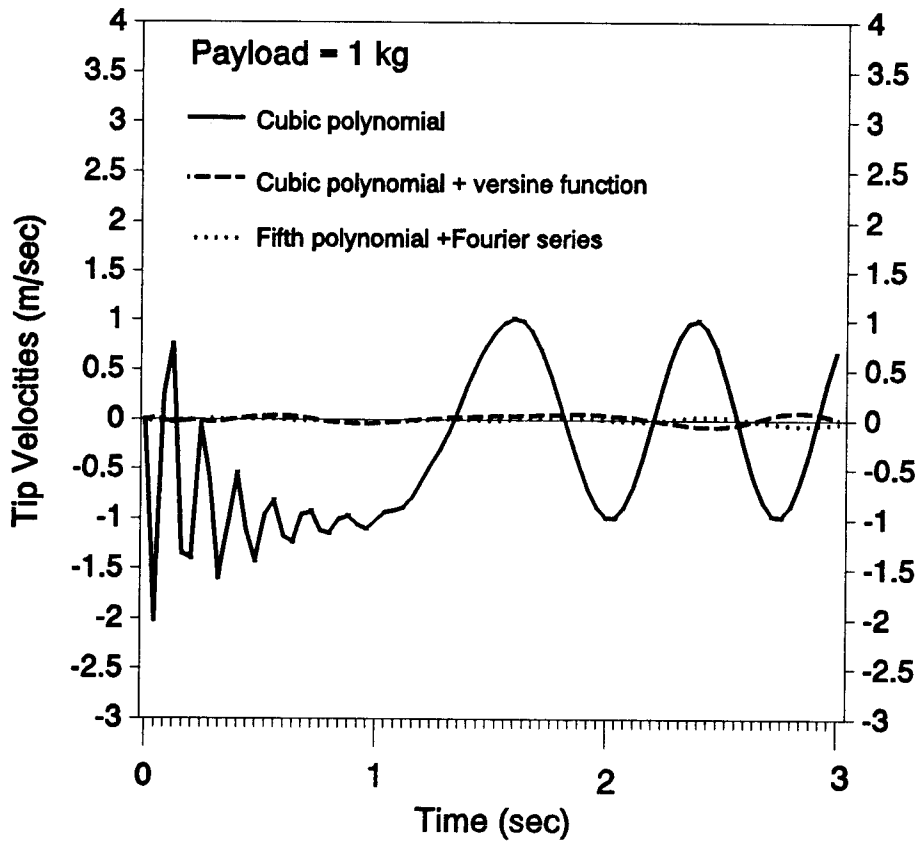


Figure 4.35 Tip vibrational velocities for proposed trajectories with payload = 1 kg.

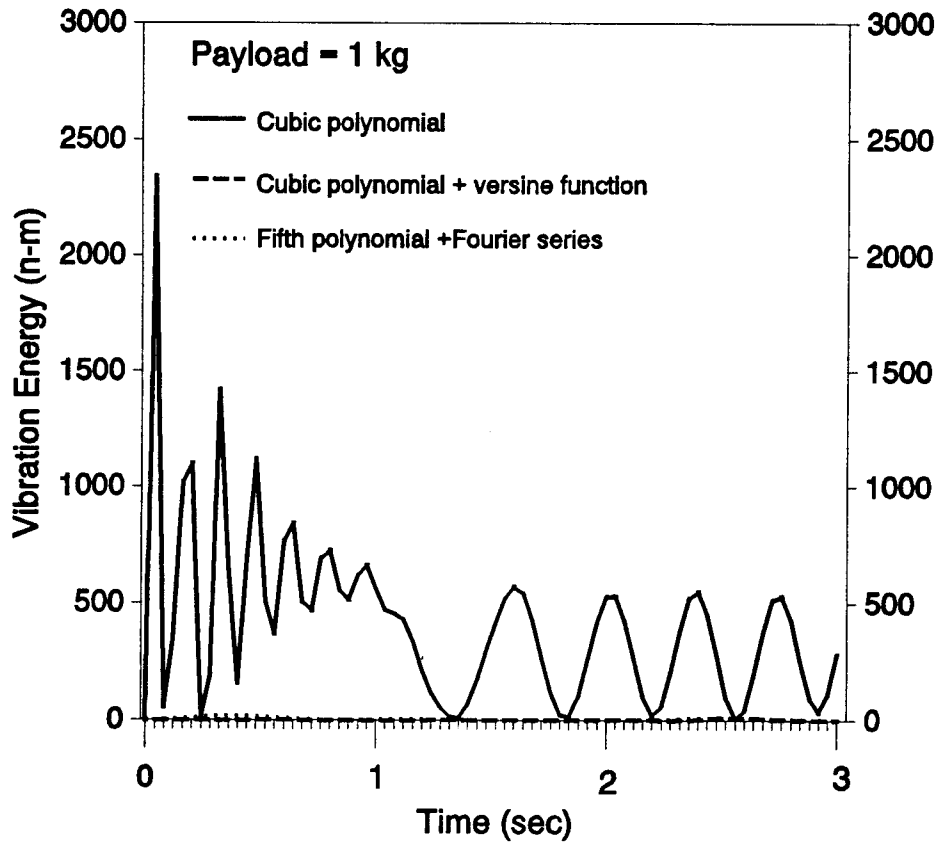


Figure 4.36 Vibrational energy for proposed trajectories with payload = 1 kg.

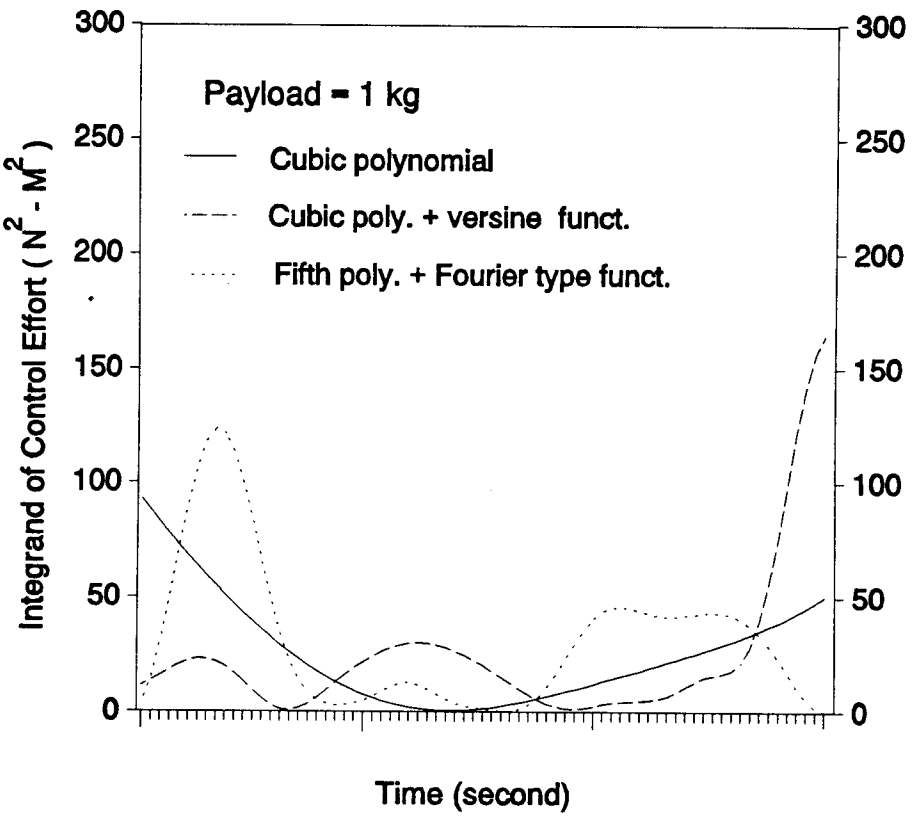


Figure 4.37 Integrand of control effort ($\tau_1^2+\tau_2^2$) with payload = 1 kg.

instability may occur when an inaccurate, linearizied model is used with a large payload. This suggests that the proposed two-stage control is better suited for the light-weight, high-speed motion manipulator.

## 4.5. On-Line Control Simulation Results

To evaluate the on-line real time control, two types of feedback controllers based on pole-placement method and linear quadratic regulator (LQR) are used for simulation. The feedback gains in both controllers were adjusted experimentally to illustrate the effect on the control of the actual flexible manipulator. For the pole-placement method, the gains were adjusted to achieve a critically damped ($\zeta$=1) characteristic because this will produce the fastest non-oscillatory response. The sampling frequency was chosen to be 80 Hz. Although further improvement in computation time is possible, this speed was adequate in demonstrating the dynamic compensation.

The system information is the same as that used in the first part of simulations discussed previously. Fifth order polynomial plus Fourier-type based series path is used as an planned path in this on-line control simulation and the corresponding reference positions, velocities, and the feedforward torques can be generated by a microprocessor and input to the independent joint analog servos.

Torque disturbances of 5 N·m, constant throughout the interval 0.1s < t < 0.102s, were injected to both shoulder and elbow joint. These disturbances were purposely introduced during the motion to observe the behavior of the feedback systems.

The simulation results are presented in Figure 4.38-4.44 for three different loading conditions. Figure 4.38 and 4.39 shows the velocity responses of the actual flexible manipulator using proposed linear feedback controller found by either pole-placement method or LQR. The initial planned velocity (solid line) and the actual velocity profiles (dash line) are superimposed with each other in the figures. Both controllers show very stable response to the external disturbances. Figure 4.38 indicates that link 1 was less affected by the external disturbance than was the second link. Figure 4.39 shows that for $\zeta_1=\zeta_2=1$ and $\omega_1=\omega_2=1$, the pole-placement-based controller quickly drives the second link back to the planned trajectory without oscillating. On the contrary, for $\mathbf{Q}$ = diag[$10^4$,$10^4$,1,1] and $\mathbf{R}$ = diag[0.1,0.1], the bottom scheme shows the LQR obtains larger oscillation before returning to the planned path . Comparison of these two feedback controllers in Figure 4.38 and 4.39 shows that the LQR controller takes longer to drive the link back to the planned trajectory than the pole-placement-based controller with selected $\zeta_i,\omega_i$ and weight matrices $\mathbf{Q}$ and $\mathbf{R}$.

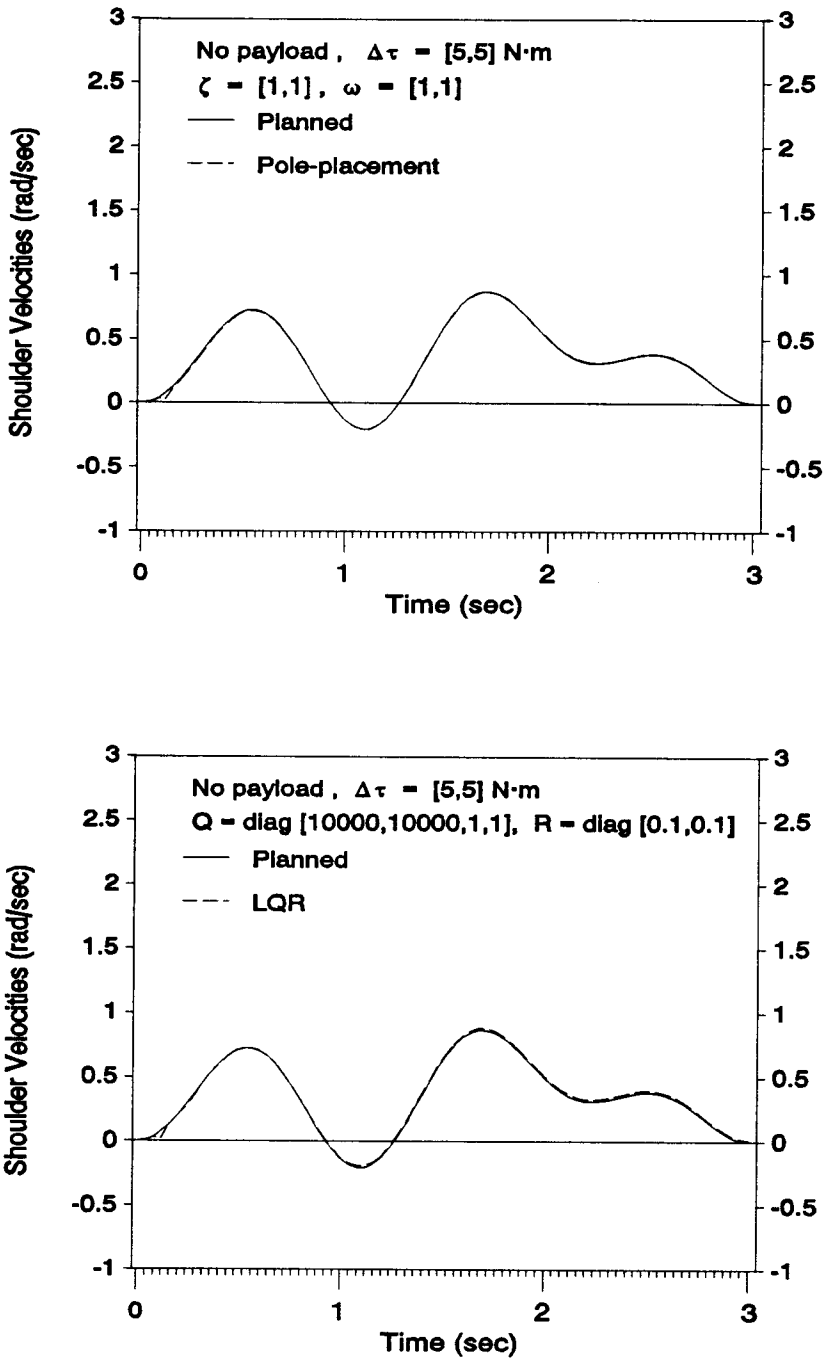


Figure 4.38 Shoulder velocities with proposed controllers ( $m_p = 0\,kg$, $\Delta\tau = [5, 5]\,N \cdot m$, $\zeta = \omega = [1, 1]$, $Q=diag[10^4, 10^4, 1, 1]$, $R=diag[10^{-1}, 10^{-1}]$)

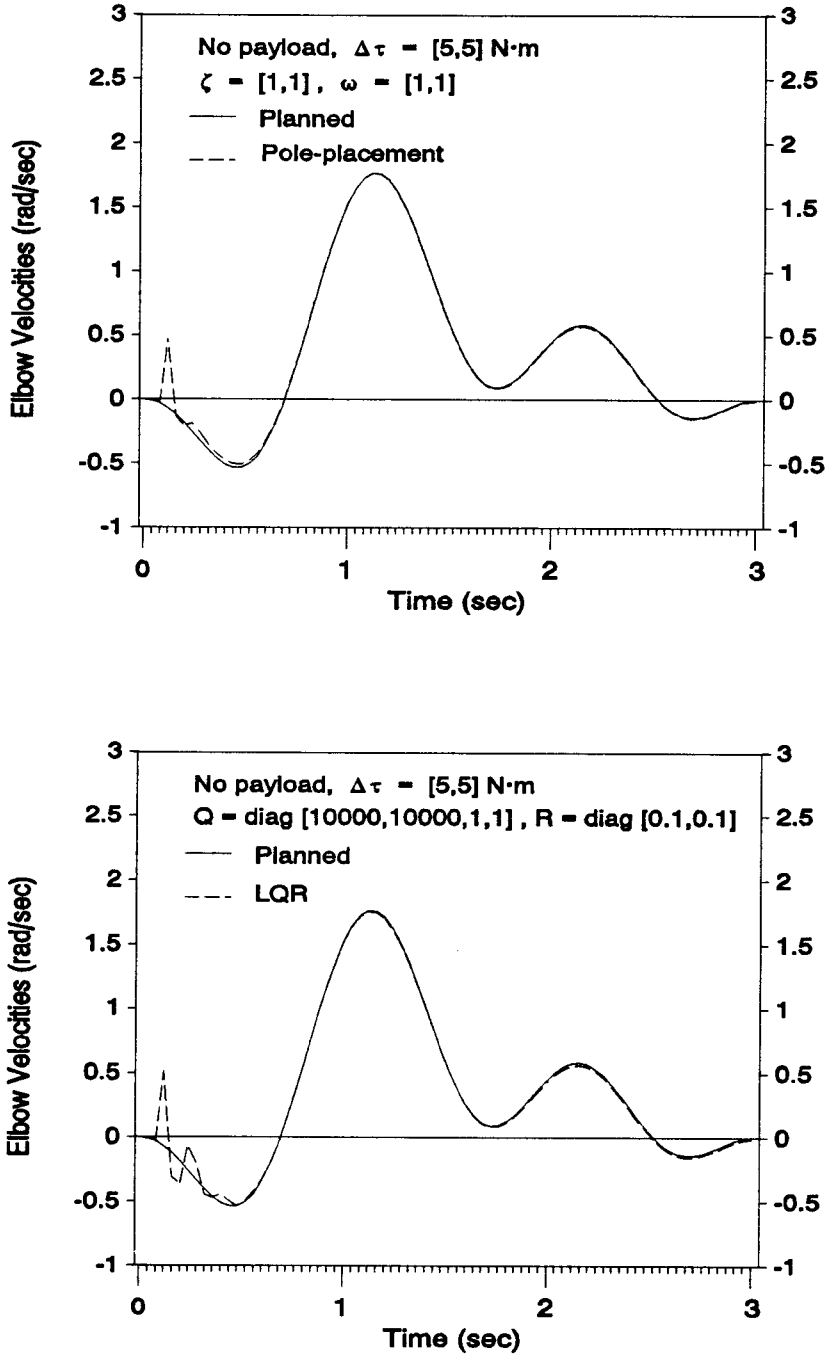


Figure 4.39 Elbow velocities with proposed controllers ( $m_p = 0\,kg$, $\Delta\tau = [5,5]\,N\cdot m$, $\zeta = \omega = [1,1]$, $Q=diag[10^4,10^4,1,1]$, $R=diag[10^{-1},10^{-1}]$).

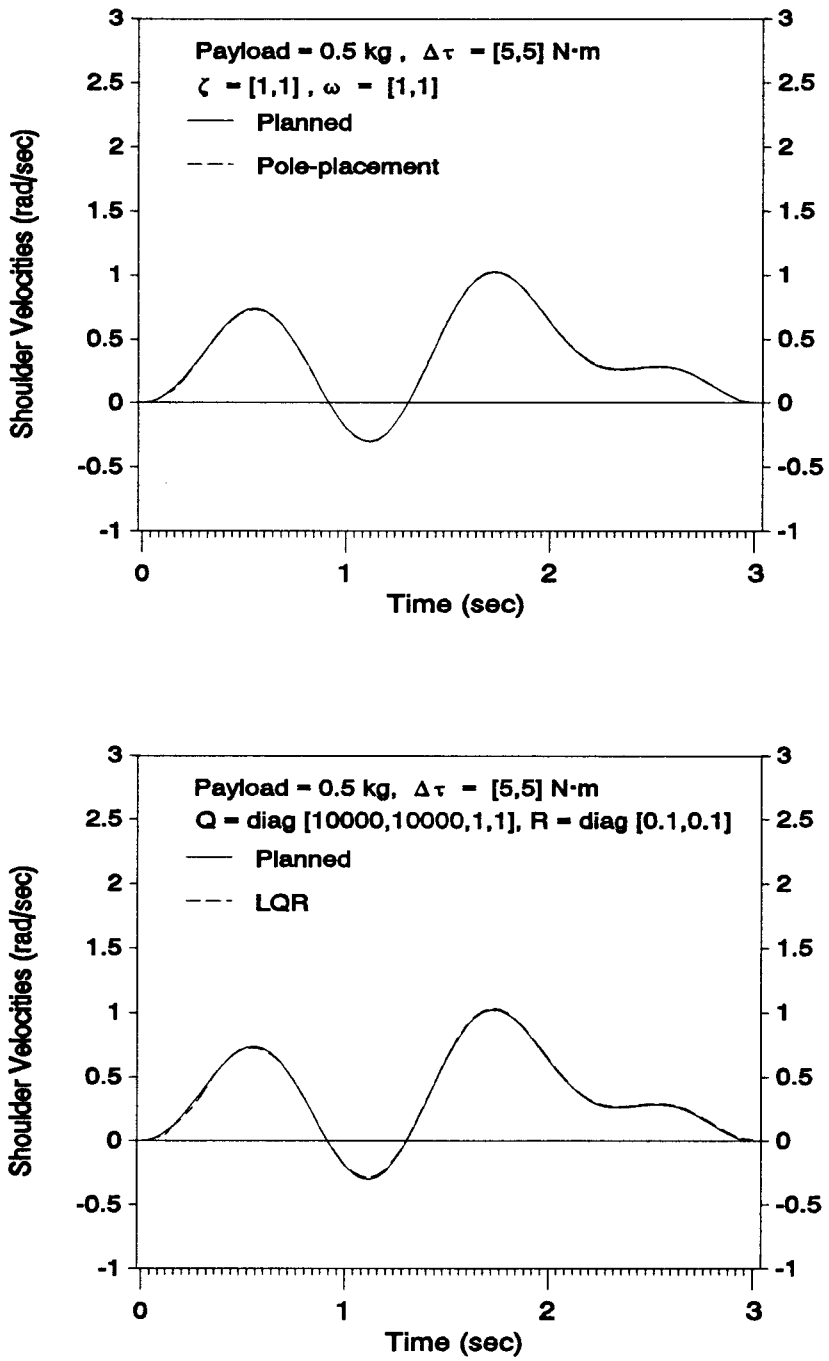


Figure 4.40 Shoulder velocities with proposed controllers ( $m_p$=0.5 kg, $\Delta\tau$=[5,5] N·m, $\zeta$=$\omega$=[1,1], Q=diag[$10^4$,$10^4$,1,1], R=[$10^{-1}$,$10^{-1}$]).

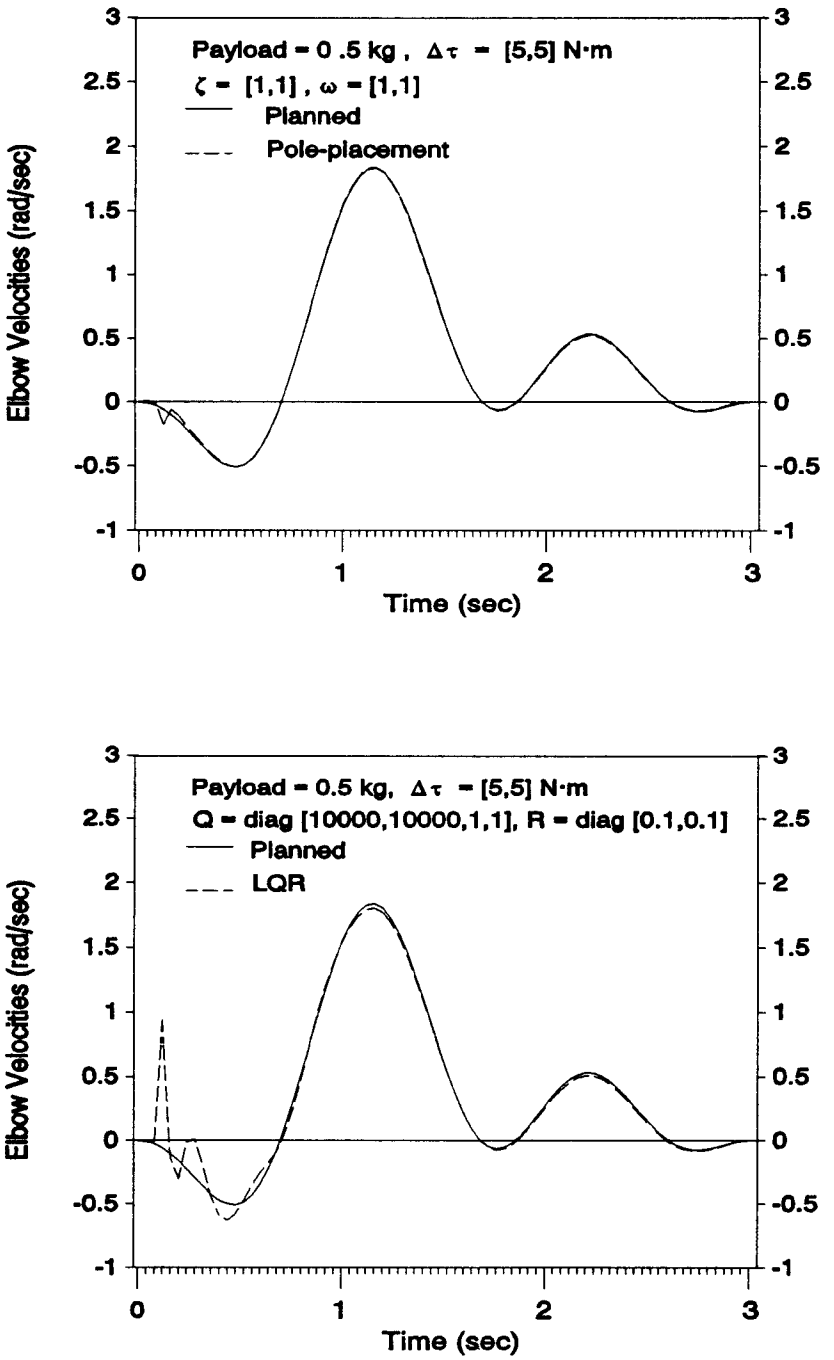


Figure 4.41 Elbow velocities with proposed controller ($m_p$=0.5kg, $\Delta\tau$=[5,5] N·m, $\zeta$=$\omega$=[1,1], Q=[$10^4$,$10^4$,1,1], R=[$10^{-1}$,$10^{-1}$]

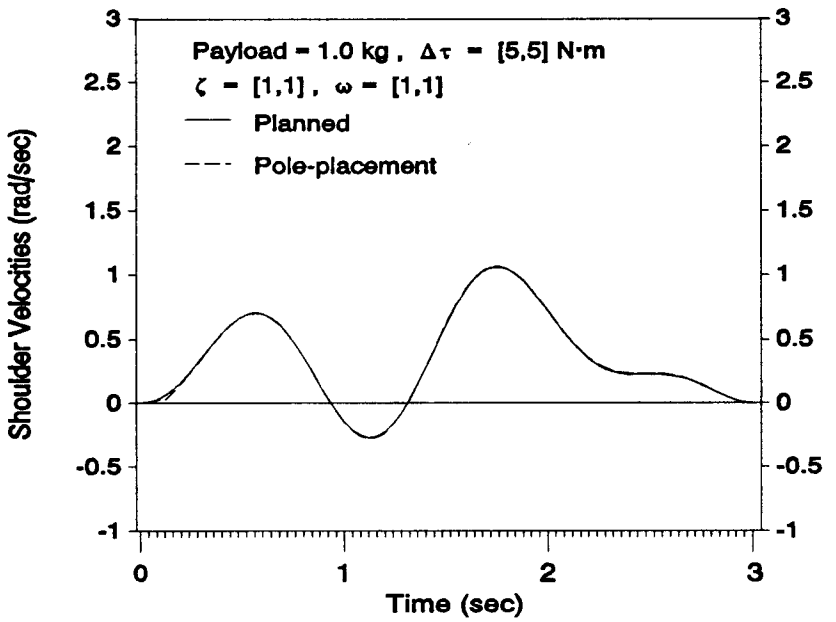


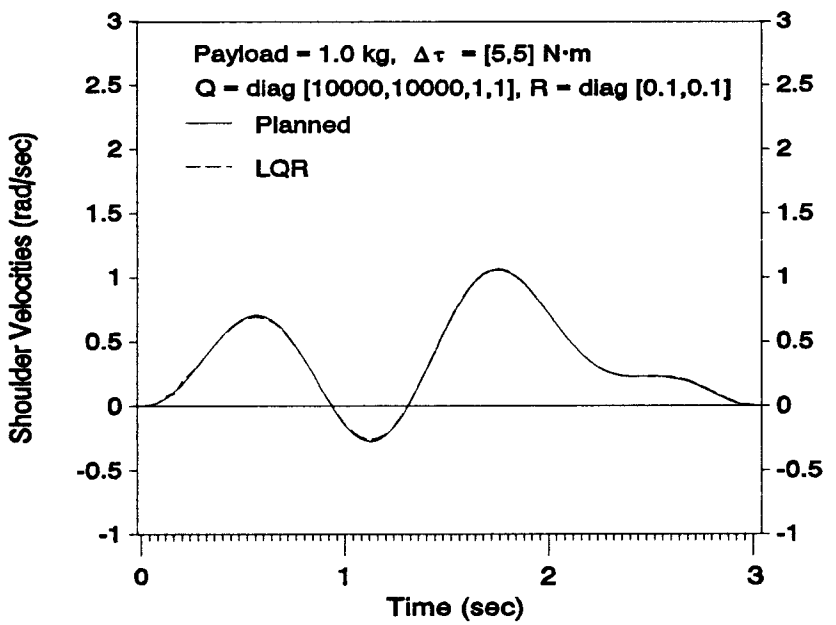


Figure 4.42 Shoulder velocities with proposed controllers ($m_p$=1kg, $\Delta\tau$=[5,5]N·m, $\zeta$=$\omega$=[1,1], Q=[$10^4$,$10^4$,1,1], R=[$10^{-1}$,$10^{-1}$]).

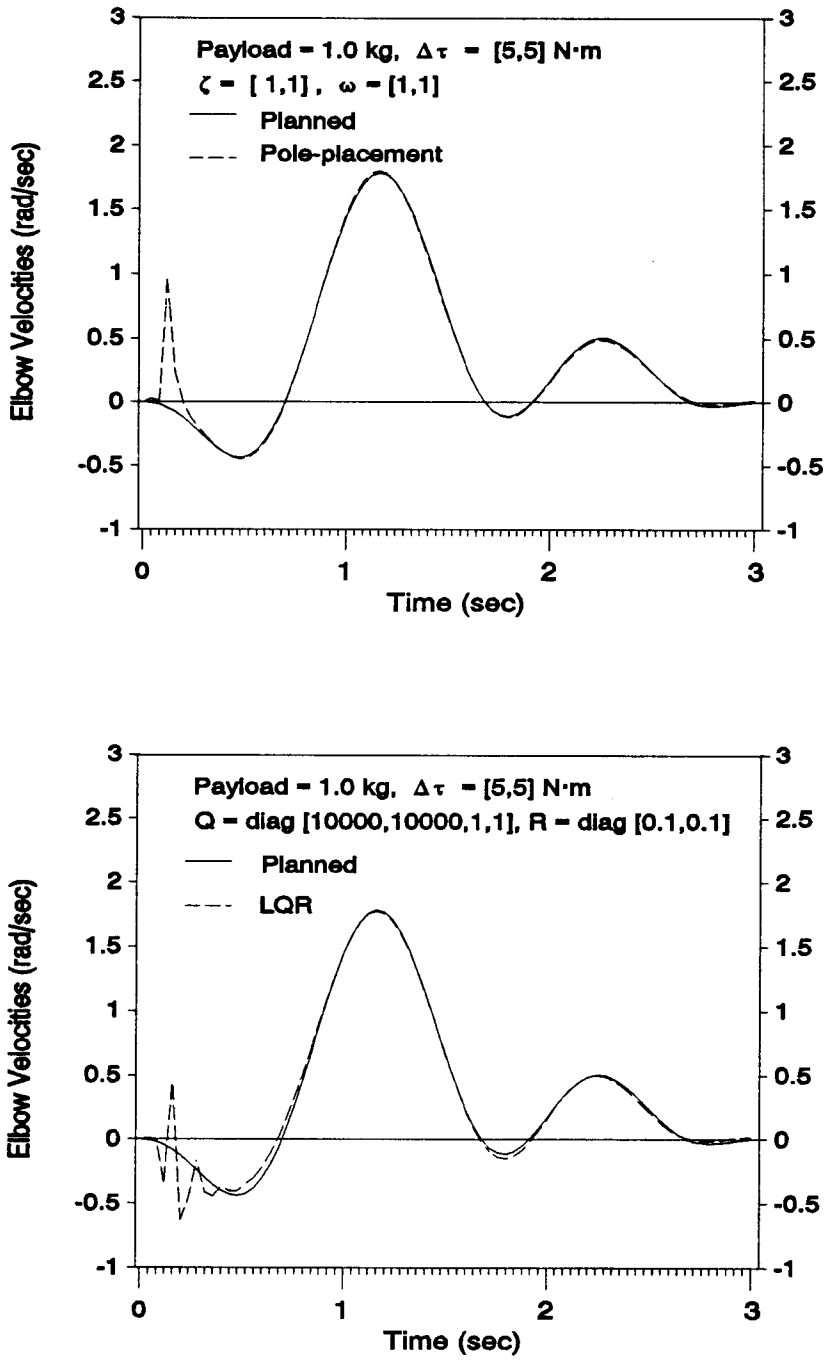


Figure 4.43 Elbow velocities with proposed controllers ($m_p$=1kg,$\Delta\tau$=[5,5] N·m, $\zeta$=$\omega$=[1,1], $Q$=[$10^4$,$10^4$,1,1], $R$=[$10^{-1}$,$10^{-1}$]).

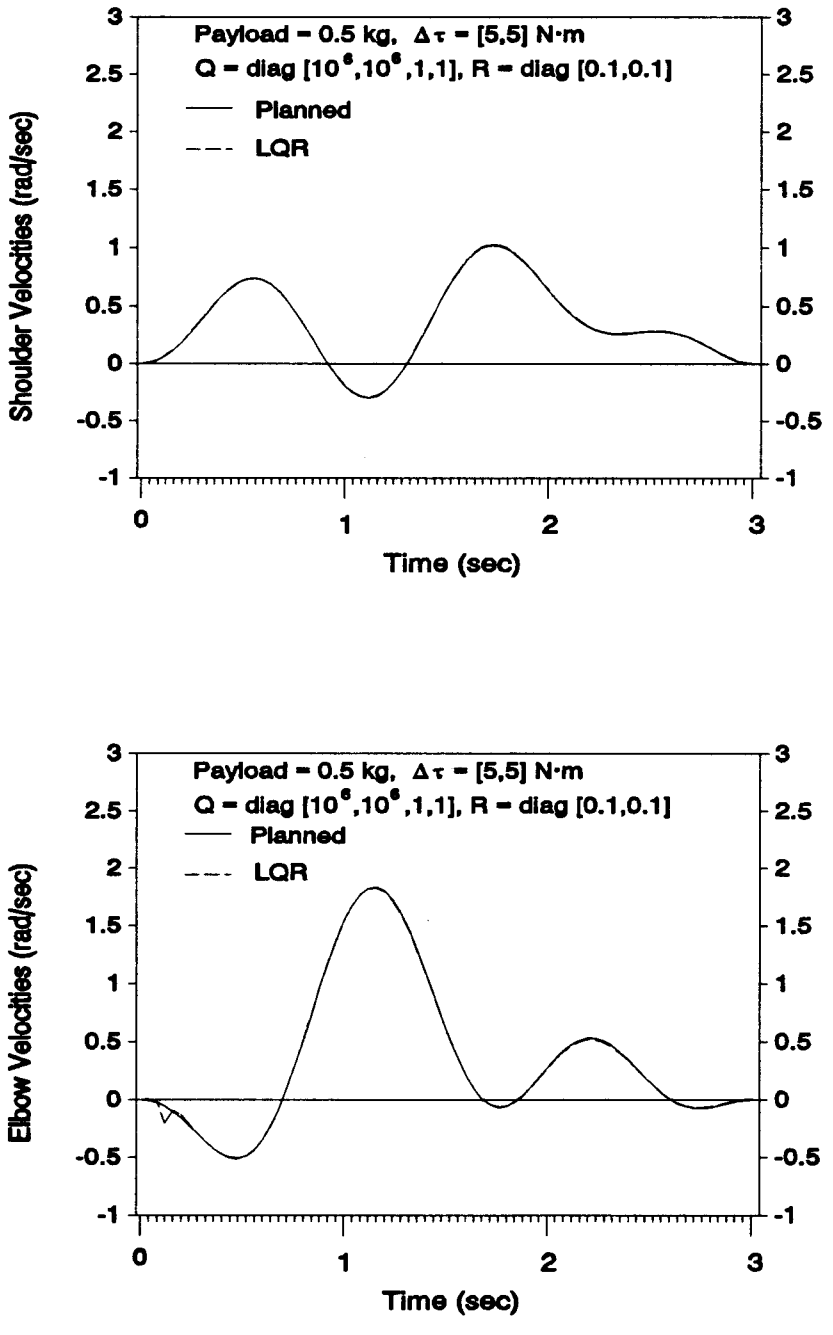


Figure 4.44 Joint velocities with LQR controller ($Q=[10^6,10^6,1,1]$ and $R=[10^{-1},10^{-1}]$, $\Delta\tau=[5,5]N\cdot m$) for $m_p=0.5kg$.

Figure 4.40 - 4.43 show that the proposed two-stage control strategy can be applied to maximum payload up to 1 kg with very stable results, even with the external disturbance is added to the system.

## 4.6. Selection of the Weighting Matrices **Q** and **R**

The selection of the weighting matrices **Q** and **R** is usually made on the basis of experience together with simulation of the results for different trial values. The **Q** and **R** are commonly selected to be diagonal so that the specific components of the state and control vectors can be handled individually. This enables the designer to visualize the effects of the trial values for **Q** and **R**.

In fact, high performance and less oscillation can be achieved by LQR with selected higher control gains. This can be done by putting more weight on matrix **Q** in Equation (3.46). Generally, the larger the elements of **Q**, the larger the gain matrix **K** elements, and the faster the velocity approaches the planned trajectory. On the other hand, the larger the elements of **R**, the smaller the elements of **K** and the slower the response. Figure 4.44 shows that the performance of LQR can be improved by choosing $\mathbf{Q} = \text{diag}[10^6, 10^6, 1, 1]$ and $\mathbf{R} = \text{diag}[0.1, 0.1]$.

A technique for choosing the **Q** and **R** that turns out to be quite reasonable is suggested by Bryson and Ho [1981], and this is presented here as a technique for the first

quess of **Q** and **R**:

1. Make, for lack of better knowledge, the off-diagonal elements of **Q** and **R** zero.

2. Pick the diagonal elements as follows:

$\mathbf{Q}^{-1}$ = n($t_f$-$t_0$) × maximum acceptable value of diag $\mathbf{x}(t)\mathbf{x}^T(t)$.

$\mathbf{R}^{-1}$ = m($t_f$-$t_0$) × maximum acceptable value of diag $\mathbf{\Gamma}(t)\mathbf{\Gamma}^T(t)$.

here, the dimensions of $\mathbf{x}(t)$ and $\mathbf{\Gamma}$ are n and m, respectively.

For special cases, the **Q**, **R** matrices can be chosen as time varying in order to achieve the best performance of the control system.

# CHAPTER 5. CONCLUSIONS AND FUTURE WORK

The primary objective of this study was to verify that the tip position of a flexible manipulator can be effectively controlled by simple controllers using only rigid body model for reference.

A two-link rigid/flexible robot is used as the focus for this study. The dynamic model for the robot includes the effect of the distributed mass and elasticity of the last link. The assumed modes method is used to approximate the dynamics of the distributed-parameter link. This approximation incorporates a truncated modal description of the dynamic beam, and Lagrange's equations are used to derived the equation of motion.

In order to control the flexible robot arm, the two-stage control scheme was proposed. First, the optimal control problem was formulated as a manipulator-trajectory-planning problem in order to avoid the computational difficulty. A reduced order model HRRA serves as a good approximation of the actual RFRA system behavior through the proposed trajectory planning algorithm. A parameter-optimization approach was adopted to find the optimal trajectories form this simplified HRRA system. This approach offers significant advantages in computational efficiency compared with the dynamic-programming-based methods which require extensive computer

storage. When compared to calculus-of-variations-based methods, the approach eliminates the requirement of solving a two-point boundary-value problem and therefore is more robust and efficient.

At the second stage, two linear state feedback controllers based on the pole-placement method and the linear quadratic method were designed to control the actual RFRA system using only simplified HRRA system. Compared with the flexible feedback control (FFC) which requires additional sensors for deflection information, this control design greatly simplifies the design of control of a flexible robot. Although a tabulation method was suggested in obtaining the time-varying optimal feedback gains, a more efficient method e.g. "One-Step" optimal control algorithm was implemented for real time on-line control.

The dynamic model and the proposed control algorithm are applied as the basis for the simulation. The results indicated, as expected, that good trajectory planning helps to avoid any unnecessary excitation of vibration. High frequency term in the beam deflections can be damped, thus reducing the vibration, which in turn, improves the overall stability and performance. The results also show that with properly selected of time-varying feedback gains, fast, accurate movement can be achieved even when external disturbances are intentionally introduced to the

system. Instability is not detected on both controllers but undesired performance is possible when the payload exceeds the maximum loading condition (i.e., $m_p$ = 1.0 kg).

A pre-calculated method was suggested in obtaining the system parameters of the linearized rigid model for on-line trajectory tracking; however, inaccurate knowledge of the actual flexible manipulator may be a significant factor contributing to inaccurate results. Uncertainties in the actual system, such as compliance in joints, temperature variation, or gear friction and backlash which will reduce the achievable performance from the proposed design. Therefore, there is a need for more accurate system information before the proposed control algorithm is utilized. One such parameter-identification technique for robotic application has already been proposed by Everett and Hsu [1988].

The future tasks recommended for further study may be summarized as follows:

1. experimental verification.
2. definition of a formal procedure to find the linear optimal control gains.
3. finding a method to choose closed-loop poles which maximize the feedback and still stabilize the flexible manipulator.
4. improve the optimal numerical method to increase the optimization efficiency.

5. inclusion of prismatic joints and closed-loop mechanisms.

# BIBLIOGRAPHY

Albert, T.E., Xia, H., and Chen, Y., 1990, "Dynamic analysis to evaluate viscoelastic passive damping augmentation for the space shuttle remote manipulator system," *ASME DSC-Vol.20*, pp.35-41.

Anderson, D.O. and Moore, J.B., 1990, *Optimal Control; Linear Quadratic Method*. Prentice-Hall, Inc., Englewood Cliffs, NJ.

Atkeson, C. G., An, C. H., and Hollerbach, J. M., 1986, "Estimation of inertial parameters of manipulator loads and links," *The International Journal of Robotics Reseach*, Vol. 5, No. 3, pp 101-119.

Balas, M. J., 1978a, "Modal control of certain flexible dynamic systems," *SIAM J. Control and Optimization*, Vol. 16, No. 3, pp. 450-462.

Balas, M. J., 1978b, "Feedback control of flexible systems," *IEEE Transactions on Automatic Control*, Vol. AC-23, No. 4, pp. 673-679.

Benati, M. and Morro, A., 1988, "Dynamics of chain of flexible links," *ASME Journal of Dynamic Systems, Measurement, and Control*, Vol. 110, pp. 410-415.

Beveridge, G.S. and Schechter, R.S., 1970, *Optimization: Theory and Practice*. McGraw-Hill, Inc., New York, NY.

Biswas, S.K. and Klafter, R.D., 1988, "Dynamic modeling and optimal control of flexible robotic manipulators," *IEEE International Conference on Robotics & Automation*, pp. 15-20.

Blanck, N.E., 1988, "Two time-variant control designs for a manipulator: optimal control and pole-placement," *IFAC Theroy of Robots*, Proceedings series; no. 3 pp. 199-203.

Bobrow, J.E., Dubowsky, S., and Gibson, J.S., 1985, "Time-optimal control of robotic manipulators along specified paths," *The International Journal of Robotics Research*, Vol. 4, No. 3, pp. 3-17.

Book, W.J., Dickerson, S.L., Hastings, G., Cetinkunt, S., and Alberts, T.,1985, "Combined approaches to lightweight arm utilization," *Robotics and Manufacturing Automation*, PED- Vol. 15, pp. 97-107.

Book, W.J., 1984, "Recursive Lagrangian dynamics of flexible manipulator arm," *The International Journal of Robotics Reseach*, Vol. 3, No. 3, pp. 87-101.

Book, W.J., Alberts, T.E., and Hastings, G.G., 1986, "Design strategies for high-speed lightweight robots,", *Computers in Mechanical Engineering*, pp. 26-33.

Book, W.J., Maizza-Neto, O., and Whitney, D.E., 1975, "Feedback control of two joint system with distributed flexibility," *ASME Journal of Dynamic Systems, Measurement, and Control*, Dec., pp. 424-431.

Bryson, A.E.,Jr. and Ho, Y.C., *Applied Optimal Control; Optimization, Estimation, and Control*. John Wiley, New York.

Cannon, Jr., R.H. and Schmitz, E., 1984, "Initial experiments on end-point control of a flexible one-link robot," *The International Journal of Robotics Reseach*, Vol. 3, No. 3, pp. 62-75.

Castelazo, I.A. and Lee, H., 1990, "Nonlinear compensation for flexible manipulators," *ASME Journal of Dynamic Systems, Measurement, and Control*, Vol. 112, pp. 62-68.

Chalhoub, N.G. and Ulsoy, A.G., 1987, "Control of a flexible robot arm: experimental and theoretical results," *ASME Journal of Dynamic Systems, Measurement, and Control*, Vol. 109, Dec., pp. 299-309.

Chalhoub, N.G. and Ulsoy, A.G., 1986, "Dynamic simulation of a leadscrew driven flexible robot arm and controller," *ASME Journal of Dynamic Systems, Measurement, and Control*, Vol. 108, June., pp. 119-126.

Chen, C. T., 1984. *Linear System Theory and Design*. Holt, Rinehart and Winston.

Christian, A.D. and Seering, W.P., 1989, "Design considerations for an earth based flexible robotic system," *IEEE International Conference on Robotics and Automation*, Vol. 3, pp. 1396-1401.

Craig, J.J., 1986, *Introduction to robotics: mechanics and control*. Reading, Mass.: Addison-Wesley publishing company.

Craig, J.J., Hsu, P., and Sastry, S.S., 1987, "Adaptive control of mechanical manipulators," *The International Journal of Robotics Reseach*, Vol. 6, No. 2, pp. 16-28.

Craig, R., 1981, *Structural Dynamics - An Introduction to Computer Methods*. John Wiley & Sons, Inc.

Desoyer, K., Kopacek, P., Lugner, P., and Troch, I., 1986, "Felexible robots - a survey," *IFAC Theory of Robots*, Vienna, Austria, pp. 23-34.

Dick, G.M., 1986, "End-point control of a two-link compliant manipulator," *Recents Trends in Robotics: Modeling, Control, and Education*, Jamshidi, M., Luh, L.Y.S., and Shahinpoor, M., Editors, pp. 137-143.

Everett, L.J. and Hsu, T.W., 1988, "The theory of kinematic parameter identification for industrial robots," *ASME Journal of Dynamic Systems, Measurement, and Control*, Vol. 110, pp. 96-100.

Everett, L. J., 1989, "An extension of Kane's method for deriving equations of motion of flexible manipulators," *IEEE International conference on Robotics & Automation*, pp. 716-721.

Fiacco, A.V. and McCormick, G.P.,1969, *Nonlinear Programming: Sequential Unconstrained Minimization techniques*. Wiley, New York.

Fukuda, T., 1985, "Flexibility control of elastic robot arms," *Journal of Robotic Systems*, Vol. 2, No. 1, pp. 73-88.

Gebler, B., 1987, "Feed-forward control strategy for an industrial robot with elastic links and joints," *IEEE International Conference on Robotics & Automation*, pp. 923-928.

Geering, H.P., Guzzella, L., Hepner, S.A.R., and Onder, C.H., 1986, "Time-optimal motions of robots in assembly tasks," *IEEE Transactions on Automatic Control*, Vol. AC-31, No.6, pp.512-518.

Hastings, G.G. and Book, W.J., 1986, "Verfication of a linear dynamic model for flexible robotic manipulators," *IEEE International Conference on Robotics & Automation*, pp. 1024-1029.

Huston, R.L., 1981, "Multi-body dynamics including the effects of flexibility and compliance," *Computers & Structures*, Vol. 14, No. 5-6, pp. 443-451.

Huston, R.L. and Kelly, F.A., 1982, "New approaches in robot dynamics and control," *Proceedings of the 2nd ASME International Computers in Engineering Conference*, San Diego.

Jacquot, R. G., 1981, *Modern digital control system*. Marcel Dekker, Inc., NY.

Jamshidi, M. and Malek-Zavarei, M., 1986, *Linear Control System; A Computer-Aided Approach*. Pergamon Books Ltd..

Johnson, C.D.,1968, "Optimal control of the linear regulator with constant disturbances," *IEEE Transactions on Automatic Control*, pp. 416-421.

Johnson, C.D.,1971, "Accommodation of external distrubances in linear regulator and servomechanism problems," *IEEE Transactions on Automatic Control*, Vol. AC-16, No. 6, pp. 635-645.

Kane, T.R. and Levinson, D.A., 1983, "The use of Kane's dynamical equations in robotics," *The International Journal of Robotics Research*, Vol. 2, No. 3, pp. 3-21.

Kane, T.R., Linkins, P.W., and Levinson, D.A., 1983, *Spacecraft dynamics*. New York: McGraw-Hill.

Kanoh, H. and Lee, H.G., 1985, "Vibration control of one-link flexible arm," *Proceedings of 24th Conference on Decision and Control*, Ft. Lauderdale, FL..

Kirt, D.E., 1970, *Optimal Control Theroy: An Introduction*. Prentice-Hall, Inc., Englewood Cliffs, NJ.

Kleemann, U.,1986, "Dynamics and control of a robotic system with elastic arms," *Recents Trends in Robotics: Modeling, Control, and Education*, Jamshidi, M., Luh, L.Y.S., and Shahinpoor, M., Editors, pp. 487-492.

Lee, J.D., Haynes, L.S., Wang, B.L., and Tsai, K.H., 1987, "Control of flexible robot arm," *ASME DSC-Vol.6*, pp. 241-251.

Lee, B.K., 1989, "A model reference adaptive system for control of a flexible mechanical manipulator." *Ph.D. thesis*, Dept. of Mechanical Engineering, Oregon State University.

Lee, C.S.G. and Chung, M.J., 1984, "An adaptive control strategy for mechanical manipulators," *IEEE Transactions on Automatic Control*, Vol. AC-29, No. 9, pp. 837-840.

Leu, M.C. and Hemati, N., 1986, "Automated symbolic derivation of dynamic equations of motion for robotic manipulators," *ASME Journal of Dynamic Systems, Measurement, and Control*, Vol. 108, pp. 172-179.

Liao, D.X., Sung, C.K., and Tompson, B.S., 1987, "The design of flexible robotic manipulators with optimal arm geometries fabricated from composite laminates with optimal material properties," *The International Journal of Robotics Research*, Vol.6, No.3, pp. 116-130.

Lin, C.S., Chang, P.R., and Luh, J.Y.S., 1983, "Formulation and optimization of cubic polynomial joint trajectories for industrial robots," *IEEE Transactions on Automatic Control*, Vol. AC-28, No. 12, pp. 1066-1074.

Luh, J.Y.S., Walker, M.W., and Paul, R.P., 1980, "On-line computational schemes for mechanical manipulators," ASME *Journal of Dynamic Systems, Measurement, and Control*, Vol. 102, pp. 69-76.

Luh, J.Y.S. and Lin, C.S., 1981, "Optimum path planning for mechanical manipulators," ASME *Journal of Dynamic Systems, Measurement, and Control*, Vol. 102, pp. 142-151.

*MACSYMA Reference Manual*. 1983, The Mathlab Group, Laboratory for Computer Science, MIT.

Maizza-Neto, O., 1974, "Modal analysis and control of flexible manipulator arms," *Ph.D. thesis*, Dept. of Mechanical Engineering, MIT.

Meckl, P.H. and Seering, W.P., 1987, "Reducing residual vibration in systems with time-varing resonances," *IEEE International Conference on Robotics & Automation*, pp. 1690-1695.

Meckl, P.H. and Seering, W.P., 1988, "Shaping reference input to reduce residual vibration for a cartesian robot," *Symposium on Robotics*, DSC-Vol. 11, pp. 225-240.

Meirovitvh, L., 1967, *Analytical Methods in Vibrations*. The MacMillian Co..

Meirovitch, L., 1970, *Methods of Analytical Dynamics*. McGraw-Hill.

Melsa, J.L. and Jones, S.K., 1973, *Computer Program for Computational Assistance in the Study of Linear Control Theory*. 2nd ed. McGraw-Hill, Inc..

Nagurka, M.L. and Yen, V., 1987, "Designing manipulator trajectories by nonlinear programming," *ASME DSC-Vol.6*, pp. 377-384.

Nelder, J.A. and Mead, R., 1965, "A simplex method for function minimization," *Computer Journal*, Vol. 7, pp. 308-313.

Nicosia, S., Tomei, D., and Tornambe, A., 1986, "Dynamic modelling of flexible robot manipulators," *Proc. IEEE Conf. on Robotics and Automation*, San Francisco, USA, pp. 365-372.

Owens, D.H., 1988, "Optimal Control," *Industrial Digital Control System*. edited by Warwick, E. and Rees, D., pp. 213-225.

Palm, W. J., 1983, *Modeling, Analysis, and Control of Dynamic System*. John Wiley & Sons, Inc..

Paul, R.P., 1985, *Robot manipulators; Mathematics, Programming and Control*. Cambridge, Mass. : MIT Press.

Petterson, B.J., Robinett, R.D., and Werner, J.C., 1990, "Parameter-scheduled trajectory planning for suppression of coupled horizontal and vertical vibrations in a flexible rod," *IEEE International conference on Robotics & Automation*, Vol. 2, pp. 916-921.

Pfeiffer, F. and Johanni, R., 1986, "A concept for manipulator trajectory planning," *IEEE International conference on Robotics & Automation*, pp. 1399-1405.

Pfeiffer, F. and Kleemann, U., 1989, "Elasticity and vibration control for manipulators," *IEEE International Conference on Control & Applications*, pp. 1-7.

Pfeiffer, F. and Gebler, B., 1988, "A multistage-approach to the dynamics and control of elastic robots," *IEEE International Conference on Robotics and Automation*, pp. 2-8.

Powell, M.J.D., 1964, "An efficient method for finding the minimum of a function of several variables without calculating derivatives," *The computer Journal*, 7, pp.155-162.

Press, W. H., Flannery, B. P., Teukolsky, S. A., and Vetterling, W. T., 1989, *Numerical recipes*. Cambridge University Press.

Reddy, J. N., 1986, *Applied Functional Analysis and Variational Methods in Engineering*. McGraw-Hill Book Comp..

Schmitt, D., Soni, A.H.,Srinivasan, V., Naganathan, G., 1985, "Optimal motion programming of robot manipulators," *ASME Journal of Mechanisms, Transmissions, and Automation in Design*, Vol. 107, pp. 239-244.

Schmitz, E., 1989, "Modeling and control of a planar manipulator with an elastic forearm," *IEEE International Conference on Robotics & Automation*, Vol. 2, pp. 894-899.

Serna, M.A. and Bayo, E., 1990, "Trajectory planning for flexible manipulators," *IEEE International conference on Robotics & Automation*, pp. 910-915.

Shin, K.G. and Mckay, N.D., 1985, "Minimum-time control of robotic manipulators with geometric path constrains," *IEEE Transactions on Automatic Control*, Vol. AC-30, No. 6, pp. 531-541.

Shin, K.G. and Mckay, N.D., 1986a, "A dynamic programming approach to trajectory planning of robotics manipulators," *IEEE Transactions on Automatic Control*, Vol. AC-31, No. 6, pp. 491-500.

Shin, K.G. and Mckay, N.D., 1986b, "Selection of near-minimum time geometric paths for robotic manipulators," *IEEE Transactions on Automatic Control*, Vol. AC-31, No. 6, pp. 501-511.

Silver, W.M., 1982, "On the equivalence of Lagrangian and Newton-Euler dynamics for manipulators," *International Journal of Robotics Research*, Vol. 1, No. 2, pp. 60-70.

Singh, S. and Leu, M.C., 1987, "Optimal trajectory generation for robotic manipulators using dynamic programming," *ASME Journal of Dynamic Systems, Measurement, and Control*, Vol. 109, pp. 88-96.

Singhose, W.E., Seering, P.W., and Singer, N.C., 1990, "Shaping inputs to reduce vibration: a vector diagram approach," *IEEE International Conference on Robotics and Automation*, Vol. 2, pp. 922-927.

Smith, C. E., 1985, personal communication.

Spong, M.W. and Vidyasagar, M., 1989, *Robot Dynamics and Control*. John Wiley & Sons, Inc..

Sunada, W. and Dubowsky, S., 1981, "The application of finite element methods to the dynamic analysis of flexible spatial and co-planar linkage system," *ASME Journal of Mechanical Design*, Vol.103, No.3, pp.643-651.

Thompson, B.S. and Sung, C.K., 1984, "A variational formulation for the dynamic viscoelastic finite element analysis of robotic manipulators constructed from composite materials," *Journal of Mechanisms, Transmissions, and Automation in Design*, Vol. 106, pp. 183-190.

Usoro, P.B., Nadira, R., and Mahil, S.S., 1986, "A finite element/Lagrange approach to modeling light-weight flexible manipulators," *ASME Journal of Dynamic Systems, Measurement, and Control*, Vol. 108, No. 3, pp. 88-96.

Vukobratović, M. and Stokić, D., 1982, *Control of Manipulation Robots : Theory and Application*. Springer-Verlag Berlin, Heidelberg.

Wang, P.K.C. and Wei, J.D., 1987, "Feedback control of vibrations in a moving flexible robot arm with rotary and prismatic joints," *IEEE International Conference on Robotics & Automation*, Vol. 3, pp. 15-20.

Whitney, D. E., June 1974, "Design and control coordinations for industrial and space manipulators," *JACC Proceedings*, pp. 591-598.

Yang, S. and Tomizuka, M., 1988, "Pulse control for vibration attenuation in nonlinear mechanical systems," *Symposium on Robotics*, DSC - Vol. 11, pp. 103-114.

Yen, V. and Nagurka, M., 1989, "Optimal trajectory planning of robotic manipulators via quasi-linearization and state parameterization," *IEEE International conference on Robotics & Automation*, pp. 1116-1121.

Yuan, B.S. and Book, W.J., 1987, "A robust scheme for direct adaptive control of flexible arms," *ASME Annual Winter Meeting*, pp. 261-268.

Zalucky, A. and Hardt, D.E., 1984, "Active control of robot structure deflections," *ASME Journal of Dynamic Systems, Measurement, and Control*, Vol. 106, pp. 63-69.